

Variants of SGD for Lipschitz Continuous Loss Functions in Low-Precision Environments

Michael R. Metel*

Huawei Noah's Ark Lab, Montréal, Qc, Canada

June 21, 2023

Abstract

Motivated by neural network training in low-bit floating and fixed-point environments, this work studies the convergence of variants of SGD using adaptive step sizes with computational error. Considering a general stochastic Lipschitz continuous loss function, an asymptotic convergence result to a Clarke stationary point, and the non-asymptotic convergence to an approximate stationary point are presented assuming that only an approximation of the loss function's stochastic gradient can be computed, as well as error in computing the SGD step itself. Different variants of SGD are tested empirically in a variety of low-precision arithmetic environments, where improved test set accuracy is observed compared to SGD for two image recognition tasks.

1 Introduction

This paper studies the convergence of variants of stochastic gradient descent (SGD) using adaptive steps sizes in an environment with non-negligible computational error. The assumptions are given in a general form but are motivated by the error from using low-bit finite precision arithmetic for neural network training. Given the continuously increasing size of deep learning models, there is a strong motivation to do training in lower-bit formats. The majority of research in this area is focused on hardware design using number formats of different precision for different types of data (gradients, weights, etc.) to accelerate training and reduce memory requirements while aiming to incur minimal accuracy degradation, see (Wang et al., 2022, Table 1). Our work is complementary to this line of research, with a focus on trying to gain a better understanding of low-bit training from the perspective of the training algorithm, namely, we seek to understand what level of error can be imposed while still maintaining a theoretical convergence guarantee, and to observe empirically to what extent simple variants of SGD can improve a model's accuracy in challenging low-bit environments.

The theoretical convergence analysis in Section 5 focuses on using variants of perturbed SGD

*michael.metel@huawei.com

(PSGD) with adaptive step sizes to find an (approximate) stationary point of the function

$$f(w) := \mathbb{E}[F(w, \xi)], \quad (1)$$

where $w \in \mathbb{R}^d$, $\xi \in \mathbb{R}^r$ is a random vector from a probability space (Ω, \mathcal{F}, P) , and $F(w, \xi)$ is assumed to be a stochastic Lipschitz continuous function in $w \in \mathbb{R}^d$, with the precise details given in Section 2. Unlike assuming that $F(w, \xi)$ is convex or that it has a Lipschitz continuous gradient, this assumption is much closer to reality as a wide range of neural network architectures are known to be at least locally Lipschitz continuous (Davis et al., 2020).

Section 6 examines the empirical performance of variants of SGD, focusing on image recognition tasks in floating and fixed-point environments. Given that the training was performed in low-bit settings with observed variation in accuracy over different runs, emphasis was placed on algorithms' robustness, with their evaluation based not only on their average, but also their minimum achieved accuracy.

Before these results, an overview of floating and fixed-point arithmetic using rounding to nearest and stochastic rounding is given in Section 3. In Section 4, relevant past work studying optimization with computational error is discussed, with the paper concluding in Section 7. The appendices contain all of the proofs of the theoretical results, as well as the detailed results and plots from the numerical experiments.

2 Lipschitz Continuous Loss Functions

This section contains the required assumptions and resulting properties for functions $f(w)$ of form (1). It is assumed that $F(w, \xi)$ is continuous in w for each $\xi \in \mathbb{R}^r$, and Borel measurable in ξ for each $w \in \mathbb{R}^d$. For almost all $\xi \in \mathbb{R}^r$,

$$|F(w, \xi) - F(w', \xi)| \leq L_0(\xi) \|w - w'\|_2,$$

for all $w, w' \in \mathbb{R}^d$, where $L_0(\xi)$ is a real-valued measurable function which is square integrable, $Q := \mathbb{E}[L_0(\xi)^2] < \infty$. It follows that $f(w)$ is $L_0 := \mathbb{E}[L_0(\xi)]$ -Lipschitz continuous (Metel, 2023, Proposition 2). As is common for loss functions used in machine learning applications, we assume that $f(w) \geq 0$ for all $w \in \mathbb{R}^d$ without serious loss of generality: If $\inf_{w \in \mathbb{R}^d} f(w) \geq -b > -\infty$ for some $b > 0$, $f(w)$ can be redefined as $f(w) := \mathbb{E}[F(w, \xi)] + b$.

Let $m(S)$ denote the Lebesgue measure of any measurable set S . Let $B_\epsilon^p(w) := \{x \in \mathbb{R}^d : \|x - w\|_p < \epsilon\}$ and $\overline{B}_\epsilon^p(w) := \{x \in \mathbb{R}^d : \|x - w\|_p \leq \epsilon\}$, for $\epsilon \geq 0$ and $p \geq 1$, and for simplicity let $B_\epsilon^p := B_\epsilon^p(0)$ and $\overline{B}_\epsilon^p := \overline{B}_\epsilon^p(0)$.

The Clarke ϵ -subdifferential (Goldstein, 1977) has been defined using the Euclidean norm for a function $g(w)$ as

$$\partial_\epsilon g(w) := \text{co}\{\partial g(x) : x \in \overline{B}_\epsilon^2(w)\},$$

where co denotes the convex hull, and $\partial g(x)$ denotes the Clarke subdifferential, which for a locally Lipschitz continuous function $g(w)$ is equal to

$$\partial g(w) = \text{co}\{v : \exists x^k \rightarrow w, x^k \in D, \nabla g(x^k) \rightarrow v\},$$

where D is the domain of $\nabla g(w)$. The Clarke ϵ -subdifferential is a commonly used relaxation of the Clarke subdifferential for use in the development and analysis of algorithms for the minimization of non-smooth non-convex Lipschitz continuous loss functions. In particular, for any $\epsilon_1, \epsilon_2 > 0$, algorithms have been developed with non-asymptotic convergence guarantees in expectation and with high probability for the approximate stationary point $\text{dist}(0, \partial_{\epsilon_1} f(w)) \leq \epsilon_2$, see for example (Davis et al., 2022; Metel, 2023; Tian et al., 2022; Zhang et al., 2020d). At times it is more convenient to consider different norms, so we define a generalization for $p \geq 1$ as

$$\partial_\epsilon^p g(w) := \text{co}\{\partial g(x) : x \in \overline{B}_\epsilon^p(w)\},$$

and we will also consider a smaller subdifferential, removing the convex hull:

$$\hat{\partial}_\epsilon^p g(w) := \{\partial g(x) : x \in \overline{B}_\epsilon^p(w)\}.$$

Proposition 1. *Let $g(w)$ be a locally Lipschitz continuous function for $w \in \mathbb{R}^d$. For $\epsilon \geq 0$ and $p \geq 1$, $\partial_\epsilon^p g(w)$ and $\hat{\partial}_\epsilon^p g(w)$ are compact and outer semicontinuous for $w \in \mathbb{R}^d$.*

Let $\{\alpha_k\}$ be a sequence such that $\alpha_k > 0$ for all $k \in \mathbb{N}$ with $\lim_{k \rightarrow \infty} \alpha_k = 0$. The next proposition proves the continuous convergence (Rockafellar and Wets, 2009, Definition 5.41) of the sequences of set-valued mappings $\{\partial_{\alpha_k}^p g\}$ and $\{\hat{\partial}_{\alpha_k}^p g\}$ to the Clarke subdifferential of $g(w)$.

Proposition 2. *Let $g(w)$ be a locally Lipschitz continuous function for $w \in \mathbb{R}^d$. The sequences of mappings $\{\partial_{\alpha_k}^p g\}$ and $\{\hat{\partial}_{\alpha_k}^p g\}$ converge continuously to $\partial g(w)$ for all $w \in \mathbb{R}^d$.*

It is not assumed that $f(w)$ nor $F(w, \xi)$ are differentiable. We instead define $\tilde{\nabla} F(w, \xi)$ to be a Borel measurable function which equals the gradient of $F(w, \xi)$ almost everywhere it exists. This can be computed using back propagation for a wide range of neural network architectures made up of elementary (measurable) functions, see (Bolte and Pauwels, 2020, Proposition 3 & Theorem 2) for more details.

In the convergence analysis in Section 5, iterate perturbation is used with samples of a random variable $u : \Omega \rightarrow \mathbb{R}^d$ which is uniformly distributed over $\overline{B}_{\frac{\alpha}{2}}^\infty(w)$ for an $\alpha > 0$, denoted as $u \sim U(\overline{B}_{\frac{\alpha}{2}}^\infty)$. Let $f_\alpha(w) := \mathbb{E}[f(w + u)]$ for $u \sim U(\overline{B}_{\frac{\alpha}{2}}^\infty)$ be the expected value of the perturbed loss function (1). We will now list some useful properties.

Proposition 3. (Metel, 2023, Propositions 3 & 6) & (Metel and Takeda, 2022, Lemma 4.2)

1. For any $w \in \mathbb{R}^d$ and $\alpha > 0$, with $u \sim U(\overline{B}_{\frac{\alpha}{2}}^\infty)$, $\mathbb{E}[\tilde{\nabla} F(w + u, \xi)] = \nabla f_\alpha(w)$ and
2. the gradient of $f_\alpha(w)$ is $L_1^\alpha := 2\alpha^{-1}\sqrt{d}L_0$ -Lipschitz continuous.
3. For almost all $(w, \xi) \in \mathbb{R}^{d+p}$, $\|\tilde{\nabla} F(w, \xi)\|_2 \leq L_0(\xi)$.

We will also need the following proposition, connecting the gradient of $f_\alpha(w)$ with the L_∞ -norm Clarke $\frac{\alpha}{2}$ -subdifferential of $f(w)$.

Proposition 4. *For all $w \in \mathbb{R}^d$ and $\alpha > 0$, it holds that $\nabla f_\alpha(w) \in \partial_{\frac{\alpha}{2}}^\infty f(w)$.*

3 Finite Precision Environments

This section sets the notation for floating and fixed-point arithmetic environments and gives some preliminary results. We will use the notation $\mathbb{F} \subset \mathbb{R}$ to denote a general finite precision environment when further specification is not required. The notation $\mathbb{L} \subset \mathbb{R}$ and $\mathbb{I} \subset \mathbb{R}$ will denote a floating and fixed-point environment, respectively. For $m, n \in \mathbb{Z}_{\geq 0}$, with $m \leq n$, let $[n]_m := [m, \dots, n]$, and in particular $[n] := [n]_1$.

Following the notation of (Higham, 2002, Chapter 2), a number $y \in \mathbb{L}$ can be represented as

$$y = \pm \beta^e \times .d_1 d_2 \dots d_t, \quad (2)$$

where \pm is chosen using a sign bit (0 for positive, 1 for negative), $\beta \in \mathbb{Z}_{>1}$ is the base, $t \in \mathbb{Z}_{>0}$ is the number of precision digits, the exponent $e \in [e_{\min}, e_{\max}] \subset \mathbb{Z}$ for $e_{\min} \leq e_{\max} \in \mathbb{Z}$, $d_i \in \mathbb{Z}_{\geq 0}$, and $d_i < \beta$ for $i \in [t]$. To enforce a unique representation, the normalized floating-point numbers \mathbb{L}_N have $d_1 \neq 0$, with $\lambda_N := \beta^{e_{\min}-1}$ being the smallest positive representable number in \mathbb{L}_N .

Following (Gupta et al., 2015), all $y \in \mathbb{I}$ are represented in the form of

$$[e_r e_{r-1} (\dots) e_1 . d_1 d_2 (\dots) d_t], \quad (3)$$

written in radix complement (Weik, 2001, Page 1408), using $r \in \mathbb{Z}_{\geq 0}$ digits to represent the integer part and $t \in \mathbb{Z}_{\geq 0}$ digits to represent the fractional part of y , with $r+t > 0$, $0 \leq e_i < \beta$ for all $i \in [r]$, and $0 \leq d_i < \beta$ for all $i \in [t]$, for a base $\beta \in \mathbb{Z}_{>1}$.

For any \mathbb{F} , let Λ^- , λ , and Λ^+ denote the smallest, the smallest positive, and the largest representable numbers, respectively. Their explicit values as well as further background on finite precision environments can be found in Appendix B. The next proposition verifies that the set of elements representable in floating and fixed-point environments are countable.

Proposition 5. *Let $\widehat{\mathbb{F}} := \{y \in \mathbb{L}_{t, e_{\min}}^{\beta, e_{\max}} : \beta \in \mathbb{Z}_{>1}, t \in \mathbb{Z}_{>0}, \mathbb{Z} \ni e_{\min} \leq e_{\max} \in \mathbb{Z}\} \cup \{y \in \mathbb{I}_{r, t}^\beta : \beta \in \mathbb{Z}_{>1}, r \in \mathbb{Z}_{\geq 0}, t \in \mathbb{Z}_{\geq 0}, r+t \in \mathbb{Z}_{>0}\}$ be the set of all elements representable by finite precision environments of the form (2) and (3), where $\mathbb{L}_{t, e_{\min}}^{\beta, e_{\max}}$ denotes an \mathbb{L} in base β with t precision digits and an exponent range of $[e_{\min}, e_{\max}]$, and $\mathbb{I}_{r, t}^\beta$ denotes an \mathbb{I} in base β with r integer digits and t fractional digits. It holds that $\widehat{\mathbb{F}} = \mathbb{Q}$.*

The range of an \mathbb{F} is defined as $\mathcal{R}_{\mathbb{F}} := \{x \in \mathbb{R} : \Lambda^- \leq x \leq \Lambda^+\}$, whereas the exponent range as used in Proposition 5 can be taken simply as $\{x \in \mathbb{Z} : e_{\min} \leq x \leq e_{\max}\}$. We will consider two forms of rounding: rounding to nearest and stochastic rounding. Given an $x \in \mathcal{R}_{\mathbb{F}}$, let $[x]_{\mathbb{F}} := \max\{y \in \mathbb{F} : y \leq x\}$ and $\lceil x \rceil_{\mathbb{F}} := \min\{y \in \mathbb{F} : y \geq x\}$, and let $R(x) \in \mathbb{F}$ denote

a function which performs one of the two rounding methods. For rounding to nearest an $x \in \mathcal{R}_{\mathbb{F}}$,

$$R(x) \in \operatorname{argmin}_{y \in \{\lfloor x \rfloor_{\mathbb{F}}, \lceil x \rceil_{\mathbb{F}}\}} |y - x|.$$

When $\lceil x \rceil_{\mathbb{F}} - x = x - \lfloor x \rfloor_{\mathbb{F}}$, this work does not depend on the use of a specific tie-breaking rule, but for simplicity we assume that it is deterministic, such as rounding to even or away (IEEE Computer Society, 2019, Section 4.3.1). We note that for odd bases there is no need for tie-breaking rules when rounding to nearest a $y \in \mathbb{F}$ to an environment of the same type (\mathbb{L} or \mathbb{I}) with the same β , see Proposition 29 in Appendix B.

For stochastic rounding an $x \in \mathcal{R}_{\mathbb{F}}$,

$$R(x) := \begin{cases} \lceil x \rceil_{\mathbb{F}} & \text{with probability } p = \frac{x - \lfloor x \rfloor_{\mathbb{F}}}{\lceil x \rceil_{\mathbb{F}} - \lfloor x \rfloor_{\mathbb{F}}} \\ \lfloor x \rfloor_{\mathbb{F}} & \text{with probability } 1 - p. \end{cases}$$

Considering the error $\delta := R(x) - x$, it is well known that $\mathbb{E}[\delta] = 0$, e.g. (Connolly et al., 2021, Lemma 5.1). We will also need a bound on the variance.

Proposition 6. *It holds that*

$$\mathbb{E}[\delta] = 0 \text{ and } \operatorname{Var}(\delta) = \mathbb{E}[\delta^2] \leq \frac{\beta^{2(e-t)}}{4},$$

where e is the exponent of the representation of $\lfloor |x| \rfloor_{\mathbb{F}}$ or $e = 0$, when $\mathbb{F} = \mathbb{L}$ or \mathbb{I} , respectively.

When $x \notin \mathcal{R}_{\mathbb{F}}$, for rounding to nearest and stochastic rounding, we assume that $R(x) = \operatorname{argmin}_{y \in \{\Lambda^-, \Lambda^+\}} |y - x|$, which is similar to how overflows are handled when using rounding towards zero (IEEE Computer Society, 2019, Section 7.4).

For stochastic rounding in the next proposition, we consider sampling from $U([0, 1])$ to generate the random output to determine whether to round up or down, with further details given in the proof.

Proposition 7. *Rounding to nearest and stochastic rounding are Borel measurable functions.*

As is standard (IEEE Computer Society, 2019, Section 5.4), we make the following assumption.

Assumption 8. *The basic operations $\operatorname{op} \in \{+, -, \times, \div\}$ and $\sqrt{\cdot}$ performed on any $y, z \in \mathbb{R}$ ($z \in \mathbb{R}_{\geq 0}$) resulting in $x = y \operatorname{op} z$ ($x = \sqrt{z}$) is rounded to $R(x)$ as if x was first computed exactly in \mathbb{R} .*

4 Past Work on Optimization with Computational Error

Research on optimization in environments with error is vast when considering stochastic optimization as a subset. The minimization of a stochastic function with further computational

error seems to be a topic much less explored. We highlight a few papers which were found to be most relevant to the current research.

An influential paper for this work was (Bertsekas and Tsitsiklis, 2000), where the convergence of a gradient method of the form $w^{k+1} = w^k + \eta^k(s^k + e^k)$ is studied, where η^k is a step size, s^k is a direction of descent, e^k is a deterministic or stochastic error, and it is assumed that $f(w)$ has a Lipschitz continuous gradient. It was proven that $f(w^k)$ converges, and if the limit is finite, then $\nabla f(w^k) \rightarrow 0$, without any type of boundedness assumptions.

In (Solodov and Zavriev, 1998), a parallel projected incremental algorithm onto a convex compact set is proposed for solving finite-sum problems. It is assumed that there is non-vanishing bounded error when computing subgradients $g_i(w) \in \partial f_i(w)$ of each subfunction, with a convergence result to an approximate stationary point with an error level relative to the error in computing the subgradients. Each subfunction $f_i(w)$ is assumed to be Lipschitz continuous but regular, i.e. its one-sided directional derivative exists and for all $v \in \mathbb{R}^d$ $f'_i(w; v) = \max_{g \in \partial f_i(w)} \langle g, v \rangle$ (Clarke, 1990, Section 2.3), which precludes functions with downward cusps such as $(1 - \text{ReLU}(x))^2$ (Davis et al., 2020, Section 1).

Recent work studying the convergence of gradient descent for convex loss functions with a Lipschitz continuous gradient in a low-precision floating-point environment is presented in (Xia et al., 2022). Besides proposing biased stochastic rounding schemes which prevent small gradients from being rounded to zero, inequalities are provided involving the step size, the unit roundoff, and the norms of the gradient and iterates which guarantee either a convergence rate to the optimal solution, or at least the (expected) monotonicity of the loss function values.

We also mention the paper (Yang et al., 2019), which studies the algorithm $w^{k+1} = R(w^k - \eta^k \nabla \tilde{f}(w^k))$, where $\nabla \tilde{f}(w)$ is a stochastic gradient and $R(\cdot)$ performs stochastic rounding into an \mathbb{L} . It is assumed that the loss function $f(w)$ is strongly convex, with Lipschitz continuous gradient and Hessian, with $\nabla \tilde{f}(w^k)$ being uniformly bounded from $\nabla f(w^k)$ for all $k \geq 1$. Convergence to a neighbourhood of the optimal solution is proven which depends on the precision of \mathbb{L} , with an improved dependence proven when considering an exponential moving average of iterates computed in full-precision.

5 Perturbed SGD with Computational Errors

We will first describe the PSGD algorithm over the real numbers in order to more easily describe the modelling of PSGD with computational error. Given an initial iterate $w^1 \in \mathbb{R}^d$, we consider a perturbed mini-batch SGD algorithm of the form

$$w^{k+1} = w^k - \frac{\eta_k}{M} \sum_{i=1}^M \tilde{\nabla} F(w^k + u^k, \xi^{k,i}), \quad (4)$$

where $\eta_k \geq 0$ is the step size, $M \in \mathbb{Z}_{>0}$ is the mini-batch size, $u^k \sim U(\overline{B}_{\frac{\alpha_k}{2}}^\infty)$ is a sample from a uniform distribution with parameter $\alpha_k > 0$, and $\{\xi^{k,i}\}$ are M samples of ξ . The following

proposition follows directly from Proposition 3, and serves as the basis for the assumptions of PSGD with computational error.

Proposition 9. For all $w \in \mathbb{R}^d$ and $\alpha > 0$, with $u \sim U(\overline{B}_{\frac{\alpha}{2}}^\infty)$,

$$\langle \mathbb{E}[\tilde{\nabla}F(w + u, \xi)], \nabla f_\alpha(w) \rangle \geq \|\nabla f_\alpha(w)\|_2^2, \quad (5)$$

and

$$\mathbb{E}[\|\tilde{\nabla}F(w + u, \xi)\|_2^2] \leq Q. \quad (6)$$

The proposed model of PSGD with computational error takes the form

$$w^{k+1} = w^k - \frac{\eta_k}{M} \sum_{i=1}^M \widehat{\nabla}F(w^k + \hat{u}^k, \xi^{k,i}, b^{k,i}) + e^k, \quad (7)$$

which addresses three types of error in finite-precision environments from attempting to

1. compute the approximate stochastic gradient $\tilde{\nabla}F(w, \xi)$,
2. sample from the continuous distribution $U(\overline{B}_{\frac{\alpha}{2}}^\infty)$ for $\alpha > 0$, and
3. perform the basic arithmetic operations in (4) given w^k , η_k , M , and $\{\tilde{\nabla}F(w^k + u^k, \xi^{k,i})\}$.

A fourth error will be discussed after the full assumptions of η_k are given. To address error 1, $\tilde{\nabla}F(w, \xi)$ is replaced by an approximation $\widehat{\nabla}F(w, \xi, b)$ which is subject to errors which are a function of $(w, \xi, b) \in \mathbb{R}^{d+p+s}$. The inclusion of the random vector $b \in \mathbb{R}^s$ is to model the use of (approximate) stochastic rounding. The size $s \in \mathbb{N}$ of b would then equal the number of basic arithmetic operations required to approximately compute $\tilde{\nabla}F(w, \xi)$, see (Croci et al., 2022, Section 7) for an overview of the implementation of stochastic rounding in practice. It is assumed that for all $k \geq 1$ and $j \in [s]$, b_j^k is a discrete uniformly distributed random variable over a finite set $V_j^k \subset \mathbb{R}$, i.e. $\mathbb{P}(b_j^k \in V_j^k) = 1$, and in (7), the set $\{b^{k,i}\} \subset \mathbb{R}^s$ are M samples of $b^k \in \mathbb{R}^s$.

For error 2, $u^k \sim U(\overline{B}_{\frac{\alpha_k}{2}}^\infty)$ is replaced by a sample $\hat{u}^k \in \mathbb{R}^d$ from a probability distribution \widehat{P}^k . The choice of the distributions $\{\widehat{P}^k\}$ is discussed in Section 5.2, including an analysis of using a discrete approximation of $\{U(\overline{B}_{\frac{\alpha_k}{2}}^\infty)\}$.

We will now describe the probabilistic assumptions for the analysis of (7), after which we can continue describing our modelling assumptions, including the sequence of random vectors $\{e^k\} \subset \mathbb{R}^d$, which is used to address error 3. The sampling of \hat{u}^k , $\{\xi^{k,i}\}$, and $\{b^{k,i}\}$ is assumed to be done independently. We consider a filtration $\{\mathcal{F}_k\}$ on the probability space (Ω, \mathcal{F}, P) , where $\mathcal{F}_k := \sigma(\hat{u}^j, \{\xi^{j,i}\}, \{b^{j,i}\}, e^j : j \in [k])$ and a sequence of σ -algebras $\{\mathcal{G}_k\}$, where $\mathcal{G}_k := \sigma(\hat{u}^k, \{\xi^{k,i}\}, \{b^{k,i}\})$. We note that w^k is \mathcal{F}_{k-1} -measurable, setting $\mathcal{F}_0 := \{\emptyset, \Omega\}$ and assuming that $w^1 \in \mathbb{R}^d$ is given. We assume that the sequences $\{\alpha_k\}$, $\{V_j^k\}$, and $\{P^k\}$ are deterministic.

Given the assumed error in computing (4) we consider adaptive step sizes, motivated by methods such as gradient normalization and clipping, in an attempt to stabilize the algorithm steps (7) and improve performance in practice. We assume that for all $k \geq 1$,

$\eta_k = \hat{\eta}_k \psi_k$, where $\hat{\eta}_k > 0$ is deterministic and $\psi_k \geq 0$ is $\sigma(\mathcal{F}_{k-1}, \mathcal{G}_k)$ -measurable. More detailed assumptions concerning $\{\psi_k\}_{k=1}^\infty$ are given in Assumption 11 after the following definition.

Definition 10. (Rambaud, 2011, Proposition 1) *A sequence of random variables $\{x_k\}_{k=1}^\infty \subset \mathbb{R}$ converges almost surely uniformly to a random variable $x \in \mathbb{R}$ if for all $\phi > 0$, there exists a $K_\phi \geq 1$ such that $|x_k - x| \leq \phi$ almost surely for all $k \geq K_\phi$.*

Assumption 11. *We assume that*

1. $\{\psi_k\}_{k=1}^\infty$ are essentially bounded by \mathcal{F}_{k-1} -measurable random variables $0 \leq \Psi_k^L \leq \Psi_k^U < \infty$, $\mathbb{P}(\Psi_k^L \leq \psi_k \leq \Psi_k^U) = 1$ for all $k \geq 1$,
2. $\{\Psi_k^U\}_{k=1}^\infty$ are essentially uniformly bounded by constants $0 < \underline{\Psi}^U \leq \overline{\Psi}^U < \infty$, $\mathbb{P}(\underline{\Psi}^U \leq \Psi_k^U \leq \overline{\Psi}^U) = 1$ for all $k \geq 1$, and
3. $\{\Delta_k\}_{k=1}^\infty$, where $\Delta_k := \Psi_k^U - \Psi_k^L$, almost surely uniformly converges to 0.

Assumption 11.3 is restrictive, requiring the length of the range of ψ_k , Δ_k , to decrease with $\lim_{k \rightarrow \infty} \psi_k = \lim_{k \rightarrow \infty} \Psi_k^U$ almost surely. Our analysis allows adaptive step sizes, but in the limit the adaptiveness can only be with respect to \mathcal{F}_{k-1} -measurable quantities. Assumption 11.3 stems from the difficulty in analyzing $\mathbb{E}[\psi_k \widehat{\nabla} F(w^k + \hat{u}^k, \xi^{k,i}, b^{k,i}) | \mathcal{F}_{k-1}]$, given that ψ_k can change the expected step direction. A number of recent papers have presented convergence analysis for gradient clipping algorithms for non-convex stochastic optimization. We show under what conditions their required step sizes follow Assumption 11 in Section 5.1.

The fourth error in computing (4) is from the rounding error in computing η_k . Given our intended step size $\eta'_k \in \mathbb{R}_{\geq \lambda}$ for $\hat{\eta}_k$, we can set $\hat{\eta}_k = R(\eta'_k)$. In the following proposition we give as an example of how the rounding error of $\hat{\eta}_k$ can be bounded.

Proposition 12. *Assume that $\mathbb{F} = \mathbb{L}$, $t > 1$, and that $\eta'_k \in [\lambda_N, \Lambda^+]$ (the range of \mathbb{L}_N). The rounded step size $R(\eta'_k) \in [\frac{1}{2}\eta'_k, \frac{3}{2}\eta'_k]$, whether rounding to nearest or stochastic rounding is used.*

If rounding to nearest is used, $\{\hat{\eta}_k\}_{k=1}^\infty$ remains a deterministic positive sequence by the monotonicity of rounding to nearest (Higham, 2002, Page 38). Given a $\sigma(\mathcal{F}_{k-1}, \mathcal{G}_k)$ -measurable random variable $\psi'_k \in \mathbb{R}_{\geq 0}$, we can clip it using \mathcal{F}_{k-1} -measurable random variables $\mathbb{R}_{\geq 0} \ni \widehat{\Psi}_k^L \leq \widehat{\Psi}_k^U \in \mathbb{R}_{\geq \lambda}$ by considering $\psi''_k := \max(\widehat{\Psi}_k^L, \min(\psi'_k, \widehat{\Psi}_k^U))$. If again rounding to nearest is used, $\psi_k = R(\psi''_k)$ is a $\sigma(\mathcal{F}_{k-1}, \mathcal{G}_k)$ -measurable random variable with $\psi_k \in [\Psi_k^L, \Psi_k^U]$, where $\Psi_k^L := R(\widehat{\Psi}_k^L)$ and $\Psi_k^U := R(\widehat{\Psi}_k^U)$, and $\underline{\Psi}^U = \lambda$ and $\overline{\Psi}^U = \Lambda^+$ are valid bounds for Ψ_k^U . In order to satisfy Assumption 11.3, for all $k \geq K'$ for any $K' \in \mathbb{N}$, we can set $\widehat{\Psi}_k^L = \widehat{\Psi}_k^U$.

The vector $e^k \in \mathbb{R}^d$ in (7) is random with $\mathbb{E}[e^k | \mathcal{F}_{k-1}, \mathcal{G}_k] = 0$, which models the error from computing the addition, subtraction, multiplication, and division with finite precision in (7) given w^k , η_k , M , and $\{\widehat{\nabla} F(w^k + \hat{u}^k, \xi^{k,i}, b^{k,i})\}$. The zero-mean assumption can be justified if stochastic rounding is used, see Proposition 18.

The requirements of the approximations $\widehat{\nabla} F(w, \xi, b)$ and $\hat{u}^k \sim \widehat{P}^k$ are contained in the following assumption, which can be seen as a relaxation of Proposition 9. These assumptions

are of a general form, and are not dependent on specifics such as the number of basic arithmetic operations or the rounding method, allowing the convergence analysis to be applicable for a potentially wide range of computational error.

Assumption 13. *There exists constants $c_1 > 0, c_2 > 0$, and a $K_1 \in \mathbb{N}$ such that for all $k \geq K_1$,*

$$\langle \mathbb{E}[\widehat{\nabla}F(w^k + \hat{u}, \xi, b) | \mathcal{F}_{k-1}], \nabla f_{\alpha_k}(w^k) \rangle \geq c_1 \|\nabla f_{\alpha_k}(w^k)\|_2^2 \quad (8)$$

and

$$\mathbb{E}[\|\widehat{\nabla}F(w^k + \hat{u}, \xi, b)\|_2^2 | \mathcal{F}_{k-1}] \leq c_2 Q \quad (9)$$

almost surely, where $\hat{u} \sim \widehat{P}^k$, $f_{\alpha_k}(w) := \mathbb{E}[f(w + u)]$ for $u \sim U(\overline{B}_{\frac{\alpha_k}{2}}^\infty)$, and recalling that $Q = \mathbb{E}[L_0(\xi)^2]$.

In our non-asymptotic convergence analysis, we will assume that $\lim_{k \rightarrow \infty} \alpha_k = 0$, so for any $\bar{\alpha} > 0$, $K_1 \in \mathbb{N}$ can be chosen such that (8) and (9) are only required to hold almost surely for $\alpha_k \leq \bar{\alpha}$. Inequalities (8) and (9) are variants of classic error assumptions, see (Levitin and Polyak, 1966, Equations (4.3) & (4.4)) and (Bertsekas and Tsitsiklis, 2000, Equation (1.5)), tailored to our problem setting. Inequality (8) states that in expectation, $-\widehat{\nabla}F(w^k + \hat{u}, \xi, b)$ must be a direction of descent for f_{α_k} at w^k almost surely when $k \in \mathbb{N}$ is sufficiently large. When $\widehat{\nabla}F(w, \xi, b) = \widetilde{\nabla}F(w, \xi)$ and $\hat{u} \sim U(\overline{B}_{\frac{\alpha_k}{2}}^\infty)$, Assumption 13 is satisfied with $c_1 = c_2 = 1$ from inequalities (5) and (6). Given that any $0 < c_1 < 1$ and $1 < c_2 < \infty$ are valid, Assumption 13 allows $\widehat{\nabla}F(w + \hat{u}, \xi, b)$ to be an approximation of $\widetilde{\nabla}F(w + u, \xi)$ with nontrivial error, which is only enforced in expectation.

We assume that $\widehat{\nabla}F(w, \xi, b)$ is a Borel measurable function in $(w, \xi, b) \in \mathbb{R}^{d+p+s}$. The following proposition considers the case where $\widehat{\nabla}F(w, \xi, b)$ approximates $\widetilde{\nabla}F(w, \xi)$ at a countable number of points, such as in a finite precision environment for all $(w, \xi) \in \mathbb{F}^{d+p}$.

Proposition 14. *Assume that $\widehat{\nabla}F(w, \xi, b)$ approximates $\widetilde{\nabla}F(w, \xi)$ at a countable set of points $\{w^i, \xi^i\}_{i=1}^\infty \subset \mathbb{R}^{d+p}$. It can be extended into a Borel measurable function in $(w, \xi, b) \in \mathbb{R}^{d+p+s}$ equal to $\widetilde{\nabla}F(w, \xi)$ for almost all $(w, \xi) \in \mathbb{R}^{d+p}$.*

Even when $\hat{u} \sim U(\overline{B}_{\frac{\alpha}{2}}^\infty)$ and stochastic rounding is used when approximately computing $\widetilde{\nabla}F(w + u, \xi)$, it cannot be assumed in general that $c_1 = 1$, which is highlighted in the next proposition for batch normalization (Ioffe and Szegedy, 2015), which is used in the Resnet models of our experiments in Section 6.

Proposition 15. *The expected rounding error from computing batch normalization and its gradient using stochastic rounding is in general non-zero.*

For simplicity let $\widehat{\nabla}F^{k,i}(w^k) := \widehat{\nabla}F(w^k + \hat{u}^k, \xi^{k,i}, b^{k,i})$ for $i \in [M]$, and $\widehat{\nabla}\overline{F}^k(w^k) := \frac{1}{M} \sum_{i=1}^M \widehat{\nabla}F^{k,i}(w^k)$. We will require the following bound.

Proposition 16. *For all $k \geq K_1$, almost surely*

$$\mathbb{E}[\|\widehat{\nabla}\overline{F}^k(w^k)\|_2^2 | \mathcal{F}_{k-1}] \leq c_2 Q.$$

Our convergence analysis requires a bound on $\mathbb{E}[\|e^k\|_2^2|\mathcal{F}_{k-1}]$ given in the following assumption. We show that this holds, as well as that $\mathbb{E}[e^k|\mathcal{F}_{k-1}, \mathcal{G}_k] = 0$ in the next proposition assuming that the computation is done in an \mathbb{I} with stochastic rounding and with no overflow occurring.

Assumption 17. *There exists a constant $c_3 > 0$ and a $K_2 \in \mathbb{N}$ such that for all $k \geq K_2$, almost surely*

$$\mathbb{E}[\|e^k\|_2^2|\mathcal{F}_{k-1}] \leq c_3 \hat{\eta}_k^2.$$

Proposition 18. *Assume that*

$$w^k \ominus (\eta_k \otimes M) \otimes (\hat{\nabla} F^{k,1}(w^k) \oplus \dots \oplus \hat{\nabla} F^{k,M}(w^k)) = w^k - \frac{\eta_k}{M} \sum_{i=1}^M \hat{\nabla} F^{k,i}(w^k) + e^k, \quad (10)$$

where the “o” symbols represent the corresponding operation in a fixed-point environment $\mathbb{I}_{r,t}^\beta \subset \mathbb{R}$ in base $\beta \in \mathbb{Z}_{>1}$, with $t \in \mathbb{Z}_{\geq 0}$ fractional and $r \in \mathbb{Z}_{\geq 0}$ integer digits with $r + t > 0$, using stochastic rounding. Assume that $w^k, \hat{\nabla} F^{k,i}(w^k) \in (\mathbb{I}_{r,t}^\beta)^d$ for $i \in [M]$, and that $\eta_k, M \in \mathbb{I}_{r,t}^\beta$. If $r \geq 0$ can be chosen to ensure that no overflow will occur in the computation of the left-hand side of (10), it holds that

$$\mathbb{E}[e^k|\mathcal{F}_{k-1}, \mathcal{G}_k] = 0,$$

and for $c_3 = \frac{M}{4}(Mc_2Q + 1)(\bar{\Psi}^U)^2$, almost surely

$$\mathbb{E}[\|e^k\|_2^2|\mathcal{F}_{k-1}] \leq c_3 \hat{\eta}_k^2.$$

Our asymptotic convergence result requires the following bound on Δ_k , which will also be used in our non-asymptotic convergence analysis.

Assumption 19. *There exists a constant $c_4 > 0$ and a $K_3 \in \mathbb{N}$ such that for all $k \geq K_3$, almost surely*

$$\Delta_k \leq c_4 \frac{\hat{\eta}_k}{\alpha_k}.$$

We now present our non-asymptotic convergence result to a Clarke stationary point.

Theorem 20. *Assume that Perturbed SGD (7) is run using step sizes $\eta_k = \hat{\eta}_k \psi_k \geq 0$ such that Assumption 11 holds, Assumption 13 holds for a non-increasing sequence $\{\alpha_k\}$, with $\{\alpha_k\}$ and $\{\hat{\eta}_k\}$ chosen such that*

$$\sum_{k=1}^{\infty} \alpha_k^d \hat{\eta}_k = \infty, \quad \sum_{k=1}^{\infty} \alpha_k^{d-1} \hat{\eta}_k^2 < \infty,$$

and $\lim_{k \rightarrow \infty} \alpha_k = 0$. Assume further that Assumptions 17 and 19 hold. Almost surely, there exists a subsequence of indices $\{k_i\}$ such that

$$\lim_{i \rightarrow \infty} \|\nabla f_{\alpha_{k_i}}(w^{k_i})\|_2 = 0$$

and for every accumulation point w^* of $\{w^{k_i}\}$,

$$\text{dist}(0, \partial f(w^*)) = 0.$$

The next proposition gives a family of sequences $\{\alpha_k\}$ and $\{\hat{\eta}_k\}$ which satisfy the conditions of Theorem 20 and Assumption 11.3 given Assumption 19.

Proposition 21. *For $0.5 < q < 1$, $p = \frac{(1-q)}{d}$, and constants $0 < c \leq c' < \infty$, setting $\alpha_k = \frac{1}{k^p}$ and $\hat{\eta}_k \in [\frac{c}{k^q}, \frac{c'}{k^q}]$ for $k \geq 1$ satisfies the conditions of Theorem 20, as well as Assumption 11.3 given the bound on Δ_k in Assumption 19.*

Assuming that $\lim_{k \rightarrow \infty} \alpha_k = 0$ has the appealing property of minimizing a sequence of approximating functions $\{f_{\alpha_k}\}_{k=1}^{\infty}$ which converge to the true function $f(w)$ (Metel, 2023, Proposition 5(2)). However, giving an asymptotic convergence result in Theorem 20 in a setting motivated by finite precision arithmetic may seem contradictory, in particular, how $\lim_{k \rightarrow \infty} \hat{\eta}_k = 0$ in Proposition 21. We could consider a sequence of environments $\{\mathbb{F}_{t_j}\}_{j=1}^{\infty}$ with increasing precision/fractional digits, $t_{j+1} > t_j$ for all $j \in \mathbb{N}$, then a schedule could be followed where we use \mathcal{F}_{t_1} for iterations $[1, \hat{K}_1]$, \mathcal{F}_{t_2} for iterations $[\hat{K}_1 + 1, \hat{K}_2]$, ..., for a predetermined sequence $\{\hat{K}_j\}_{j=1}^{\infty} \subset \mathbb{N}$, which could accommodate our decreasing step sizes. This idea of increasing the number of fractional digits through time was successfully used in (Gupta et al., 2015, Figure 3) where neural network training in an \mathbb{I} was performed with $t = 12$ until stagnation occurred, after which the fractional digits were increased to $t = 16$, resulting in a rapid accuracy improvement. Another, perhaps more practical approach is to simply consider a fixed $\alpha_k = \alpha > 0$, allowing for a non-asymptotic convergence bound in expectation using a fixed $\hat{\eta}_k = \hat{\eta} > 0$, which we now show for the L_{∞} -norm Clarke $\frac{\alpha}{2}$ -subdifferential.

Theorem 22. *For a $K \in \mathbb{N}$, assume that Perturbed SGD (7) is run for $\hat{k} \sim U([K - 1]_0)$ iterations uniformly sampled over $[K - 1]_0$, using step sizes $\eta_k = \hat{\eta}\psi_k \geq 0$, where $\hat{\eta} = \frac{c_5}{\sqrt{K}}$ for a constant $c_5 > 0$, such that Assumption 11 holds. Assume that Assumption 13 holds for $\alpha_k = \alpha > 0$ and $K_1 = 1$, as well as Assumptions 17 and 19 for $K_2 = K_3 = 1$. Assume also that for a constant c_6 such that $0 < c_6 < c_1 \underline{\Psi}^U$, $K \geq \left(\frac{c_4 c_5}{2\alpha(c_1 \underline{\Psi}^U - c_6)}\right)^2$.*

Defining $\hat{w} := w^{\hat{k}+1}$, it holds that

$$\mathbb{E}[\text{dist}(0, \partial_{\frac{\alpha}{2}}^{\infty} f(\hat{w}))^2] \leq \frac{f_{\alpha}(w^1)}{c_5 c_6 \sqrt{K}} + \frac{c_4 c_5 c_2 Q}{2\alpha c_6 \sqrt{K}} + \frac{\sqrt{d} L_0 c_5}{\alpha c_6 \sqrt{K}} ((\underline{\Psi}^U)^2 c_2 Q + c_3),$$

and to guarantee that

$$\mathbb{E}[\text{dist}(0, \partial_{\frac{\alpha}{2}}^{\infty} f(\hat{w}))] \leq \nu,$$

for any $\nu > 0$ requires $K = O(\alpha^{-2} \nu^{-4})$.

5.1 Comparison of Assumption 11 with previous work on gradient clipping

We will now compare Assumption 11 to the assumptions used in four recent papers which studied gradient clipping. All of these papers prove a non-asymptotic convergence result after running for $K \in \mathbb{N}$ iterations. As K is increased, we will show under what conditions these algorithms stop clipping the gradient almost surely, switching to SGD, or must do so in order to guarantee convergence.

There are slight variations of gradient clipping in the four papers, so we will first consider a general gradient clipping algorithm,

$$w^{k+1} = w^k - \hat{\eta} \min \left(h \left(\frac{1}{\|g(w^k)\|_2} \right), 1 \right) g(w^k), \quad (11)$$

where $g(w)$ is a stochastic gradient of a loss function $f(w)$, and $h(\cdot)$ is a non-negative function of potentially other omitted parameters. Taking $\psi_k = \min \left(h \left(\frac{1}{\|g(w^k)\|_2} \right), 1 \right)$, for $k \geq 1$, $\Psi_k^L = 0$ and $\Psi_k^U = \underline{\Psi}^U = \overline{\Psi}^U = 1$ are valid bounds for Assumption 11.

When the gradient is not clipped, i.e. $h \left(\frac{1}{\|g(w^k)\|_2} \right) \geq 1$, (11) takes the form of SGD with a fixed step size,

$$w^{k+1} = w^k - \hat{\eta} g(w^k).$$

If there exists a $K_5 \in \mathbb{N}$ such that gradient clipping does not occur almost surely for all $k \geq K_5$, then for all $k \geq K_5$, $\Psi_k^L = 1$ is valid, $\Delta_k = 0$, and Assumption 11 is satisfied. We will show how each paper's step sizes fit within Assumption 11 by giving the conditions for the existence of a $K_5 \in \mathbb{N}$ for which this holds.

For the first three papers this is shown to hold under the following bounded stochastic gradient assumption.

Assumption 23. *There exists a constant $G > 0$ such that $\|g(w^k)\|_2 \leq G$ almost surely for all $k \geq 1$.*

In the second and fourth papers, the following is assumed by the authors.

Assumption 24. *There exists a constant $\sigma > 0$ such that $\|g(w) - \nabla f(w)\|_2 \leq \sigma$ almost surely for all $w \in \mathbb{R}^d$.*

Given this assumption, a $K_5 \in \mathbb{N}$ exists with the additional assumption that their algorithms converge to within a neighbourhood of a stationary point, stated next as Assumption 25, where for the second paper (Zhang et al., 2020b) $G > 0$ can take any value, and for the fourth paper (Zhang et al., 2020a) it must hold that $G \leq 4\sigma$.

Assumption 25. *There exists a $G > 0$ and a $K_6 \in \mathbb{N}$ such that for all $k \geq K_6$, $\|\nabla f(w^k)\|_2 \leq G$ almost surely.*

We now examine the convergence results of each paper in detail.

5.1.1 (Zhang et al., 2020c)

In this paper, gradient clipping of the form

$$w^{k+1} = w^k - \hat{\eta} \min\left(\frac{\tau}{\|g(w^k)\|_2}, 1\right) g(w^k) \quad (12)$$

is considered. In their non-convex convergence result (Zhang et al., 2020c, Theorem 2), the parameter choices are¹

$$\begin{aligned} \hat{\eta} &= \min\left(\frac{1}{4L}, \frac{1}{L\tau^\alpha}, \frac{1}{24L\tau}\right), \text{ and} \\ \tau &= \max(2, 48^{1/(\alpha-1)}\sigma^{\alpha/(\alpha-1)}, 48\sigma, \sigma K^{1/(3\alpha-2)}), \end{aligned}$$

where L is the Lipschitz constant of $\nabla f(w)$, and it is assumed that for an $\alpha \in (1, 2]$, $\mathbb{E}[\|g(w) - \nabla f(w)\|_2^\alpha] \leq \sigma^\alpha$ for all $w \in \mathbb{R}^d$. Taking K sufficiently large,

$$\tau = \sigma K^{1/(3\alpha-2)} \quad \text{and} \quad \hat{\eta} = \frac{1}{L\sigma^\alpha K^{\alpha/(3\alpha-2)}}.$$

Taking $\psi_k = \min\left(\frac{\tau}{\|g(w^k)\|_2}, 1\right)$, and using Assumption 23, for K sufficiently large $\frac{\tau}{G} \geq 1$, and no gradient clipping will be performed for $k \geq 1$ almost surely.

5.1.2 (Zhang et al., 2020b)

In (Zhang et al., 2020b, Theorem 7), a variant of gradient clipping of the form

$$w^{k+1} = w^k - \hat{\eta} \min\left(\frac{1}{16\hat{\eta}^2 L_1 (\|g(w^k)\|_2 + \sigma)}, 1\right) g(w^k)$$

is considered, where it is assumed that for all $w \in \mathbb{R}^d$, $\|\nabla^2 f(w)\|_2 \leq L_0 + L_1 \|\nabla f(w)\|_2$ for constants $L_0, L_1 > 0$, and Assumption 24 is assumed. The step size $\hat{\eta}$ is chosen as

$$\hat{\eta} = \min\left(\frac{1}{20L_0}, \frac{1}{128L_1\sigma}, \frac{1}{\sqrt{K}}\right).$$

Taking $\psi_k = \min\left(\frac{1}{16\hat{\eta}^2 L_1 (\|g(w^k)\|_2 + \sigma)}, 1\right)$, for K sufficiently large, $\hat{\eta} = \frac{1}{\sqrt{K}}$ and

$$\psi_k = \min\left(\frac{K}{16L_1 (\|g(w^k)\|_2 + \sigma)}, 1\right). \quad (13)$$

If Assumption 23 holds, taking K sufficiently large, $\frac{K}{16L_1(G+\sigma)} \geq 1$, and no gradient clipping will be performed almost surely for all $k \geq 1$.

¹There seems to be a discrepancy between the theorem statement in the body of the text and the proof in the appendix for these parameter values. These are the parameter values used in the proof on page 14 in the appendix of their work.

If Assumption 23 does not hold, for all $w \in \mathbb{R}^d$, almost surely,

$$\begin{aligned}\sigma &\geq \|g(w) - \nabla f(w)\|_2 \\ &\geq \|g(w)\|_2 - \|\nabla f(w)\|_2 \\ \Rightarrow \|g(w)\|_2 &\leq \sigma + \|\nabla f(w)\|_2,\end{aligned}\tag{14}$$

using the reverse triangle inequality, hence

$$\frac{K}{16L_1(\|g(w^k)\|_2 + \sigma)} \geq \frac{K}{16L_1(\|\nabla f(w^k)\|_2 + 2\sigma)}$$

almost surely. For any $G > 0$, assume that $K \geq 16L_1(G + 2\sigma)$ and that K is sufficiently large such that (13) holds, and that there exists a $K_6 \leq K$ such that Assumption 25 holds for the chosen $G > 0$. It holds almost surely for $k \geq K_5 := K_6$ that

$$\begin{aligned}\psi_k &\geq \min\left(\frac{K}{16L_1(\|\nabla f(w^k)\|_2 + 2\sigma)}, 1\right) \\ &\geq \min\left(\frac{16L_1(G + 2\sigma)}{16L_1(G + 2\sigma)}, 1\right) \\ &\geq 1,\end{aligned}$$

and no gradient clipping will be performed almost surely.

5.1.3 (Koloskova et al., 2023)

This work studies the gradient clipping algorithm (12). Their work on stochastic non-convex problems (Koloskova et al., 2023, Theorem 3.3) gives a convergence bound of

$$\min_{k \in [0, K]} \mathbb{E} \|\nabla f(x_k)\|_2 \leq O\left(\min\left(\sigma, \frac{\sigma^2}{\tau}\right) + \sqrt{\hat{\eta}(L_0 + \tau L_1)}\sigma + \sqrt{\frac{F_0}{\hat{\eta}K} + \frac{F_0}{\hat{\eta}K\tau}}\right),\tag{15}$$

where it is assumed for all $w \in \mathbb{R}^d$ that $\mathbb{E}[\|g(w) - \nabla f(w)\|_2^2] \leq \sigma^2$ for a $\sigma > 0$ and $\|\nabla^2 f(w)\|_2 \leq L_0 + L_1\|\nabla f(w)\|_2$ for constants $L_0, L_1 > 0$, and that $F_0 := f(w^0) - \min_{w \in \mathbb{R}^d} f(w)$. In order for the right-hand side of (15) to converge to 0, we require τ to be increasing and $\hat{\eta}$ to be decreasing in K , for example, choosing $\tau = K^{\frac{1}{5}}$ and $\hat{\eta} = K^{-\frac{3}{5}}$,

$$\begin{aligned}&O\left(\min\left(\sigma, \frac{\sigma^2}{\tau}\right) + \sqrt{\hat{\eta}(L_0 + \tau L_1)}\sigma + \sqrt{\frac{F_0}{\hat{\eta}K} + \frac{F_0}{\hat{\eta}K\tau}}\right) \\ &= O\left(\min\left(\sigma, \sigma^2 K^{-\frac{1}{5}}\right) + \sqrt{K^{-\frac{3}{5}}L_0 + K^{-\frac{2}{5}}L_1}\sigma + \sqrt{F_0}K^{-\frac{1}{5}} + F_0 K^{-\frac{3}{5}}\right) \\ &= O(K^{-\frac{1}{5}}),\end{aligned}$$

ignoring all constants. If Assumption 23 holds, for K sufficiently large $\frac{\tau}{G} \geq 1$, and no gradient clipping will be performed almost surely for all $k \geq 1$.

5.1.4 (Zhang et al., 2020a)

This work studies a general clipping framework, which allows for mixing gradient clipping and momentum clipping. For simplicity, and to match our algorithm which does not use momentum, we will consider their algorithm with $\beta = 0$ in their notation, resulting in the form

$$w^{k+1} = w^k - \hat{\eta} \min\left(\frac{\tau}{\hat{\eta}(\|g(w^k)\|_2)}, 1\right) g(w^k).$$

In their stochastic convergence result, (Zhang et al., 2020a, Theorem 3.2), it is assumed that

$$\hat{\eta} = \frac{\tau}{5\sigma} \quad \text{and} \quad \tau \leq \frac{\epsilon}{2\sigma} \min\left(\frac{\epsilon}{1.01L_0}, \frac{1}{1.01L_0}, \frac{1}{25.25L_1}\right),$$

where, like in (Zhang et al., 2020b), it is assumed that for all $w \in \mathbb{R}^d$, $\|\nabla^2 f(w)\|_2 \leq L_0 + L_1\|\nabla f(w)\|_2$ for constants $L_0, L_1 > 0$ and Assumption 24 is used. Their theorem proves that their algorithm can produce a solution $\hat{w} \in \mathbb{R}^d$ such that $\mathbb{E}[\|\nabla f(\hat{w})\|_2] \leq 3\epsilon$ for an $\epsilon > 0$ when $K \in \mathbb{N}$ is chosen sufficiently large.

Taking $\psi_k = \min\left(\frac{\tau}{\hat{\eta}\|g(w^k)\|_2}, 1\right)$, plugging in $\tau = 5\sigma\hat{\eta}$ and the bound (14),

$$\begin{aligned} \psi_k &= \min\left(\frac{5\sigma}{\|g(w^k)\|_2}, 1\right) \\ &\geq \min\left(\frac{5\sigma}{\sigma + \|\nabla f(w)\|_2}, 1\right) \end{aligned}$$

almost surely. Assume that Assumption 25 holds for $G \leq 4\sigma$, then for all $k \geq K_5 := K_6$, $\psi_k \geq 1$ and no gradient clipping will be performed almost surely.

5.2 Choice of \hat{P}^k

If (8) were to hold, the simplest choice for \hat{P}^k would be a degenerate distribution with $\mathbb{P}(\hat{u}^k = 0) = 1$, with (7) simplifying to an implementation of SGD. Assuming that this is not the case, Proposition 9 motivates the choice of $\hat{P}^k = U(\overline{B}_{\frac{\alpha}{2}}^\infty)$, but this is not compatible with finite precision arithmetic, so we will now study its approximation.

For the remainder of this section we will consider a sequence of finite-precision environments $\{\mathbb{F}_{t_j}\}_{j=1}^\infty$ which have a fixed β , r or pair (e_{min}, e_{max}) , but increasing t , with $t_{j+1} > t_j$ for all $j \in \mathbb{N}$. We assume that $\overline{B}_{\frac{\alpha}{2}}^\infty$ for a chosen $\alpha > 0$ is contained in the range $[\Lambda^-, \Lambda^+]^d$ of the d -dimensional finite precision environment $\mathbb{F}_{t_1}^d$.² We denote by $R_{t_j}(\cdot) : \mathbb{R}^v \rightarrow \mathbb{F}_{t_j}^v$ rounding to nearest into $\mathbb{F}_{t_j}^v$ for $v = 1$ or d .

Assume that there exists a random number generator which can output samples of a discrete random variable \hat{u}_{t_j} taking on values $\{\hat{u}_{t_j}^k\} \subset \mathbb{F}_{t_j}^d$, and that the probability $\mathbb{P}(\hat{u}_{t_j} = \hat{u}_{t_j}^k) = \mathbb{P}(R_{t_j}(u) = \hat{u}_{t_j}^k)$ for $u \sim U(\overline{B}_{\frac{\alpha}{2}}^\infty)$. It is convenient to model the random number generator as

²This implies that $\overline{B}_{\frac{\alpha}{2}}^\infty$ is contained in the range of $\mathbb{F}_{t_j}^d$ for all $j \geq 1$.

receiving a sample of u which it then rounds to $R_{t_j}(u)$ to generate a sample of \hat{u}_{t_j} instead of considering a deterministic method such as using pseudorandom number generators. In general $\{\hat{u}_{t_j}^k\} \not\subset \overline{B}_{\frac{\alpha}{2}}^\infty$, i.e., u can be rounded outside of $\overline{B}_{\frac{\alpha}{2}}^\infty$. For simplicity we will assume that $\frac{\alpha}{2} \in \mathbb{F}_{t_1}$, from which it holds that $\{\hat{u}_{t_j}^k\} \subset \overline{B}_{\frac{\alpha}{2}}^\infty$ for all $j \geq 1$ by the monotonicity of rounding to nearest (Higham, 2002, Page 38), which is without much loss of generality as t_1 can be chosen arbitrarily large in the next theorem. Let $\hat{u}_\infty := \{\hat{u}_{t_j}^k \in \overline{B}_{\frac{\alpha}{2}}^\infty \cap \mathbb{F}_{t_j}^d : j \geq 1\}$ be the set of all vectors contained in $\overline{B}_{\frac{\alpha}{2}}^\infty$ which are representable in a finite-precision environment $\mathbb{F}_{t_j}^d$, which is countable as the Cartesian product of a finite number of countable sets from Proposition 5.

Assumption 13 was chosen to fit with sequences generated by PSGD (7) for general $\{\hat{P}^k\}$ including discrete distributions. For the next theorem, which considers sampling from $u \sim U(\overline{B}_{\frac{\alpha}{2}}^\infty)$, we use the following assumption on $\hat{\nabla}F(w, \xi, b)$ which can be seen as a direct relaxation of Proposition 3(3).

Assumption 26. *There exists a constant $c_2 > 0$ such that for almost all $w \in \mathbb{R}^d$,*

$$\mathbb{E}[\|\hat{\nabla}F(w, \xi, b)\|_2^2] \leq c_2 Q.$$

The following theorem studies the expected absolute error from quantization as the number of precision/fractional digits $t_j \rightarrow \infty$.

Theorem 27. *Assume that Assumption 26 holds, and for an $\alpha > 0$ with $\frac{\alpha}{2} \in \mathbb{F}_{t_1}$, $u \sim U(\overline{B}_{\frac{\alpha}{2}}^\infty)$. For all $\hat{u}^k \in \hat{u}_\infty$, $i \in [d]$, and almost all $w \in \mathbb{R}^d$,*

$$\lim_{j \rightarrow \infty} \mathbb{E}[\|\hat{\nabla}F_i(w + \hat{u}^k, \xi, b) - \hat{\nabla}F_i(w + u, \xi, b)\| \mid u \in \overline{B}_{\frac{\alpha}{2}}^\infty \cap R_{t_j}^{-1}(\hat{u}^k)] = 0.$$

6 Empirical Analysis of SGD Variants in Low-Precision Environments

This section compares different variants of SGD to improve the test set accuracy for image recognition tasks in low-precision arithmetic environments. The focus is on two Resnet models: Resnet 20 trained on CIFAR-10 (R20C10) and Resnet 32 trained on CIFAR-100 (R32C100). The experiments were conducted using QPyTorch (Zhang et al., 2019b), which enabled the simulation of training using floating and fixed-point arithmetic with rounding to nearest and stochastic rounding. For all experiments we train for 200 epochs, with an initial SGD step size of $\hat{\eta}_k = 0.1$ (before rounding), which is divided by 10 after 100 epochs, with a mini-batch size of $M = 128$. The plots are always of the mean (thick solid line), minimum (thin solid line), and maximum (dotted line) test set accuracy for each epoch over 10 runs. The tested algorithms generally achieve a reasonable level of convergence after the step size decrease after epoch 100. As the choice of 200 epochs is arbitrary, to avoid any ambiguity, accuracy is measured as the average accuracy in the last 30 epochs.

Let FLXR denote a floating-point environment with X total bits and 5 exponent bits, following IEEE binary 16 (IEEE Computer Society, 2019, Table 3.5), using rounding to nearest (R

= N) or stochastic rounding (R = S). Let FIX/YR denote a fixed-point environment where X is the total number of digits and Y is the number of fractional digits. Our use of QPyTorch followed closely the CIFAR10 Low Precision Training Example found at (Zhang et al., 2019a), which uses FL8³ and FL16. Assuming the training is done in FL8N, we will describe the changes made to the example in our implementation: all weight, gradient, and momentum quantization was done using FL8N, rounding to nearest was used throughout, no gradient accumulator was used, no gradient scaling was performed, and input parameters $\hat{\eta}_k$ and α_k were quantized. In order to do experiments in other environments, the only changes made was the choice of \mathbb{F} and the type of rounding $R(\cdot)$.

The initial focus was to determine a baseline SGD model to do experiments with. Training R20C10, momentum and weight decay were tested in FL8N and FL16N. Plain SGD was chosen as the baseline SGD model given its significantly better performance in FL8N, see Appendix D for more details. Given the large rounding error when training in FL8N, significant variation in accuracy can be observed over the 10 runs, summarized by the minimum and maximum accuracies. In all experiments we will not only consider the mean accuracy, but also the minimum accuracy of algorithms, placing value on algorithms’ ability to return solutions which are close to or above their mean accuracy.

6.1 Gradient Normalization

A simple variant that was found to improve test set accuracy was gradient normalization (GN) as presented in Algorithm 1, where $\mu \in \mathbb{F}_{>0}$ is a small positive constant to avoid division by 0, such as the minimum positive element in \mathbb{F} , $R(\cdot)$ performs the desired rounding scheme, and $\{\hat{\eta}_k\}_{k=1}^\infty$ is a baseline deterministic step size sequence.⁴ Experiments were done to compare different variants of GN using the L2 instead of L1-norm, as well as using an exponential moving average (EMA) with weight parameter $\beta = R(0.1)$, see the left-hand side of (16), instead of the simple moving average (SMA) in Algorithm 1 with $q = 10$, which is plotted in Figure 3 in Appendix D, where SGD with GN is referred to as NSGD, and μ was set to λ as suggested. All NSGD variants outperformed SGD, with NSGD using the L1-norm and an SMA (L1,SMA) dominating the other variants, with its mean accuracy being equal to if not greater than the maximum accuracies of the (L1,EMA) and (L2,SMA) variants, with its minimum accuracy being similar to the mean accuracy of the (L2,EMA) variant.

Algorithm 1 GN: Gradient Normalization (by step size update for iteration $k > 1$)

Input: $\widehat{\nabla}F(w^k) \in \mathbb{F}^d$, $\{g_{nrm}^i\}_{i=\max(1,k-q)}^{k-1} \subset \mathbb{F}_{>0}$; $\hat{\eta}_k, \mu \in \mathbb{F}_{>0}$

$$g_{nrm}^k = \max(R(\|\widehat{\nabla}F(w^k)\|_1), \mu)$$

$$m_{ave}^{k-1} = R\left(\frac{1}{\min(k-1,q)} \sum_{i=\max(1,k-q)}^{k-1} g_{nrm}^i\right)$$

Output: $\eta_k = R(\hat{\eta}_k * m_{ave}^{k-1} / g_{nrm}^k)$

³The number of exponent bits equals 2. This does not include the hidden bit, so in the representation of equation (2), $t = 3$, but d_1 is not required to be stored in memory.

⁴When $k = 1$, η_1 is set to $\hat{\eta}_1$.

Table 1: Mean value of η_k for different variants of GN.

$\hat{\eta}_k = 0.09375$	(L1,SMA)	(L2,SMA)
mean(η_k)	0.09753	0.09520
	(L1,EMA)	(L2,EMA)
mean(η_k)	0.12117	0.15317

If the norm of the gradient is larger (smaller) than average, then the baseline step size $\hat{\eta}_k$ is decreased (increased). For the more common form of NSGD, $\eta_k = R(\hat{\eta}_k/g_{nrm}^k)$ (Shor, 1998, Equation (2.7), Nesterov, 2004, Section 3.2.3), it seems unclear how to choose $\hat{\eta}_k$ a priori, whereas with NSGD, if $\text{mean}(\eta_k - \hat{\eta}_k) \approx 0$, the need to tune $\{\hat{\eta}_k\}$ can be avoided given that for any training task $\{\hat{\eta}_k\}$ can be set to what has previously been found to be a good step size schedule for SGD, with NSGD approximately following the same step size schedule on average, which also allows for a clearer comparison between SGD with and without gradient normalization.

In the experiments plotted in Figure 3 in Appendix D, for the first 100 epochs $\hat{\eta}_k = R(0.1) = 0.09375$. The mean value of η_k was computed over all steps in the first 100 epochs over the 10 runs, recorded in Table 1. It can be observed that for all cases $\text{mean}(\eta_k) > 0.09375$. For a successful training algorithm, the gradient norms will start out being relatively large and then decrease on average as the algorithm (hopefully) approaches a stationary point, so that on average the current gradient norm is smaller than previous ones. If the norm of the stochastic gradient is positively correlated to the true gradient norm over the iterates of the training algorithm, this could explain why the average step sizes are larger than $\hat{\eta}_k$. Using an SMA, the bias is small compared to using an EMA, for which the upward bias seems to be exacerbated by its “stickiness” in low precision, in the sense that

$$R((1 - \beta)m_{ave}^{k-1} + \beta g_{nrm}^k) = m_{ave}^{k-1} \quad (16)$$

can hold for a wide range of values. For example, if $g_{nrm}^k = 2$ and $1 \leq m_{ave}^{k-1} \leq 7$ with $\beta = R(0.1)$ in FL8N, then (16) holds.

In our implementation of GN, only one rounding operation is performed in each line of Algorithm 1. This implicitly assumes that intermediate steps are stored in sufficiently high precision such that no additional rounding errors are observable in the final low-precision output. This choice is consistent with the implementation of rounding using QPyTorch, where a quantization layer is added after each layer which induces rounding errors. If this assumption does not hold, it may be possible to devise rounding aware approximations which reduce the overall error after rounding, see for example (Wang et al., 2022, Section 3.5) where a Taylor series is used to approximately compute the gradient of cross entropy loss for use in low-precision fixed-point training.

In Algorithm 2 we present a family of step size sequences which fit within Assumption 11 if $R(\cdot)$ performs rounding to nearest, ψ_k is $\sigma(\mathcal{F}_{k-1}, \mathcal{G}_k)$ -measurable, $\hat{\Psi}_k$ is \mathcal{F}_{k-1} -measurable, and Δ_k is an element of a deterministic decreasing sequence converging to 0. The values $\Psi_k^L \geq 0$ and $\Psi_k^U > 0$ are chosen as evenly and as far apart as possible from $\hat{\Psi}_k$, with $\Psi_k^U - \Psi_k^L = 0$ when $\Delta_k = 0$. The parameters Ψ_k^L and Ψ_k^U must be chosen in general before ψ_k is known,

so if $\widehat{\Psi}_k$ is our best guess of what ψ_k is expected to equal, with $\widehat{\Psi}_k \approx \mathbb{E}[\psi_k]$, Algorithm 2 would approximately maximize $\min(\mathbb{E}[\psi_k] - \Psi_k^L, \Psi_k^U - \mathbb{E}[\psi_k])$, minimizing the probability of clipping assuming that the distribution of ψ_k is symmetric and unimodal.

Algorithm 2 General Adaptive Step Size Sequence

Input: $\psi_k, \widehat{\Psi}_k, \hat{\eta}_k \in \mathbb{F}_{>0}; \frac{\Delta_k}{2} \in \mathbb{F}_{\geq 0}$
 $v_k = \min(\frac{\Delta_k}{2}, \widehat{\Psi}_k)$
 $\Psi_k^L = R(\widehat{\Psi}_k - v_k)$
 $\Psi_k^U = R(\widehat{\Psi}_k + \Delta_k - v_k)$
 $\Upsilon_k = \min(\max(\Psi_k^L, \psi_k), \Psi_k^U)$
Output: $\eta_k = R(\hat{\eta}_k * \Upsilon_k)$

We now consider a particular instance of Algorithm 2 using what we call Delayed GN (DGN), which simply replaces g_{nrm}^k with g_{nrm}^{k-1} in the output of Algorithm 1, i.e. $\eta_k = R(\hat{\eta}_k * m_{ave}^{k-1}/g_{nrm}^{k-1})$. We note that when using rounding to nearest, GN is $\sigma(\mathcal{F}_{k-1}, \mathcal{G}_k)$ -measurable, DGN is \mathcal{F}_{k-1} -measurable, and if the gradient norms $\|\widehat{\nabla}F(w^k)\|_1$ and $\|\widehat{\nabla}F(w^{k-1})\|_1$ are positively correlated, DGN could still aid in stabilizing the algorithm steps (7). In Algorithm 2, setting $\psi_k = R(m_{ave}^{k-1}/g_{nrm}^k)$ and $\widehat{\Psi}_k = R(m_{ave}^{k-1}/g_{nrm}^{k-1})$, GN and DGN with an extra rounding operation, $\eta_k = R(\hat{\eta}_k * R(m_{ave}^{k-1}/g_{nrm}^k))$ and $\eta_k = R(\hat{\eta}_k * R(m_{ave}^{k-1}/g_{nrm}^{k-1}))$, respectively, can be seen as two extremes of this step size sequence, where GN is the step size which is guaranteed to occur when $\frac{\Delta_k}{2} = \Lambda^+$ with no clipping occurring, and DGN is the step size when $\frac{\Delta_k}{2} = 0$. In the experiments described in the next section, we will test GN and DGN based on Algorithm 1, with a single rounding operation in the output. These two step sizes occur in the following Algorithm 3 with the given choices of $\frac{\Delta_k}{2}$, where we assume all intermediate steps can be computed in sufficiently high precision to not induce any rounding error.

Algorithm 3 Restricted Gradient Normalization (for $k > 1$)

Input: $m_{ave}^{k-1}, g_{nrm}^{k-1}, g_{nrm}^k, \hat{\eta}_k \in \mathbb{F}_{>0}; \frac{\Delta_k}{2} \in \mathbb{F}_{\geq 0}$
 $v_k = \min(\frac{\Delta_k}{2}, \frac{m_{ave}^{k-1}}{g_{nrm}^{k-1}})$
 $\Psi_k^L = \frac{m_{ave}^{k-1}}{g_{nrm}^{k-1}} - v_k$
 $\Psi_k^U = \frac{m_{ave}^{k-1}}{g_{nrm}^{k-1}} + \Delta_k - v_k$
 $\Upsilon_k = \min(\max(\Psi_k^L, \frac{m_{ave}^{k-1}}{g_{nrm}^k}), \Psi_k^U)$
Output: $\eta_k = R(\hat{\eta}_k * \Upsilon_k)$

6.2 Training in Low-Precision Environments

We now compare the performance of SGD, NSGD, DNSGD, PSGD, PNSGD, and PDNSGD, where PSGD, PNSGD, and PDNSGD are SGD, NSGD, and DNSGD (SGD with DGN) with iterate perturbation. For the perturbed algorithms, the perturbation level was always kept at $\alpha_k = 0.1\hat{\eta}_k$, with the low-precision forward and back propagation computed at $w^k + u^k$ for $u^k = R(u)$, where $u \sim U(\overline{B}_{R(\frac{\alpha_k}{2})}^\infty)$.

We group the experiments into four categories: fixed-point with rounding to nearest, fixed-point with stochastic rounding, floating-point with rounding to nearest, and floating-point with stochastic rounding. Three different methods for ranking algorithms were used. The first method, Sum of Accuracies (SoA), summed each algorithm’s mean and minimum accuracies over each category’s experiments. The second method, Sum of Relative Accuracies (SoR), summed each algorithm’s relative mean and minimum accuracies over each category’s experiments, which were computed by dividing each algorithm’s mean (minimum) accuracy by the highest mean (minimum) accuracy observed in each category’s experiments. The third method, Sum of Scores (SoS) is a method we propose to overcome shortcomings found with the former two methods, described in the following section. A list of each experiment conducted, the resulting accuracies, relative accuracies, and scores, and the SoA, SoR, and SoS of each algorithm are presented in Tables 2 (all fixed-point experiments), 3 (floating-point rounding to nearest experiments), and 4 (floating-point stochastic rounding experiments) in Appendix D. It was generally too difficult to interpret a plot of all six algorithms, so for each experiment, a maximum of three algorithms were plotted in the following priority: SGD, the algorithm with the highest mean accuracy, the highest minimum accuracy, the lowest mean accuracy, and the lowest minimum accuracy, which are found in Figures 4, 5, and 6 in Appendix D.

6.2.1 Sum of Scores

To prevent algorithms from being deemed superior or inferior over trivial differences in accuracy, algorithms are considered to have equal performance, in principle, when the difference in their accuracies is less than $\chi := 0.5\%$. This was implemented using hierarchical clustering to partition the algorithms in each experiment: algorithms’ accuracies are initially placed in their own subsets, $\{p_i\}_{i=1}^6$. The dissimilarity between subsets is measured as

$$\Delta(p_i, p_j) := \max_{a \in p_i, a' \in p_j} |a - a'|, \tag{17}$$

where a and a' are accuracies of algorithms in subsets p_i and p_j . If there are at least two subsets with $\Delta(p_i, p_j) < \chi$, the pair with the smallest $\Delta(p_i, p_j)$ is combined together. This is repeated until $\Delta(p_i, p_j) \geq \chi$ for all subsets with $i \neq j$. Using the criterion (17) ensures that all algorithms whose accuracies are placed in the same subset p_i have a difference of accuracy less than χ , and are then considered as having the same ranking for the given experiment.

In order to rank the performance of algorithms over multiple experiments, scores equal to $\{5, 3, 1, -1, -3, -5\}$ are given starting from the algorithm with the highest to the lowest accuracy, with an averaged score given to algorithms with the same ranking. These scores were chosen since they are symmetrical, evenly spaced, and result in all averaged scores remaining integer valued, simplifying the presentation. The motivation to weight each experiment equally, by awarding fixed scores, is for our findings to be more robust to our choice of experiments: an algorithm may perform exceptionally well or bad relative to the other algorithms for a particular choice of neural network architecture, data set, and number format, skewing the overall rankings when using SoA or SoR, but this exceptional performance may not be representative over all potential experiments for the given category. With SoS, we limit the influence of any single experiment on the overall rankings.

6.2.2 Training in Low-Bit Fixed-Point Environments

Neural network training in fixed-point environments is of greater practical interest given the simpler arithmetic, resulting in reduced hardware complexity and energy consumption, see (Wang et al., 2022, Table 2), so we will begin with these experiments. In trying to determine the appropriate ratio of fractional bits, we were guided by the results of (Gupta et al., 2015), and experimented with a majority of bits being fractional, given that in their experiments with FI16, the best accuracy occurred with $Y=14$, with further improvement using FI20/16S (Gupta et al., 2015, Figures 1, 2, & 3). The choice of each fixed-point environment FIX/YR was determined by finding the smallest X for which all algorithms did not eventually collapse to random guessing.

The experimental results are given in Table 2 in Appendix D. For the fixed-point rounding to nearest experiments, the differentiating factor was whether perturbation was used or not. All of the perturbed and non-perturbed algorithms received the same scores, respectively. The top two plots in Figure 4 in Appendix D are of these experiments, where the mean accuracies of SGD are difficult to see given that they are almost identical to DNSGD and NSGD. The mean accuracies have a cascading waterfall appearance from single runs collapsing at different epochs. This instability from using rounding to nearest can also be observed in (Gupta et al., 2015, Figure 3), with the training and test set error increasing out of the plot. Considering all methods of ranking, PDNSGD would be considered the best algorithm. Given the almost identical performance of the perturbed algorithms though, PSGD could also be considered the best algorithm given that gradient normalization is not required, making it more computationally efficient.

For the fixed-point stochastic rounding experiments, PNSGD is the best performing algorithm according to all methods of ranking. SoA and SoR deemed SGD as the worst performing algorithm, whereas SoS ranked PSGD as the worst. SGD tied for the best mean accuracy in the first experiment, whereas PSGD always had a below average (negative) score in each experiment.

6.2.3 Training in Low-Bit Floating-Point Environments

Following the halving of bits from single to half precision, our initial choice was to try FL8 for our floating-point experiments with rounding to nearest and stochastic rounding. Although using FL8 and FL9⁵ for our R20C10 and R32C100 experiments allowed for a fairly clear comparison between the different algorithms, the maximum test set accuracies achievable by all of the algorithms were substantially lower than with single precision, and evidence of overfitting was also visible. To give more credence to the results, another set of experiments were done, where for each initial experiment, another mantissa bit was added to increase the overall accuracy, or weight decay was added when there was evidence of overfitting, for a total of 8 floating-point experiments. We note that the additional 4 experiments did not change the best algorithm determined by any of the methods of ranking based on the original 4 experiments, so these additional experiments simply reinforce our initial findings.

⁵Initial training of R32C100 in FL8N with SGD had a test set accuracy of approximately 2%, so the mantissa was increased by one bit in the initial experiments.

Table 3 and Figure 5 in Appendix D contain and plot the experimental results for the floating-point rounding to nearest experiments, where the initial experiments of training R20C10 in FL8N and R32C100 in FL9N were augmented with experiments training R20C10 in FL9N, and R32C100 in FL10N. In this setting iterate perturbation seems to have a detrimental effect, with all non-perturbed variants outperforming the perturbed variants. All methods of ranking agree that NSGD is the best performing algorithm, with PSGD being the worst. There is strong evidence of the benefit of gradient normalization, not only in how NSGD performed best overall, but for all methods of ranking NSGD>DNSGD>SGD and PNSGD>DNSGD>PSGD. Even among the algorithms with perturbation, the one using GN performed best, with both perturbed and non-perturbed DGN performing better than having no gradient normalization at all.

Table 4 and Figure 6 in Appendix D contain and plot the experimental results for the floating-point stochastic rounding experiments, where the initial experiments of training R20C10 in FL8S and R32C100 in FL9S were augmented with experiments using weight decay equal to $R(1e - 4)$, given the apparent overfitting of the models by all algorithms. With an inverted result compared to the floating-point rounding to nearest experiments, with stochastic rounding, all algorithms using iterate perturbation outperformed the algorithms without based on SoS, with PNSGD performing the best according to all methods of ranking. According to SoR and SoS, NSGD performed the worst in this set of experiments, with SGD performing the worst according to SoA.

6.2.4 Summary of Experimental Results

Based on the three methods of ranking, the algorithms which were found to perform best were PDNSGD for fixed-point rounding to nearest, PNSGD for fixed-point stochastic rounding, NSGD for floating-point rounding to nearest, and PNSGD for floating-point stochastic rounding environments. Of all methods, PNSGD seems to be the most promising algorithm for future use given that it dominated in the experiments using stochastic rounding, which is the rounding method of choice for low-precision deep learning (Gupta et al., 2015; Wang et al., 2022; Yang et al., 2019).

7 Conclusion

This paper studied the theoretical and empirical convergence of variants of SGD with computational error. A new asymptotic convergence result to a Clarke stationary point, as well as the non-asymptotic convergence to an approximate stationary point were presented for Perturbed SGD with adaptive step sizes, applied to a stochastic Lipschitz continuous loss function with error in computing its stochastic gradient, as well as the SGD step itself. Variants of SGD using gradient normalization and iterate perturbation were compared empirically to SGD in low-precision floating and fixed-point environments using rounding to nearest and stochastic rounding. In each case, variants were found to have improved test set accuracy compared to SGD, in particular PNSGD for experiments using stochastic rounding.

References

- Dimitri P. Bertsekas and John N. Tsitsiklis. Gradient Convergence in Gradient Methods with Errors. *SIAM Journal on Optimization*, 10(3):627–642, 2000.
- Jérôme Bolte and Edouard Pauwels. A mathematical model for automatic differentiation in machine learning. In H. Larochelle, M. Ranzato, R. Hadsell, M.F. Balcan, and H. Lin, editors, *Advances in Neural Information Processing Systems*, pages 10809–10819. Curran Associates, Inc., 2020.
- Frank H. Clarke. *Optimization and Nonsmooth Analysis*. SIAM, 1990.
- Michael P. Connolly, Nicholas J. Higham, and Theo Mary. Stochastic Rounding and Its Probabilistic Backward Error Analysis. *SIAM Journal on Scientific Computing*, 43(1): A566–A585, 2021.
- Matteo Croci, Massimiliano Fasi, Nicholas J. Higham, Theo Mary, and Mantas Mikaitis. Stochastic rounding: implementation, error analysis and applications. *Royal Society Open Science*, 9(3):211631, 2022.
- Damek Davis, Dmitriy Drusvyatskiy, Sham Kakade, and Jason D. Lee. Stochastic subgradient method converges on tame functions. *Foundations of Computational Mathematics*, 20(1):119–154, 2020.
- Damek Davis, Dmitriy Drusvyatskiy, Yin Tat Lee, Swati Padmanabhan, and Guanghao Ye. A gradient sampling method with complexity guarantees for Lipschitz functions in high and low dimensions. *arXiv preprint arXiv:2112.06969*, 2022.
- Gerald B. Folland. *Real Analysis: Modern Techniques and Their Applications*. Wiley, 1999.
- A.A. Goldstein. Optimization of Lipschitz continuous functions. *Mathematical Programming*, 13(1):14–22, 1977.
- Suyog Gupta, Ankur Agrawal, Kailash Gopalakrishnan, and Pritish Narayanan. Deep Learning with Limited Numerical Precision. In Francis Bach and David Blei, editors, *International Conference on Machine Learning*, pages 1737–1746. PMLR, 2015.
- Kaiming He, Xiangyu Zhang, Shaoqing Ren, and Jian Sun. Deep Residual Learning for Image Recognition. In *Proceedings of the IEEE Conference on Computer Vision and Pattern Recognition*, pages 770–778, 2016.
- Nicholas J. Higham. *Accuracy and Stability of Numerical Algorithms*. SIAM, 2002.
- IEEE Computer Society. IEEE Standard for Floating-Point Arithmetic. *IEEE Std 754-2019 (Revision of IEEE 754-2008)*, pages 1–84, 2019.
- Sergey Ioffe and Christian Szegedy. Batch Normalization: Accelerating Deep Network Training by Reducing Internal Covariate Shift. In Francis Bach and David Blei, editors, *International Conference on Machine Learning*, pages 448–456. PMLR, 2015.

- Anastasia Koloskova, Hadrien Hendrikx, and Sebastian U. Stich. Revisiting Gradient Clipping: Stochastic bias and tight convergence guarantees. In *International Conference on Machine Learning*. PMLR, 2023.
- Evgeny S. Levitin and Boris T. Polyak. Constrained Minimization Methods. *USSR Computational Mathematics and Mathematical Physics*, 6(5):1–50, 1966.
- Michael R. Metel. Sparse Training with Lipschitz Continuous Loss Functions and a Weighted Group L0-norm Constraint. *Journal of Machine Learning Research*, 24(103):1–44, 2023.
- Michael R. Metel and Akiko Takeda. Perturbed Iterate SGD for Lipschitz Continuous Loss Functions. *Journal of Optimization Theory and Applications*, 195(2):504–547, 2022.
- Yurii Nesterov. *Introductory Lectures on Convex Optimization: A Basic Course*. Springer Science+Business Media, 2004.
- Salvador Cruz Rambaud. A note on almost sure uniform and complete convergences of a sequence of random variables. *Stochastics*, 83(3):215–221, 2011.
- Herbert Robbins and David Siegmund. A Convergence Theorem for Non Negative Almost Supermartingales and Some Applications. In Jagdish S. Rustagi, editor, *Optimizing Methods in Statistics*, pages 233–257. Elsevier, 1971.
- R. Tyrrell Rockafellar and Roger J-B Wets. *Variational Analysis*. Springer, 2009.
- Rolf Schneider. *Convex Bodies: The Brunn-Minkowski Theory*. Cambridge University Press, 2014.
- Naum Z. Shor. *Nondifferentiable Optimization and Polynomial Problems*. Springer, 1998.
- M. V. Solodov and S. K. Zavriev. Error Stability Properties of Generalized Gradient-Type Algorithms. *Journal of Optimization Theory and Applications*, 98(3):663–680, 1998.
- Lai Tian, Kaiwen Zhou, and Anthony Man-Cho So. On the Finite-Time Complexity and Practical Computation of Approximate Stationarity Concepts of Lipschitz Functions. In Kamalika Chaudhuri, Stefanie Jegelka, Le Song, Csaba Szepesvari, Gang Niu, and Sivan Sabato, editors, *International Conference on Machine Learning*, pages 21360–21379. PMLR, 2022.
- Maolin Wang, Seyedramin Rasoulinezhad, Philip HW Leong, and Hayden K-H So. NITI: Training Integer Neural Networks Using Integer-Only Arithmetic. *IEEE Transactions on Parallel and Distributed Systems*, 33(11):3249–3261, 2022.
- Martin H. Weik. *Computer Science and Communications Dictionary*. 2001.
- J.H. Wilkinson. *Rounding Errors in Algebraic Processes*. Prentice-Hall, 1965.
- Lu Xia, Stefano Massei, Michiel Hochstenbach, and Barry Koren. On the influence of round-off errors on the convergence of the gradient descent method with low-precision floating-point computation. *arXiv preprint arXiv:2202.12276*, 2022.

- Guandao Yang, Tianyi Zhang, Polina Kirichenko, Junwen Bai, Andrew Gordon Wilson, and Chris De Sa. SWALP: Stochastic Weight Averaging in Low-Precision Training. In Kamalika Chaudhuri and Ruslan Salakhutdinov, editors, *International Conference on Machine Learning*, pages 7015–7024. PMLR, 2019.
- Bohang Zhang, Jikai Jin, Cong Fang, and Liwei Wang. Improved Analysis of Clipping Algorithms for Non-convex Optimization. In H. Larochelle, M. Ranzato, R. Hadsell, M.F. Balcan, and H. Lin, editors, *Advances in Neural Information Processing Systems*, pages 15511–15521. Curran Associates, Inc., 2020a.
- Jingzhao Zhang, Tianxing He, Suvrit Sra, and Ali Jadbabaie. Why Gradient Clipping Accelerates Training: A Theoretical Justification for Adaptivity. In *International Conference on Learning Representations*, 2020b.
- Jingzhao Zhang, Sai Praneeth Karimireddy, Andreas Veit, Seungyeon Kim, Sashank Reddi, Sanjiv Kumar, and Suvrit Sra. Why are Adaptive Methods Good for Attention Models? In H. Larochelle, M. Ranzato, R. Hadsell, M.F. Balcan, and H. Lin, editors, *Advances in Neural Information Processing Systems*, pages 15383–15393. Curran Associates, Inc., 2020c.
- Jingzhao Zhang, Hongzhou Lin, Stefanie Jegelka, Suvrit Sra, and Ali Jadbabaie. Complexity of Finding Stationary Points of Nonconvex Nonsmooth Functions. In Hal Daumé III and Aarti Singh, editors, *International Conference on Machine Learning*, pages 11173–11182. PMLR, 2020d.
- Tianyi Zhang, Zhiqiu Lin, Guandao Yang, and Christopher De Sa. QPyTorch’s documentation. <https://qpytorch.readthedocs.io>, 2019a. Accessed: 2022-09-29.
- Tianyi Zhang, Zhiqiu Lin, Guandao Yang, and Christopher De Sa. QPyTorch: A Low-Precision Arithmetic Simulation Framework. In *2019 Fifth Workshop on Energy Efficient Machine Learning and Cognitive Computing - NeurIPS Edition (EMC2-NIPS)*, pages 10–13. IEEE, 2019b.

Appendix A Proofs of Section 2

Proof. (Proposition 1): Let \mathcal{N}_ϵ be a neighbourhood of the set $\overline{B}_\epsilon^p(w)$, with L_ϵ being a Lipschitz constant of $g(x)$ restricted to \mathcal{N}_ϵ . Given that $\|\xi\|_2 \leq L_\epsilon$ for all $\xi \in \partial g(x)$, for all $x \in \overline{B}_\epsilon^p(w)$ (Clarke, 1990, Proposition 2.1.2 (a)), the set $\hat{\partial}_\epsilon^p g(w)$ is bounded. Since $\partial g(w)$ is outer semicontinuous (Clarke, 1990, Proposition 2.1.5 (d)), $\partial g(C)$ is closed if C is compact (Rockafellar and Wets, 2009, Theorem 5.25 (a)), hence $\hat{\partial}_\epsilon^p g(w) = g(\overline{B}_\epsilon^p(w))$ is compact. Since the convex hull of a compact set is compact (Rockafellar and Wets, 2009, Corollary 2.30), it also holds that $\partial_\epsilon^p g(w)$ is compact.

We next prove that $\hat{\partial}_\epsilon^p g(w)$ is outer semicontinuous following (Rockafellar and Wets, 2009, Definition 5.4). Let $w^k \rightarrow w$ and $u^k \rightarrow u$, with $u^k \in \hat{\partial}_\epsilon^p g(w^k)$. There exists at least one $y^k \in \overline{B}_\epsilon^p(w^k)$ such that $u^k \in \partial g(y^k)$. We can assume $\{w^k\}$ is bounded, implying that $\{y^k\}$ is as well. There then exists a subsequence $\{y^{k_i}\}$ which converges to a value y . Let the sequences $\{w^k\}$, $\{u^k\}$, and $\{y^k\}$ be redefined as the subsequences indexed by $\{k_i\}$. For an arbitrary $v \in \mathbb{R}^d$, it holds that

$$f^\circ(y^k; v) \geq \langle u^k, v \rangle,$$

where $f^\circ(w; v)$ is the Clarke generalized directional derivative at $w \in \mathbb{R}^d$ in the direction of $v \in \mathbb{R}^d$ (Clarke, 1990, Proposition 2.1.2 (b)). Given that $f^\circ(w; v)$ is upper semicontinuous (Clarke, 1990, Proposition 2.1.1 (b)),

$$f^\circ(y; v) \geq \limsup_{k \rightarrow \infty} f^\circ(y^k; v) \geq \limsup_{k \rightarrow \infty} \langle u^k, v \rangle = \langle u, v \rangle.$$

As v was chosen arbitrarily, $u \in \partial g(y)$ (Clarke, 1990, Proposition 2.1.5 (a)).

Considering $\overline{B}_\epsilon^p(w)$ as a set-valued mapping in $w \in \mathbb{R}^d$, it is outer semicontinuous: For any $\gamma > 0$, $\overline{B}_\epsilon^p(B_\gamma^p(w)) = \{x : \exists y \in B_\gamma^p(w), \|x - y\|_p \leq \epsilon\} = \{x : \|x - w\|_p < \epsilon + \gamma\} = B_{\epsilon+\gamma}^p(w)$ (Rockafellar and Wets, 2009, Theorem 5.19). It follows that $y \in \overline{B}_\epsilon^p(w)$, and

$$u \in \partial g(y) \subseteq \hat{\partial}_\epsilon^p g(w),$$

proving that $\hat{\partial}_\epsilon^p g(w)$ is outer semicontinuous. It holds again by (Rockafellar and Wets, 2009, Theorem 5.19) that for any $\gamma > 0$, there exists a $\delta > 0$ such that

$$\hat{\partial}_\epsilon^p g(x) \subseteq \hat{\partial}_\epsilon^p g(w) + B_\gamma^p(w)$$

for all $x \in B_\delta^p(w)$. Taking the convex hulls of both sides,

$$\partial_\epsilon^p g(x) \subseteq \partial_\epsilon^p g(w) + B_\gamma^p(w)$$

(Schneider, 2014, Theorem 1.1.2) for all $x \in B_\delta^p(w)$, proving that $\partial_\epsilon^p g(w)$ is outer semicontinuous as well. \square

Proof. (Proposition 2): Consider any $w \in \mathbb{R}^d$ and any $\epsilon > 0$. The proof uses (Rockafellar and Wets, 2009, Proposition 5.49) and (Rockafellar and Wets, 2009, Inequality 4(13)).

For any $\alpha_k > 0$, the Pompeiu-Hausdorff distance (Rockafellar and Wets, 2009, Example 4.13) between $\hat{\partial}_{\alpha_k}^p g(w)$ and $\partial g(w)$ with respect to the chosen p -norm⁶ equals

$$\begin{aligned} & d_\infty^p(\hat{\partial}_{\alpha_k}^p g(w), \partial g(w)) \\ &= \inf\{\gamma \geq 0 : \hat{\partial}_{\alpha_k}^p g(w) \subseteq \partial g(w) + \overline{B}_\gamma^p(w), \partial g(w) \subseteq \hat{\partial}_{\alpha_k}^p g(w) + \overline{B}_\gamma^p(w)\} \\ &= \inf\{\gamma \geq 0 : \hat{\partial}_{\alpha_k}^p g(w) \subseteq \partial g(w) + \overline{B}_\gamma^p(w)\}. \end{aligned}$$

By the outer semicontinuity of $\partial g(w)$, there exists a $\delta > 0$, such that $\partial g(\overline{B}_\delta^p(w)) \subseteq \partial g(w) + \overline{B}_\epsilon^p(w)$. There exists a $K \in \mathbb{N}$ such that for all $j \geq K$, $\alpha_j \leq \delta$, implying that $\hat{\partial}_{\alpha_j}^p g(w) = \partial g(\overline{B}_{\alpha_j}^p(w)) \subseteq \partial g(w) + \overline{B}_\epsilon^p(w)$.

For any $j \in \mathbb{N}$, there exists a $\overline{K} \in \mathbb{N}$ such that for all $i \geq \overline{K}$, $\alpha_i \leq \frac{\alpha_j}{2}$, from which it holds that for all $i \geq \overline{K}$ and for all $x \in \overline{B}_{\alpha_{\overline{K}}}^p(w)$, $\hat{\partial}_{\alpha_i}^p g(x) \subseteq \hat{\partial}_{\alpha_j}^p g(w)$. In particular for K , there exists a $\overline{K} \geq K$ such that for all $i \geq \overline{K}$ and all $x \in \overline{B}_{\alpha_{\overline{K}}}^p(w)$, $\hat{\partial}_{\alpha_i}^p g(x) \subseteq \hat{\partial}_{\alpha_K}^p g(w) \subseteq \partial g(w) + \overline{B}_\epsilon^p(w)$, from which $d_\infty^p(\hat{\partial}_{\alpha_i}^p g(x), \partial g(w)) \leq \epsilon$. Given that $\partial g(w)$ and $\overline{B}_\epsilon^p(w)$ are convex sets, taking the convex hull of both sides, it also holds that for all $i \geq \overline{K}$ and $x \in \overline{B}_{\alpha_{\overline{K}}}^p(w)$, $\partial_{\alpha_i}^p g(x) \subseteq \partial g(w) + \overline{B}_\epsilon^p(w)$, implying that $d_\infty^p(\partial_{\alpha_i}^p g(x), \partial g(w)) \leq \epsilon$ as well, proving that $\{\partial_{\alpha_k}^p g\}$ and $\{\hat{\partial}_{\alpha_k}^p g\}$ converge continuously to $\partial g(w)$ for all $w \in \mathbb{R}^d$. \square

Proof. (Proposition 4): Let $\tilde{\nabla} f(w)$ be a Borel measurable function equal to the gradient of $f(w)$ almost everywhere it exists, see (Metel and Takeda, 2022, Example A.1) for a method of its construction. It holds that $\nabla f(w+u) \in \partial f(w+u)$ when f is differentiable at $w+u \in \mathbb{R}^d$ (Clarke, 1990, Proposition 2.2.2), which is for almost all $u \in \overline{B}_{\frac{\alpha}{2}}^\infty$ by Rademacher's theorem. It follows that for almost all $u \in \overline{B}_{\frac{\alpha}{2}}^\infty$, $\tilde{\nabla} f(w+u) \in \partial_{\frac{\alpha}{2}}^\infty f(w)$, hence $\mathbb{E}[\tilde{\nabla} f(w+u)] \in \partial_{\frac{\alpha}{2}}^\infty f(w)$. The result follows given that $\nabla f_\alpha(w) = \mathbb{E}[\tilde{\nabla} f(w+u)]$ (Metel, 2023, Proposition 3). \square

Appendix B Further Background on Finite-Precision Environments & Proofs of Section 3

Further Background on Finite-Precision Environments

Continuing from the definition of \mathbb{L}_N in Section 3, the subnormal floating-point numbers \mathbb{L}_S are the remaining small in magnitude non-zero numbers which do not use the full precision of \mathbb{L} , written as $y = \pm \beta^{e_{\min}} \times .0d_2 \dots d_t$. We do not need a signed 0 in this work, so let 0 be represented as $+\beta^{e_{\min}} \times .00(\dots)0$.

It follows that for any $y \in \mathbb{L}_N$, $\lambda_N \leq |y| \leq \beta^{e_{\max}}(1 - \beta^{-t}) =: \Lambda^+$ and for any $y \in \mathbb{L}_S$, $\lambda = \beta^{e_{\min}-t} \leq |y| \leq \lambda_N - \lambda$. In addition, it holds that $\Lambda^- = -\Lambda^+$.

⁶This is done for simplicity, with the result holding using any norm on \mathbb{R}^d given their equivalence.

For an \mathbb{I} with $\beta = 2$, the non-negative and negative numbers will have $e_r = 0$ and $e_r = 1$, respectively, and the range of representable numbers equals $[-2^{r-1}, 2^{r-1} - 2^{-t}]$. This can be generalized to arbitrary $\beta \in \mathbb{Z}_{>1}$.

Proposition 28. *The range of \mathbb{I} written in the form of (3) with base $\beta \in \mathbb{Z}_{>1}$ using radix complement equals*

$$\left[-\left\lfloor \frac{\beta^{r+t}}{2} \right\rfloor \beta^{-t}, (\beta^{r+t} - \left\lfloor \frac{\beta^{r+t}}{2} \right\rfloor - 1) \beta^{-t}\right]. \quad (18)$$

Proof. The representable numbers are centered around 0, and when β is even, the number of representable numbers, β^{r+t} , is even, with there being one more negative number, $[(\beta - 1)00\dots 0.00\dots 0]$, than there are positive numbers. When β is odd, β^{r+t} is odd, and the representable numbers are symmetric around zero.

From the range (18), there are $n = \lfloor \frac{\beta^{r+t}}{2} \rfloor$ negative numbers and $\beta^{r+t} - n$ non-negative numbers, with the difference between adjacent representable numbers equal to $\rho := \beta^{-t}$. The smallest number is $-n\rho$ and the largest number is $(\beta^{r+t} - n - 1)\rho$.

When β is even, $\lfloor \frac{\beta^{r+t}}{2} \rfloor = \frac{\beta^{r+t}}{2}$, hence the negative and non-negative numbers have been evenly divided. When β is odd, let even $m := \beta^{r+t} - 1$. It follows that $n = \lfloor \frac{\beta^{r+t}}{2} \rfloor = \lfloor \frac{m+1}{2} \rfloor = \frac{m}{2}$ and $\beta^{r+t} - \lfloor \frac{\beta^{r+t}}{2} \rfloor - 1 = m + 1 - \frac{m}{2} - 1 = \frac{m}{2}$, hence the number of negative and positive numbers are equal. \square

For an \mathbb{I} , $\Lambda^- = -\lfloor \frac{\beta^{r+t}}{2} \rfloor \beta^{-t}$, $\Lambda^+ = (\beta^{r+t} - \lfloor \frac{\beta^{r+t}}{2} \rfloor - 1) \beta^{-t}$ and $\lambda = \beta^{-t}$. The following proposition proves that tie-breaking rules are unnecessary when using rounding to nearest in an odd base \mathbb{F} by considering a number of the form $y = 0.d_1d_2\dots d_t$ with $t \in \mathbb{Z}_{>0}$. This is without loss of generality, with more discussion after the proof of the result.

Proposition 29. *Consider a $y \in \mathbb{F}$ with an odd base β and $t \in \mathbb{Z}_{>0}$ of the form $y = 0.d_1d_2\dots d_t$. For any $q \in \mathbb{Z}_{\geq 0}$, it holds that $\underset{z \in \{d'_0.d'_1d'_2\dots d'_q; 0 \leq d'_i \leq \beta-1 \forall i \in [q]_0\}}{\operatorname{argmin}} |y - z|$ is a singleton.*

Proof. The result is trivial when $q \geq t$, so we will assume that $q < t$. The argmin will not be a singleton when $d_q\beta^{-q} + d_{q+1}\beta^{-(q+1)} + \dots d_t\beta^{-t}$ is equidistant from $d_q\beta^{-q}$ and $(d_q + 1)\beta^{-q}$, i.e.

$$\begin{aligned} d_q\beta^{-q} + \dots + d_t\beta^{-t} - d_q\beta^{-q} &= (d_q + 1)\beta^{-q} - (d_q\beta^{-q} + \dots + d_t\beta^{-t}) \\ \Rightarrow d_{q+1}\beta^{-(q+1)} + \dots + d_t\beta^{-t} &= \beta^{-q} - (d_{q+1}\beta^{-(q+1)} + \dots + d_t\beta^{-t}) \\ \Rightarrow 2(d_{q+1}\beta^{-(q+1)} + \dots + d_t\beta^{-t}) &= \beta^{-q} \\ \Rightarrow 2(d_{q+1}\beta^{t-(q+1)} + \dots + d_t\beta^0) &= \beta^{t-q}, \end{aligned}$$

which is impossible given that the left-hand side is an even integer, whereas the right-hand side is odd. \square

When $\mathbb{F} = \mathbb{L}$, Proposition 29 is considering a number of the form $y = +\beta^0 \times .d_1d_2\dots d_t$. Given that all \mathbb{L} are symmetric about 0, the result also holds for when $\pm = -$. The assumption

that $e = 0$ is without loss of generality. If y gets rounded up to $y = 1.00\dots$, considering its true original exponent e , y is rounded to $y = \beta^{e+1} \times .100\dots$, with a possible overflow, see (IEEE Computer Society, 2019, Section 7.4), having no effect on the uniqueness of the rounding. If y gets rounded down, d_1 will not be decreased given that $q \in \mathbb{Z}_{>0}$ for $y \in \mathbb{L}$, hence the true exponent e will be unchanged. For the case $\mathbb{F} = \mathbb{I}$, if in fact $t = 0$, i.e. $y \in \mathbb{Z}$, increasing t to a $q \in \mathbb{Z}_{>0}$ has no rounding effect. For a $y = [e_r e_{r-1}(\dots) e_1 . d_1 d_2(\dots) d_t]$ with $r \in \mathbb{Z}_{\geq 0}$ and $t \in \mathbb{Z}_{>0}$, the uniqueness of rounding $y' = [0 . d_1 d_2(\dots) d_t]$ to $z' = [d'_0 . d'_1 d'_2(\dots) d'_q]$ implies the uniqueness of rounding y to $z = [e_r e_{r-1}(\dots) e_1 . 0(\dots) 0] + [0(\dots) d'_0 . d'_1 d'_2(\dots) d'_q]$, with again a possible overflow occurring, but with no effect on the uniqueness of the rounding operation.

Proofs of Section 3

Proof. (Proposition 5): For simplicity let $\widehat{\mathbb{L}} := \{y \in \mathbb{L}_{t, e_{min}}^{\beta, e_{max}} : \beta \in \mathbb{Z}_{>1}, t \in \mathbb{Z}_{>0}, \mathbb{Z} \ni e_{min} \leq e_{max} \in \mathbb{Z}\}$ and $\widehat{\mathbb{I}} := \{y \in \mathbb{I}_{r, t}^{\beta} : \beta \in \mathbb{Z}_{>1}, r \in \mathbb{Z}_{\geq 0}, t \in \mathbb{Z}_{\geq 0}, r + t \in \mathbb{Z}_{>0}\}$.

We first show that $\mathbb{Q} \subseteq \widehat{\mathbb{I}}$: For $y \in \mathbb{Q}$ let $|y|$ be representable as $|y| = \frac{a}{b}$ for $a \in \mathbb{Z}_{\geq 0}$ and $b \in \mathbb{Z}_{>0}$. Let $c, d \in \mathbb{Z}_{\geq 0}$ be the unique integers satisfying

$$a = cb + d \quad \text{with} \quad d < b.$$

It holds that $|y| \in \mathbb{I}_{r, 1}^b$ if r satisfies, following Proposition 28,

$$\begin{aligned} (b^{r+1} - \lfloor \frac{b^{r+1}}{2} \rfloor - 1)b^{-1} &\geq \frac{cb + d}{b} \\ \Rightarrow \quad b^{r+1} - \lfloor \frac{b^{r+1}}{2} \rfloor - 1 &\geq cb + d, \end{aligned}$$

which is satisfied when

$$\begin{aligned} \frac{b^{r+1}}{2} - 1 &\geq cb + d \\ \Rightarrow \quad r &\geq \frac{\log(2(cb + d + 1))}{\log(b)} - 1. \end{aligned}$$

For $r^* \geq \frac{\log(2(cb + d + 1))}{\log(b)} - 1$, the radix complement of $-|y|$ is in $\mathbb{I}_{r^*, 1}^b$ as well, hence $y \in \widehat{\mathbb{I}}$.

We now show that for a $y \in \widehat{\mathbb{I}}$ it holds that $y \in \mathbb{Q}$. From (3), its absolute value

$$|y| = \sum_{i=1}^r e_i \beta^{i-1} + \sum_{j=1}^t d_j \beta^{-j},$$

where each $e_i \beta^{i-1} \in \mathbb{Z}$ and each $d_j \beta^{-j} \in \mathbb{Q}$. It follows that $|y| \in \mathbb{Q}$ as a finite sum of rationals, from which it holds that $y \in \mathbb{Q}$ as well. Similarly for $y \in \widehat{\mathbb{L}}$, from (2),

$$|y| = \sum_{i=1}^t d_i \beta^{e-i}$$

is equal to a finite sum of rationals, hence $y \in \mathbb{Q}$. □

Proof. (Proposition 6): For completeness we will give a proof that $\mathbb{E}[\delta] = 0$. Let $\omega := \lceil x \rceil_{\mathbb{F}} - \lfloor x \rfloor_{\mathbb{F}}$, noting that $\lceil x \rceil_{\mathbb{F}} - x = \omega - (x - \lfloor x \rfloor_{\mathbb{F}})$.

$$\begin{aligned}\mathbb{E}[\delta] &= (\lceil x \rceil_{\mathbb{F}} - x) \frac{x - \lfloor x \rfloor_{\mathbb{F}}}{\omega} + (\lfloor x \rfloor_{\mathbb{F}} - x) \left(1 - \frac{x - \lfloor x \rfloor_{\mathbb{F}}}{\omega}\right) \\ &= (\lceil x \rceil_{\mathbb{F}} - x) \frac{x - \lfloor x \rfloor_{\mathbb{F}}}{\omega} + (\lfloor x \rfloor_{\mathbb{F}} - x) \frac{\omega - (x - \lfloor x \rfloor_{\mathbb{F}})}{\omega} \\ &= (\lceil x \rceil_{\mathbb{F}} - x) \frac{x - \lfloor x \rfloor_{\mathbb{F}}}{\omega} + (\lfloor x \rfloor_{\mathbb{F}} - x) \frac{\lceil x \rceil_{\mathbb{F}} - x}{\omega} = 0.\end{aligned}$$

Letting $\kappa := x - \lfloor x \rfloor_{\mathbb{F}}$,

$$\begin{aligned}\text{Var}[\delta] &= \mathbb{E}[\delta^2] - \mathbb{E}[\delta]^2 \\ &= (\lceil x \rceil_{\mathbb{F}} - x)^2 \frac{x - \lfloor x \rfloor_{\mathbb{F}}}{\omega} + (\lfloor x \rfloor_{\mathbb{F}} - x)^2 \left(1 - \frac{x - \lfloor x \rfloor_{\mathbb{F}}}{\omega}\right) \\ &= (\omega - \kappa)^2 \frac{\kappa}{\omega} + \kappa^2 \frac{\omega - \kappa}{\omega} \\ &= \frac{\kappa}{\omega} (\omega^2 - 2\omega\kappa + \kappa^2 + \kappa\omega - \kappa^2) \\ &= \kappa\omega - \kappa^2 \\ &\leq \frac{\omega^2}{2} - \frac{\omega^2}{4} \\ &= \frac{(\lceil x \rceil_{\mathbb{F}} - \lfloor x \rfloor_{\mathbb{F}})^2}{4},\end{aligned}\tag{19}$$

where the inequality holds given that $k = \frac{\omega}{2}$ maximizes the strongly concave function (19). From (3), $\lceil x \rceil_{\mathbb{I}} - \lfloor x \rfloor_{\mathbb{I}} \leq \beta^{-t}$, and from (2), $\lceil x \rceil_{\mathbb{L}} - \lfloor x \rfloor_{\mathbb{L}} \leq \beta^{(e-t)}$, where if $x > 0$, e is the exponent of $\lfloor x \rfloor_{\mathbb{F}}$, and if $x < 0$, e is the exponent of $\lceil x \rceil_{\mathbb{L}}$, which is the exponent of the representation of $\lfloor |x| \rfloor_{\mathbb{L}}$, see the image on (Higham, 2002, Page 38) for an intuition in $\beta = 2$. \square

Proof. (Proposition 7): For any \mathbb{F} , the number of representable numbers, denoted as $|\mathbb{F}|$, is finite: for any \mathbb{L} , $|\mathbb{L}| = 1 + 2(e_{max} - e_{min} + 1)(\beta - 1)\beta^{t-1} + 2(\beta^{t-1} - 1)$, see the solution to (Higham, 2002, Problem 2.1), and for any \mathbb{I} , $|\mathbb{I}|$ equals β^{r+t} . For any \mathbb{F} , let the representable numbers be indexed from 1 to $|\mathbb{F}|$ in ascending order, i.e. $\mathbb{F} = \{y_{\mathbb{F}}^i\}_{i=1}^{|\mathbb{F}|}$ and $y_{\mathbb{F}}^i < y_{\mathbb{F}}^{i+1}$ for all $i \in [|\mathbb{F}| - 1]$.

We first verify the measurability of $\lfloor x \rfloor_{\mathbb{F}}$ and $\lceil x \rceil_{\mathbb{F}}$:

$$\lfloor x \rfloor_{\mathbb{F}} = \Lambda^- \mathbb{1}_{\{-\infty < x < \Lambda^-\}} + \sum_{i=1}^{|\mathbb{F}|-1} y_{\mathbb{F}}^i \mathbb{1}_{\{y_{\mathbb{F}}^i \leq x < y_{\mathbb{F}}^{i+1}\}} + \Lambda^+ \mathbb{1}_{\{\Lambda^+ \leq x < \infty\}}$$

and

$$\lceil x \rceil_{\mathbb{F}} = \Lambda^- \mathbb{1}_{\{-\infty < x \leq \Lambda^-\}} + \sum_{i=2}^{|\mathbb{F}|} y_{\mathbb{F}}^i \mathbb{1}_{\{y_{\mathbb{F}}^{i-1} < x \leq y_{\mathbb{F}}^i\}} + \Lambda^+ \mathbb{1}_{\{\Lambda^+ < x < \infty\}},$$

where the domains of $\lfloor x \rfloor_{\mathbb{F}}$ and $\lceil x \rceil_{\mathbb{F}}$ have been extended to include all of \mathbb{R} , with all $x \notin \mathcal{R}_{\mathbb{F}}$ set to whichever is closest between Λ^- and Λ^+ , in the same way rounding to nearest and stochastic rounding is defined for $x \notin \mathcal{R}_{\mathbb{F}}$. Since both $\lfloor x \rfloor_{\mathbb{F}}$ and $\lceil x \rceil_{\mathbb{F}}$ are simple functions (Folland, 1999, Page 46), they are measurable. Similarly, rounding to nearest is also a simple function, hence measurable:

$$R(x) = \Lambda^- \mathbb{1}_{\{-\infty < x \lesssim \frac{\Lambda^- + y_{\mathbb{F}}^2}{2}\}} + \sum_{i=2}^{|\mathbb{F}|-1} y_{\mathbb{F}}^i \mathbb{1}_{\{\frac{y_{\mathbb{F}}^{i-1} + y_{\mathbb{F}}^i}{2} \lesssim x \lesssim \frac{y_{\mathbb{F}}^i + y_{\mathbb{F}}^{i+1}}{2}\}} + \Lambda^+ \mathbb{1}_{\{\frac{y_{\mathbb{F}}^{|\mathbb{F}|-1} + \Lambda^+}{2} \lesssim x < \infty\}},$$

where in each instance, $\lesssim = <$ or \leq , depending on the tie-breaking rule.

For stochastic rounding, for $u \in [0, 1]$, the function

$$R(x, u) = \lceil x \rceil_{\mathbb{F}} \mathbb{1}_{\{u(\lceil x \rceil_{\mathbb{F}} - \lfloor x \rfloor_{\mathbb{F}}) - (x - \lfloor x \rfloor_{\mathbb{F}}) \leq 0\}} + \lfloor x \rfloor_{\mathbb{F}} \mathbb{1}_{\{u(\lceil x \rceil_{\mathbb{F}} - \lfloor x \rfloor_{\mathbb{F}}) - (x - \lfloor x \rfloor_{\mathbb{F}}) > 0\}}$$

performs stochastic rounding of x when $u \sim U([0, 1])$ is inputted: when $x \in \mathcal{R}_{\mathbb{F}}$ and $x \notin \mathbb{F}$, $R(x, u) = \lceil x \rceil_{\mathbb{F}}$ when $u \leq \frac{x - \lfloor x \rfloor_{\mathbb{F}}}{\lceil x \rceil_{\mathbb{F}} - \lfloor x \rfloor_{\mathbb{F}}}$ and $R(x, u) = \lfloor x \rfloor_{\mathbb{F}}$ when $u > \frac{x - \lfloor x \rfloor_{\mathbb{F}}}{\lceil x \rceil_{\mathbb{F}} - \lfloor x \rfloor_{\mathbb{F}}}$. When $x \in \mathbb{F}$ or $x \notin \mathcal{R}_{\mathbb{F}}$, $\lceil x \rceil_{\mathbb{F}} = \lfloor x \rfloor_{\mathbb{F}}$ and one of x , Λ^+ , or Λ^- is correctly returned. In addition, $R(x, u)$ is measurable over the product measurable space $(\mathbb{R} \times [0, 1], \mathcal{B}_{\mathbb{R}} \otimes \mathcal{B}_{[0,1]})$, given the measurability of $\lceil x \rceil_{\mathbb{F}}$ and $\lfloor x \rfloor_{\mathbb{F}}$. \square

Appendix C Proofs of Section 5

Proof. (Proposition 12): The rounding error can be modelled as

$$R(\eta'_k) = \eta'_k(1 + \delta),$$

where $|\delta| \leq u$ for rounding to nearest (Higham, 2002, Theorem 2.2) and $|\delta| \leq 2u$ for stochastic rounding (Connolly et al., 2021, Equation (2.4a)), where $u = \frac{1}{2}\beta^{1-t}$, hence

$$(1 - 2^{-1})\eta'_k \leq (1 - \beta^{1-t})\eta'_k = (1 - 2u)\eta'_k \leq R(\eta'_k) \leq (1 + 2u)\eta'_k = (1 + \beta^{1-t})\eta'_k \leq (1 + 2^{-1})\eta'_k,$$

given that $\beta > 1$ and our assumption that $t > 1$. \square

Proof. (Proposition 14): Let $S := \{w^i, \xi^i\}_{i=1}^{\infty} \subset \mathbb{R}^{d+p}$ be the set of points where $\widehat{\nabla}F(w, \xi, b)$ approximates $\widetilde{\nabla}F(w, \xi)$, and let $V := \{b : b_j \in V_j \forall j \in [s]\}$. By assumption, $\widetilde{\nabla}F(w, \xi)$ is a Borel measurable function in \mathbb{R}^{d+p} . Define $\widehat{\nabla}F(w, \xi, b) := \widetilde{\nabla}F(w, \xi)$ for all $(w, \xi, b) \in S^c \times \mathbb{R}^s$. When $(w, \xi, b) \in S \times V^c$, define $\widehat{\nabla}F(w, \xi, b) := a$ for any $a \in \mathbb{R}^d$. For any $i \in [d]$ and $\hat{a} \in \mathbb{R}$, the set

$$\begin{aligned} & \{(w, \xi, b) \in \mathbb{R}^{d+p+s} : \widehat{\nabla}_i F(w, \xi, b) > \hat{a}\} \\ &= \{(w, \xi, b) \in S^c \times \mathbb{R}^s : \widetilde{\nabla}_i F(w, \xi) > \hat{a}\} \cup \{(w, \xi, b) \in S \times \mathbb{R}^s : \widehat{\nabla}_i F(w, \xi, b) > \hat{a}\}. \end{aligned}$$

Given that S is countable, S^c is measurable, and the set

$$\begin{aligned} & \{(w, \xi, b) \in S^c \times \mathbb{R}^s : \widetilde{\nabla}_i F(w, \xi) > \hat{a}\} \\ &= (\{(w, \xi) \in \mathbb{R}^{d+p} : \widetilde{\nabla}_i F(w, \xi) > \hat{a}\} \cap S^c) \times \mathbb{R}^d \end{aligned}$$

is measurable, given the measurability of $\widetilde{\nabla}_i F(w, \xi)$. The set

$$\begin{aligned} & \{(w, \xi, b) \in S \times \mathbb{R}^d : \widehat{\nabla}_i F(w, \xi, b) > \hat{a}\} \\ & = \{(w, \xi, b) \in S \times V : \widehat{\nabla}_i F(w, \xi, b) > \hat{a}\} \cup \{(w, \xi, b) \in S \times V^c : \widehat{\nabla}_i F(w, \xi, b) > \hat{a}\} \end{aligned}$$

is measurable given that the set $S \times V$ is countable in \mathbb{R}^{d+p+s} , and that

$$\{(w, \xi, b) \in S \times V^c : \widehat{\nabla}_i F(w, \xi, b) > \hat{a}\} = \begin{cases} \emptyset & \text{if } \hat{a} \geq a \\ S \times V^c & \text{otherwise} \end{cases}$$

is measurable given that the Borel σ -algebra on \mathbb{R}^{d+p+s} , $\mathcal{B}_{\mathbb{R}^{d+p+s}} = \mathcal{B}_{\mathbb{R}^{d+p}} \otimes \mathcal{B}_{\mathbb{R}^s}$, hence $S \times V^c \in \mathcal{B}_{\mathbb{R}^{d+p+s}}$. Given that S^c is a set of full measure, $\widehat{\nabla} F(w, \xi, b) = \widetilde{\nabla} F(w, \xi)$ for almost all $(w, \xi) \in \mathbb{R}^{d+p}$. \square

Proof. (Proposition 15): Using the notation of the definition of batch normalization written in (Ioffe and Szegedy, 2015, Algorithm 1), consider a mini-batch of size 2, with $x_1 = 2$, $x_2 = 1$, $\epsilon = 0.25$, $\gamma = 1$, and $\beta = 0$. For an \mathbb{F} with $S := \{3, 2, 1, 1.5, 0.5, 0.25, -0.5\} \subseteq \mathbb{F}$ $y_i := x_i - \mu_\beta$ for $i \in [2]$, and $z := \sigma_\beta^2 + \epsilon$ can be computed exactly with $y_1 = z = 0.5$. The batch norm output for x_1 can be written as $\frac{y_1}{\sqrt{z} + \delta_1} + \delta_2$, where δ_1 is the stochastic rounding error from the square root operation and δ_2 is the subsequent rounding error from the division. Computing the expected value of the output of batch normalization for x_1 using stochastic rounding,

$$\begin{aligned} & \mathbb{E}\left[\frac{y_1}{\sqrt{z} + \delta_1} + \delta_2\right] \\ & = \mathbb{E}\left[\mathbb{E}\left[\frac{y_1}{\sqrt{z} + \delta_1} + \delta_2 \mid y_1, z, \delta_1\right]\right] \\ & = \mathbb{E}\left[\frac{y_1}{\sqrt{z} + \delta_1} + \mathbb{E}[\delta_2 \mid y_1, z, \delta_1]\right] \\ & = \mathbb{E}\left[\frac{y_1}{\sqrt{z} + \delta_1}\right] \\ & = \frac{y_1}{\lceil \sqrt{z} \rceil_{\mathbb{F}} \lceil \sqrt{z} \rceil_{\mathbb{F}} - \lfloor \sqrt{z} \rfloor_{\mathbb{F}}} + \frac{y_1}{\lfloor \sqrt{z} \rfloor_{\mathbb{F}}} \left(1 - \frac{\sqrt{z} - \lfloor \sqrt{z} \rfloor_{\mathbb{F}}}{\lceil \sqrt{z} \rceil_{\mathbb{F}} - \lfloor \sqrt{z} \rfloor_{\mathbb{F}}}\right) \\ & = \frac{y_1}{\lceil \sqrt{z} \rceil_{\mathbb{F}} - \lfloor \sqrt{z} \rfloor_{\mathbb{F}}} \left(\frac{\sqrt{z} - \lfloor \sqrt{z} \rfloor_{\mathbb{F}}}{\lceil \sqrt{z} \rceil_{\mathbb{F}}} + \frac{\lceil \sqrt{z} \rceil_{\mathbb{F}} - \sqrt{z}}{\lfloor \sqrt{z} \rfloor_{\mathbb{F}}}\right). \end{aligned}$$

Assume that the expected error is 0:

$$\begin{aligned} & \frac{y_1}{\lceil \sqrt{z} \rceil_{\mathbb{F}} - \lfloor \sqrt{z} \rfloor_{\mathbb{F}}} \left(\frac{\sqrt{z} - \lfloor \sqrt{z} \rfloor_{\mathbb{F}}}{\lceil \sqrt{z} \rceil_{\mathbb{F}}} + \frac{\lceil \sqrt{z} \rceil_{\mathbb{F}} - \sqrt{z}}{\lfloor \sqrt{z} \rfloor_{\mathbb{F}}}\right) = \frac{y_1}{\sqrt{z}} \\ \Rightarrow & \sqrt{z} \left(\frac{\sqrt{z} - \lfloor \sqrt{z} \rfloor_{\mathbb{F}}}{\lceil \sqrt{z} \rceil_{\mathbb{F}}} + \frac{\lceil \sqrt{z} \rceil_{\mathbb{F}} - \sqrt{z}}{\lfloor \sqrt{z} \rfloor_{\mathbb{F}}}\right) = \lceil \sqrt{z} \rceil_{\mathbb{F}} - \lfloor \sqrt{z} \rfloor_{\mathbb{F}} \\ \Rightarrow & \sqrt{z} \left(\frac{\lceil \sqrt{z} \rceil_{\mathbb{F}}}{\lceil \sqrt{z} \rceil_{\mathbb{F}}} - \frac{\lfloor \sqrt{z} \rfloor_{\mathbb{F}}}{\lfloor \sqrt{z} \rfloor_{\mathbb{F}}}\right) = \lceil \sqrt{z} \rceil_{\mathbb{F}} - \lfloor \sqrt{z} \rfloor_{\mathbb{F}} + z \left(\frac{1}{\lceil \sqrt{z} \rceil_{\mathbb{F}}} - \frac{1}{\lfloor \sqrt{z} \rfloor_{\mathbb{F}}}\right). \end{aligned}$$

For any \mathbb{F} with $S \subseteq \mathbb{F}$ this is impossible to hold given that \sqrt{z} is irrational, $\lceil \sqrt{z} \rceil_{\mathbb{F}}$ and $\lfloor \sqrt{z} \rfloor_{\mathbb{F}}$ are non-zero, and rational from Proposition 5, with $\lceil \sqrt{z} \rceil_{\mathbb{F}} \neq \lfloor \sqrt{z} \rfloor_{\mathbb{F}}$, hence the left-hand side is an irrational number, whereas the right-hand side is rational.

Batch normalization suffered from biased rounding error due to the division by \sqrt{z} in this example. In back propagation, this error will also occur as this operation is required when computing the gradient of batch normalization, see $\frac{\partial l}{\partial \mu_{\beta}}$ and $\frac{\partial l}{\partial x_i}$ in (Ioffe and Szegedy, 2015, Section 3). \square

Proof. (Proposition 16):

$$\begin{aligned}
& \mathbb{E}[\|\widehat{\nabla} \overline{F}^k(w^k)\|_2^2 | \mathcal{F}_{k-1}] \\
&= \mathbb{E}[\|\frac{1}{M} \sum_{i=1}^M \widehat{\nabla} F(w^k + \hat{u}^k, \xi^{k,i}, b^{k,i})\|_2^2 | \mathcal{F}_{k-1}] \\
&= \mathbb{E}[\sum_{j=1}^d (\frac{1}{M} \sum_{i=1}^M \widehat{\nabla} F_j(w^k + \hat{u}^k, \xi^{k,i}, b^{k,i}))^2 | \mathcal{F}_{k-1}] \\
&\leq \mathbb{E}[\sum_{j=1}^d \frac{1}{M} \sum_{i=1}^M \widehat{\nabla} F_j(w^k + \hat{u}^k, \xi^{k,i}, b^{k,i})^2 | \mathcal{F}_{k-1}] \\
&= \frac{1}{M} \sum_{i=1}^M \mathbb{E}[\|\widehat{\nabla} F(w^k + \hat{u}^k, \xi^{k,i}, b^{k,i})\|_2^2 | \mathcal{F}_{k-1}] \\
&\stackrel{\text{a.s.}}{\leq} c_2 Q,
\end{aligned}$$

where the first inequality uses Jensen's inequality and the second uses (9). \square

Proof. (Proposition 18): We adapt the results of (Wilkinson, 1965, Page 4 & 5), which for the basic operations $\{+, -, \times, \div\}$ with rounding to nearest applied to $x, y \in \mathbb{I}_t^{\beta}$ gives absolute errors bounded by $\{0, 0, 0.5\beta^{-t}, 0.5\beta^{-t}\}$, respectively, assuming no overflow. With the adoption of stochastic rounding these errors are increased to $\{0, 0, \beta^{-t}, \beta^{-t}\}$, but with the benefit of the errors from the operations $\{\times, \div\}$ being unbiased.

Evaluating the left-hand side of (10), following the order of operations,

$$\begin{aligned}
& w^k \ominus (\eta_k \otimes M) \otimes (\widehat{\nabla} F^{k,1}(w^k) \oplus \dots \oplus \widehat{\nabla} F^{k,M}(w^k)) \\
&= w^k \ominus \left(\frac{\eta_k}{M} + \delta_0\right) \otimes (\widehat{\nabla} F^{k,1}(w^k) \oplus \dots \oplus \widehat{\nabla} F^{k,M}(w^k)) \\
&= w^k \ominus \left(\frac{\eta_k}{M} + \delta_0\right) \otimes \sum_{i=1}^M \widehat{\nabla} F^{k,i}(w^k) \\
&= w^k \ominus \left(\left(\frac{\eta_k}{M} + \delta_0\right) \sum_{i=1}^M \widehat{\nabla} F^{k,i}(w^k) + \delta^1\right) \\
&= w^k - \left(\left(\frac{\eta_k}{M} + \delta_0\right) \sum_{i=1}^M \widehat{\nabla} F^{k,i}(w^k) + \delta^1\right) \\
&= w^k - \frac{\eta_k}{M} \sum_{i=1}^M \widehat{\nabla} F^{k,i}(w^k) - \delta_0 \sum_{i=1}^M \widehat{\nabla} F^{k,i}(w^k) - \delta^1,
\end{aligned}$$

where $\delta_0 \in \mathbb{R}$ is the error from the division, and $\delta^1 \in \mathbb{R}^d$ is the vector of errors from the multiplication. It holds that $e^k = -\delta_0 \sum_{i=1}^M \widehat{\nabla} F^{k,i}(w^k) - \delta^1$, and

$$\begin{aligned}
& \mathbb{E}[e^k | \mathcal{F}_{k-1}, \mathcal{G}_k] \\
&= -M \mathbb{E}[\delta_0 \widehat{\nabla} \overline{F}^k(w^k) | \mathcal{F}_{k-1}, \mathcal{G}_k] - \mathbb{E}[\mathbb{E}[\delta^1 | \mathcal{F}_{k-1}, \mathcal{G}_k, \delta_0] | \mathcal{F}_{k-1}, \mathcal{G}_k] \\
&= -M \mathbb{E}[\delta_0 | \mathcal{F}_{k-1}, \mathcal{G}_k] \widehat{\nabla} \overline{F}^k(w^k) = 0.
\end{aligned}$$

Considering now $\mathbb{E}[\|e^k\|_2^2 | \mathcal{F}_{k-1}]$,

$$\begin{aligned}
& \mathbb{E}[\|e^k\|_2^2 | \mathcal{F}_{k-1}] \\
&= \mathbb{E}[\|\delta_0 M \widehat{\nabla} \overline{F}^k(w^k) + \delta^1\|_2^2 | \mathcal{F}_{k-1}] \\
&= \mathbb{E}[\|\delta_0 M \widehat{\nabla} \overline{F}^k(w^k)\|_2^2 | \mathcal{F}_{k-1}] + 2\mathbb{E}[\langle \delta_0 M \widehat{\nabla} \overline{F}^k(w^k), \delta^1 \rangle | \mathcal{F}_{k-1}] + \mathbb{E}[\|\delta^1\|_2^2 | \mathcal{F}_{k-1}] \\
&= M^2 \mathbb{E}[\delta_0^2 \|\widehat{\nabla} \overline{F}^k(w^k)\|_2^2 | \mathcal{F}_{k-1}] + 2M \mathbb{E}[\langle \delta_0 \widehat{\nabla} \overline{F}^k(w^k), \delta^1 \rangle | \mathcal{F}_{k-1}] + \mathbb{E}[\|\delta^1\|_2^2 | \mathcal{F}_{k-1}]. \tag{20}
\end{aligned}$$

Focusing on $\mathbb{E}[\delta_0^2 \|\widehat{\nabla} \overline{F}^k(w^k)\|_2^2 | \mathcal{F}_{k-1}]$,

$$\begin{aligned}
& \mathbb{E}[\delta_0^2 \|\widehat{\nabla} \overline{F}^k(w^k)\|_2^2 | \mathcal{F}_{k-1}] \\
&= \mathbb{E}[\mathbb{E}[\delta_0^2 | \mathcal{F}_{k-1}, \mathcal{G}_k] \|\widehat{\nabla} \overline{F}^k(w^k)\|_2^2 | \mathcal{F}_{k-1}] \\
&\leq \mathbb{E}\left[\frac{\beta^{-2t}}{4} \|\widehat{\nabla} \overline{F}^k(w^k)\|_2^2 | \mathcal{F}_{k-1}\right] \\
&\stackrel{\text{a.s.}}{\leq} \frac{\beta^{-2t}}{4} c_2 Q,
\end{aligned}$$

using Propositions 6 and 16. Considering now $\mathbb{E}[\langle \delta_0 \widehat{\nabla} \overline{F}^k(w^k), \delta^1 \rangle | \mathcal{F}_{k-1}]$,

$$\begin{aligned}
& \mathbb{E}[\langle \delta_0 \widehat{\nabla} \overline{F}^k(w^k), \delta^1 \rangle | \mathcal{F}_{k-1}] \\
&= \mathbb{E}[\mathbb{E}[\langle \delta_0 \widehat{\nabla} \overline{F}^k(w^k), \delta^1 \rangle | \mathcal{F}_{k-1}, \mathcal{G}_k, \delta_0] | \mathcal{F}_{k-1}] \\
&= \mathbb{E}[\langle \delta_0 \widehat{\nabla} \overline{F}^k(w^k), \mathbb{E}[\delta^1 | \mathcal{F}_{k-1}, \mathcal{G}_k, \delta_0] \rangle | \mathcal{F}_{k-1}] \\
&= 0.
\end{aligned}$$

Continuing from (20),

$$\begin{aligned}
& \mathbb{E}[||e^k||_2^2 | \mathcal{F}_{k-1}] \\
& \stackrel{\text{a.s.}}{\leq} M^2 \frac{\beta^{-2t}}{4} c_2 Q + \mathbb{E}[||\delta^1||_2^2 | \mathcal{F}_{k-1}] \\
&= M^2 \frac{\beta^{-2t}}{4} c_2 Q + \mathbb{E}[\sum_{i=1}^M (\delta_i^1)^2 | \mathcal{F}_{k-1}] \\
&= M^2 \frac{\beta^{-2t}}{4} c_2 Q + \sum_{i=1}^M \mathbb{E}[\mathbb{E}[(\delta_i^1)^2 | \mathcal{F}_{k-1}, \mathcal{G}_k, \delta_0] | \mathcal{F}_{k-1}] \\
& \leq M^2 \frac{\beta^{-2t}}{4} c_2 Q + \sum_{i=1}^M \frac{\beta^{-2t}}{4} \\
&= \frac{M}{4} (M c_2 Q + 1) \beta^{-2t} \\
& \leq \frac{M}{4} (M c_2 Q + 1) \eta^2 \\
&= \frac{M}{4} (M c_2 Q + 1) (\hat{\eta}_k \psi_k)^2 \\
& \stackrel{\text{a.s.}}{\leq} \frac{M}{4} (M c_2 Q + 1) \hat{\eta}_k^2 (\overline{\Psi}^U)^2,
\end{aligned}$$

where the second last inequality holds since β^{-t} is the smallest positive element of \mathbb{I}_t^β . \square

Lemma 30. (Robbins and Siegmund, 1971, Theorem 1) For all $k \geq 1$, let z_k , θ_k , and ζ_k be non-negative \mathcal{F}_{k-1} -measurable random variables such that

$$\mathbb{E}[z_{k+1} | \mathcal{F}_{k-1}] \leq z_k + \theta_k - \zeta_k$$

almost surely, and assume that $\sum_{k=1}^{\infty} \theta_k < \infty$ almost surely. It holds almost surely that z_k converges to a random variable, $\lim_{k \rightarrow \infty} z_k = z_\infty < \infty$, and $\sum_{k=1}^{\infty} \zeta_k < \infty$.

Proof. (Theorem 20): This proof requires a Robbins-Siegmund inequality which is given directly above as Lemma 30. There exists a $K_4 \in \mathbb{N}$ such that for all $k \geq K_4$ it holds that $\Delta_k \leq c_1 \underline{\Psi}^U$ almost surely by Assumption 11.3. We begin the analysis assuming that the algorithm has been run sufficiently long such that $k \geq \overline{K} := \max(K_1, K_2, K_3, K_4)$ and Assumptions 13, 17, and 19 hold. By the L_1^α -smoothness of $f_\alpha(w)$ (Proposition 3.2 & Nesterov

(2004, Lemma 1.2.3)),

$$\begin{aligned} f_{\alpha_k}(w^{k+1}) &\leq f_{\alpha_k}(w^k) + \langle \nabla f_{\alpha_k}(w^k), w^{k+1} - w^k \rangle + \frac{L_1^{\alpha_k}}{2} \|w^{k+1} - w^k\|_2^2 \\ &= f_{\alpha_k}(w^k) + \langle \nabla f_{\alpha_k}(w^k), -\eta_k \widehat{\nabla} \overline{F}^k(w^k) + e^k \rangle + \frac{L_1^{\alpha_k}}{2} \|w^{k+1} - w^k\|_2^2 \end{aligned} \quad (21)$$

$$\begin{aligned} \Rightarrow f_{\alpha_{k+1}}(w^{k+1}) &\leq f_{\alpha_k}(w^k) + f_{\alpha_{k+1}}(w^{k+1}) - f_{\alpha_k}(w^{k+1}) - \eta_k \langle \nabla f_{\alpha_k}(w^k), \widehat{\nabla} \overline{F}^k(w^k) \rangle \\ &\quad + \langle \nabla f_{\alpha_k}(w^k), e^k \rangle + \frac{L_1^{\alpha_k}}{2} \|w^{k+1} - w^k\|_2^2. \end{aligned} \quad (22)$$

Focusing on $f_{\alpha_{k+1}}(w^{k+1}) - f_{\alpha_k}(w^{k+1})$,

$$\begin{aligned} &f_{\alpha_{k+1}}(w^{k+1}) - f_{\alpha_k}(w^{k+1}) \\ &= f_{\alpha_{k+1}}(w^{k+1}) - \int_{-\alpha_k/2}^{\alpha_k/2} \int_{-\alpha_k/2}^{\alpha_k/2} \cdots \int_{-\alpha_k/2}^{\alpha_k/2} \frac{f(w^{k+1} + u)}{\alpha_k^d} du_1 du_2 \dots du_d \\ &= f_{\alpha_{k+1}}(w^{k+1}) - \int_{-\alpha_k/2}^{\alpha_k/2} \int_{-\alpha_k/2}^{\alpha_k/2} \cdots \int_{-\alpha_k/2}^{\alpha_k/2} \mathbb{1}_{\{u \in \mathbb{R}^d: \|u\|_\infty \leq \frac{\alpha_{k+1}}{2}\}} \frac{f(w^{k+1} + u)}{\alpha_k^d} du_1 du_2 \dots du_d \\ &\quad - \int_{-\alpha_k/2}^{\alpha_k/2} \int_{-\alpha_k/2}^{\alpha_k/2} \cdots \int_{-\alpha_k/2}^{\alpha_k/2} \mathbb{1}_{\{u \in \mathbb{R}^d: \|u\|_\infty > \frac{\alpha_{k+1}}{2}\}} \frac{f(w^{k+1} + u)}{\alpha_k^d} du_1 du_2 \dots du_d \\ &= f_{\alpha_{k+1}}(w^{k+1}) - f_{\alpha_{k+1}}(w^{k+1}) \frac{\alpha_{k+1}^d}{\alpha_k^d} \\ &\quad - \int_{-\alpha_k/2}^{\alpha_k/2} \int_{-\alpha_k/2}^{\alpha_k/2} \cdots \int_{-\alpha_k/2}^{\alpha_k/2} \mathbb{1}_{\{u \in \mathbb{R}^d: \|u\|_\infty > \frac{\alpha_{k+1}}{2}\}} \frac{f(w^{k+1} + u)}{\alpha_k^d} du_1 du_2 \dots du_d \\ &\leq f_{\alpha_{k+1}}(w^{k+1}) \left(1 - \frac{\alpha_{k+1}^d}{\alpha_k^d} \right), \end{aligned}$$

where we used the assumption that $\alpha_{k+1} \leq \alpha_k$ for the third equality, and that $\inf_{w \in \mathbb{R}^d} f(w) \geq 0$ for the inequality at the end. Plugging into (22),

$$\begin{aligned} f_{\alpha_{k+1}}(w^{k+1}) &\leq f_{\alpha_k}(w^k) + f_{\alpha_{k+1}}(w^{k+1}) \left(1 - \frac{\alpha_{k+1}^d}{\alpha_k^d} \right) - \eta_k \langle \nabla f_{\alpha_k}(w^k), \widehat{\nabla} \overline{F}^k(w^k) \rangle \\ &\quad + \langle \nabla f_{\alpha_k}(w^k), e^k \rangle + \frac{L_1^{\alpha_k}}{2} \|w^{k+1} - w^k\|_2^2 \\ \Rightarrow \frac{\alpha_{k+1}^d}{\alpha_k^d} f_{\alpha_{k+1}}(w^{k+1}) &\leq f_{\alpha_k}(w^k) - \eta_k \langle \nabla f_{\alpha_k}(w^k), \widehat{\nabla} \overline{F}^k(w^k) \rangle \\ &\quad + \langle \nabla f_{\alpha_k}(w^k), e^k \rangle + \alpha_k^{-1} \sqrt{d} L_0 \| -\eta_k \widehat{\nabla} \overline{F}^k(w^k) + e^k \|_2^2 \\ \Rightarrow \alpha_{k+1}^d f_{\alpha_{k+1}}(w^{k+1}) &\leq \alpha_k^d f_{\alpha_k}(w^k) - \alpha_k^d \eta_k \langle \nabla f_{\alpha_k}(w^k), \widehat{\nabla} \overline{F}^k(w^k) \rangle + \alpha_k^d \langle \nabla f_{\alpha_k}(w^k), e^k \rangle \\ &\quad + \alpha_k^{d-1} \sqrt{d} L_0 (\eta_k^2 \| \widehat{\nabla} \overline{F}^k(w^k) \|_2^2 - 2\eta_k \langle \widehat{\nabla} \overline{F}^k(w^k), e^k \rangle + \|e^k\|_2^2). \end{aligned} \quad (23)$$

Taking the conditional expectation of (23) with respect to \mathcal{F}_{k-1} ,

$$\begin{aligned}
& \mathbb{E}[\alpha_{k+1}^d f_{\alpha_{k+1}}(w^{k+1}) | \mathcal{F}_{k-1}] \\
& \leq \alpha_k^d f_{\alpha_k}(w^k) - \alpha_k^d \hat{\eta}_k \mathbb{E}[\psi_k \langle \nabla f_{\alpha_k}(w^k), \widehat{\nabla} \overline{F}^k(w^k) \rangle | \mathcal{F}_{k-1}] + \alpha_k^d \langle \nabla f_{\alpha_k}(w^k), \mathbb{E}[e^k | \mathcal{F}_{k-1}] \rangle \\
& \quad + \alpha_k^{d-1} \sqrt{d} L_0 (\hat{\eta}_k^2 \mathbb{E}[\psi_k^2 | \widehat{\nabla} \overline{F}^k(w^k)|_2^2 | \mathcal{F}_{k-1}] - 2 \hat{\eta}_k \mathbb{E}[\psi_k \langle \widehat{\nabla} \overline{F}^k(w^k), e^k \rangle | \mathcal{F}_{k-1}] + \mathbb{E}[|e^k|_2^2 | \mathcal{F}_{k-1}]).
\end{aligned} \tag{24}$$

It holds that $\mathbb{E}[e^k | \mathcal{F}_{k-1}] = \mathbb{E}[\mathbb{E}[e^k | \mathcal{F}_{k-1}, \mathcal{G}_k] | \mathcal{F}_{k-1}] = 0$ by assumption, $\mathbb{E}[\psi_k^2 | \widehat{\nabla} \overline{F}^k(w^k)|_2^2 | \mathcal{F}_{k-1}] \leq (\overline{\Psi}^U)^2 c_2 Q$ almost surely using Assumption 11.2 and Proposition 16,

$$\begin{aligned}
& \mathbb{E}[\psi_k \langle \widehat{\nabla} \overline{F}^k(w^k), e^k \rangle | \mathcal{F}_{k-1}] \\
& = \mathbb{E}[\mathbb{E}[\psi_k \langle \widehat{\nabla} \overline{F}^k(w^k), e^k \rangle | \mathcal{G}_k, \mathcal{F}_{k-1}] | \mathcal{F}_{k-1}] \\
& = \mathbb{E}[\psi_k \langle \widehat{\nabla} \overline{F}^k(w^k), \mathbb{E}[e^k | \mathcal{G}_k, \mathcal{F}_{k-1}] \rangle | \mathcal{F}_{k-1}] = 0,
\end{aligned}$$

and $\mathbb{E}[|e^k|_2^2 | \mathcal{F}_{k-1}] \leq c_3 \hat{\eta}_k^2$ almost surely by Assumption 17. Continuing from (24),

$$\begin{aligned}
\mathbb{E}[\alpha_{k+1}^d f_{\alpha_{k+1}}(w^{k+1}) | \mathcal{F}_{k-1}] & \stackrel{\text{a.s.}}{\leq} \alpha_k^d f_{\alpha_k}(w^k) - \alpha_k^d \hat{\eta}_k \mathbb{E}[\psi_k \langle \nabla f_{\alpha_k}(w^k), \widehat{\nabla} \overline{F}^k(w^k) \rangle | \mathcal{F}_{k-1}] \\
& \quad + \alpha_k^{d-1} \hat{\eta}_k^2 \sqrt{d} L_0 ((\overline{\Psi}^U)^2 c_2 Q + c_3).
\end{aligned} \tag{25}$$

We now focus on the conditional expectation $\mathbb{E}[-\psi_k \langle \nabla f_{\alpha_k}(w^k), \widehat{\nabla} \overline{F}^k(w^k) \rangle | \mathcal{F}_{k-1}]$,

$$\begin{aligned}
& \mathbb{E}[-\psi_k \langle \nabla f_{\alpha_k}(w^k), \widehat{\nabla} \overline{F}^k(w^k) \rangle | \mathcal{F}_{k-1}] \\
& = \mathbb{E}[\frac{\psi_k}{2} (|\nabla f_{\alpha_k}(w^k) - \widehat{\nabla} \overline{F}^k(w^k)|_2^2 - |\nabla f_{\alpha_k}(w^k)|_2^2 - |\widehat{\nabla} \overline{F}^k(w^k)|_2^2) | \mathcal{F}_{k-1}] \\
& \leq \frac{\Psi_k^U}{2} \mathbb{E}[|\nabla f_{\alpha_k}(w^k) - \widehat{\nabla} \overline{F}^k(w^k)|_2^2 | \mathcal{F}_{k-1}] - \frac{\mathbb{E}[\psi_k | \mathcal{F}_{k-1}]}{2} |\nabla f_{\alpha_k}(w^k)|_2^2 - \frac{\Psi_k^L}{2} \mathbb{E}[|\widehat{\nabla} \overline{F}^k(w^k)|_2^2 | \mathcal{F}_{k-1}] \\
& \leq \frac{\Psi_k^U}{2} \mathbb{E}[|\nabla f_{\alpha_k}(w^k) - \widehat{\nabla} \overline{F}^k(w^k)|_2^2 | \mathcal{F}_{k-1}] - \frac{\Psi_k^L}{2} |\nabla f_{\alpha_k}(w^k)|_2^2 - \frac{\Psi_k^L}{2} \mathbb{E}[|\widehat{\nabla} \overline{F}^k(w^k)|_2^2 | \mathcal{F}_{k-1}] \\
& = \frac{\Psi_k^U}{2} (|\nabla f_{\alpha_k}(w^k)|_2^2 - 2 \mathbb{E}[\langle \nabla f_{\alpha_k}(w^k), \widehat{\nabla} \overline{F}^k(w^k) \rangle | \mathcal{F}_{k-1}] + \mathbb{E}[|\widehat{\nabla} \overline{F}^k(w^k)|_2^2 | \mathcal{F}_{k-1}]) \\
& \quad - \frac{\Psi_k^L}{2} |\nabla f_{\alpha_k}(w^k)|_2^2 - \frac{\Psi_k^L}{2} \mathbb{E}[|\widehat{\nabla} \overline{F}^k(w^k)|_2^2 | \mathcal{F}_{k-1}] \\
& \stackrel{\text{a.s.}}{\leq} \frac{\Psi_k^U}{2} (|\nabla f_{\alpha_k}(w^k)|_2^2 - 2c_1 |\nabla f_{\alpha_k}(w^k)|_2^2 + \mathbb{E}[|\widehat{\nabla} \overline{F}^k(w^k)|_2^2 | \mathcal{F}_{k-1}]) \\
& \quad - \frac{\Psi_k^L}{2} |\nabla f_{\alpha_k}(w^k)|_2^2 - \frac{\Psi_k^L}{2} \mathbb{E}[|\widehat{\nabla} \overline{F}^k(w^k)|_2^2 | \mathcal{F}_{k-1}] \\
& = (\frac{\Psi_k^U}{2} - c_1 \Psi_k^U - \frac{\Psi_k^L}{2}) |\nabla f_{\alpha_k}(w^k)|_2^2 + (\frac{\Psi_k^U}{2} - \frac{\Psi_k^L}{2}) \mathbb{E}[|\widehat{\nabla} \overline{F}^k(w^k)|_2^2 | \mathcal{F}_{k-1}] \\
& \stackrel{\text{a.s.}}{\leq} (\frac{\Psi_k^U}{2} - c_1 \Psi_k^U - \frac{\Psi_k^L}{2}) |\nabla f_{\alpha_k}(w^k)|_2^2 + (\frac{\Psi_k^U}{2} - \frac{\Psi_k^L}{2}) c_2 Q
\end{aligned} \tag{26}$$

$$\stackrel{\text{a.s.}}{\leq} -\frac{c_1}{2} \underline{\Psi}^U |\nabla f_{\alpha_k}(w^k)|_2^2 + \frac{c_4}{2} \frac{\hat{\eta}_k}{\alpha_k} c_2 Q, \tag{27}$$

where the second and third inequalities use Assumption 11.1, the third inequality uses equation (8), and the last inequality uses the assumption that k is sufficiently large such that $\Delta_k \leq c_1 \underline{\Psi}^U$ almost surely, and Assumption 19. Plugging (27) into (25),

$$\begin{aligned} \mathbb{E}[\alpha_{k+1}^d f_{\alpha_{k+1}}(w^{k+1}) | \mathcal{F}_{k-1}] &\stackrel{\text{a.s.}}{\leq} \alpha_k^d f_{\alpha_k}(w^k) - \alpha_k^d \frac{\hat{\eta}_k}{2} (c_1 \underline{\Psi}^U \|\nabla f_{\alpha_k}(w^k)\|_2^2 - c_4 \frac{\hat{\eta}_k}{\alpha_k} c_2 Q) \\ &\quad + \alpha_k^{d-1} \hat{\eta}_k^2 \sqrt{d} L_0 ((\overline{\Psi}^U)^2 c_2 Q + c_3) \\ &= \alpha_k^d f_{\alpha_k}(w^k) - \alpha_k^d \hat{\eta}_k \frac{c_1}{2} \underline{\Psi}^U \|\nabla f_{\alpha_k}(w^k)\|_2^2 \\ &\quad + \alpha_k^{d-1} \hat{\eta}_k^2 (\sqrt{d} L_0 ((\overline{\Psi}^U)^2 c_2 Q + c_3) + \frac{c_4}{2} c_2 Q). \end{aligned}$$

Lemma 30 can now be applied (redefining the index from $k = \overline{K}, \overline{K}+1, \dots$ to $k = 1, 2, \dots$) with $z_k = \alpha_k^d f_{\alpha_k}(w^k)$, $\theta_k = \alpha_k^{d-1} \hat{\eta}_k^2 (\sqrt{d} L_0 ((\overline{\Psi}^U)^2 c_2 Q + c_3) + \frac{c_4}{2} c_2 Q)$, and $\zeta_k = \alpha_k^d \hat{\eta}_k \frac{c_1}{2} \underline{\Psi}^U \|\nabla f_{\alpha_k}(w^k)\|_2^2$, given that

$$\begin{aligned} &\sum_{k=\overline{K}}^{\infty} \alpha_k^{d-1} \hat{\eta}_k^2 (\sqrt{d} L_0 ((\overline{\Psi}^U)^2 c_2 Q + c_3) + \frac{c_4}{2} c_2 Q) \\ &\leq (\sqrt{d} L_0 ((\overline{\Psi}^U)^2 c_2 Q + c_3) + \frac{c_4}{2} c_2 Q) \sum_{k=1}^{\infty} \alpha_k^{d-1} \hat{\eta}_k^2 < \infty \end{aligned}$$

by assumption, proving that almost surely

$$\sum_{k=\overline{K}}^{\infty} \alpha_k^d \hat{\eta}_k \frac{c_1}{2} \underline{\Psi}^U \|\nabla f_{\alpha_k}(w^k)\|_2^2 < \infty. \quad (28)$$

It follows that $\liminf_{k \rightarrow \infty} \|\nabla f_{\alpha_k}(w^k)\|_2 = 0$ almost surely, as for any $\epsilon > 0$ if there exists a $\overline{K}_2 \geq \overline{K}$ such that $\|\nabla f_{\alpha_k}(w^k)\|_2 \geq \epsilon$ almost surely for all $k \geq \overline{K}_2$,

$$\sum_{k=\overline{K}_2}^{\infty} \alpha_k^d \hat{\eta}_k \frac{c_1}{2} \underline{\Psi}^U \|\nabla f_{\alpha_k}(w^k)\|_2^2 \stackrel{\text{a.s.}}{\geq} \frac{c_1}{2} \underline{\Psi}^U \epsilon^2 \sum_{k=\overline{K}_2}^{\infty} \alpha_k^d \hat{\eta}_k = \infty,$$

given that $\sum_{k=1}^{\infty} \alpha_k^d \hat{\eta}_k = \infty$ by assumption and that $\sum_{k=1}^{\overline{K}_2-1} \alpha_k^d \hat{\eta}_k$ is finite, contradicting (28). There then exists, almost surely, a subsequence of indices $\{k_i\}$ for which $\lim_{i \rightarrow \infty} \|\nabla f_{\alpha_{k_i}}(w^{k_i})\|_2 = \liminf_{k \rightarrow \infty} \|\nabla f_{\alpha_k}(w^k)\|_2 = 0$. If w^* is an accumulation point of $\{w^{k_i}\}$, let $\{\hat{k}_{i_j}\}$ be a subsequence of $\{k_i\}$ such that $\lim_{j \rightarrow \infty} w^{\hat{k}_{i_j}} = w^*$. Given that $\partial_{0.5\alpha_{k_{i_j}}}^{\infty} f(w^{\hat{k}_{i_j}})$ converges continuously to $\partial f(w^*)$ by Proposition 2, it holds that

$$\lim_{j \rightarrow \infty} \text{dist}(0, \partial_{0.5\alpha_{k_{i_j}}}^{\infty} f(w^{\hat{k}_{i_j}})) = \text{dist}(0, \partial f(w^*))$$

(Rockafellar and Wets, 2009, Exercise 5.42 (b)). Since $\nabla f_{\alpha_{k_{i_j}}}(w^{\hat{k}_{i_j}}) \in \partial_{0.5\alpha_{k_{i_j}}}^{\infty} f(w^{\hat{k}_{i_j}})$ from Proposition 4,

$$\text{dist}(0, \partial f(w^*)) = \lim_{j \rightarrow \infty} \text{dist}(0, \partial_{0.5\alpha_{k_{i_j}}}^{\infty} f(w^{\hat{k}_{i_j}})) \leq \lim_{j \rightarrow \infty} \|\nabla f_{\alpha_{k_{i_j}}}(w^{\hat{k}_{i_j}})\|_2 \stackrel{\text{a.s.}}{=} 0.$$

□

Proof. (Proposition 21): Setting $\alpha_k = \frac{1}{k^p}$ and $\hat{\eta}_k \in [\frac{c}{k^q}, \frac{c'}{k^q}]$, $\{\alpha_k\}$ is non-increasing with $\lim_{k \rightarrow \infty} \alpha_k = 0$ for $p > 0$. The summation conditions require that

$$\begin{aligned} \sum_{k=1}^{\infty} \alpha_k^d \hat{\eta}_k &\geq c \sum_{k=1}^{\infty} k^{-dp} k^{-q} = \infty \text{ and} \\ \sum_{k=1}^{\infty} \alpha_k^{d-1} \hat{\eta}_k^2 &\leq c' \sum_{k=1}^{\infty} k^{-(d-1)p} k^{-2q} < \infty, \end{aligned}$$

which holds when $0 < dp + q \leq 1$ and $(d-1)p + 2q > 1$, which holds when $0.5 < q < 1$ and $p = \frac{(1-q)}{d}$. Defining $\hat{q} := 2q - 1 > 0$, and assuming now that

$$\Delta_k \stackrel{\text{a.s.}}{\leq} c_4 \frac{\hat{\eta}_k}{\alpha_k} \leq c_4 c' k^{p-q} \leq c_4 c' k^{1-2q} = c_4 c' k^{-\hat{q}}$$

for $k \geq K_3$ following Assumption 19, it holds that $\{\Delta_k\}_{k=1}^{\infty}$ almost surely uniformly converges to 0. \square

Proof. (Theorem 22): Taking the conditional expectation with respect to \mathcal{F}_{k-1} of inequality (21) in the proof of Theorem 20, and simplifying the notation, letting $\alpha_k = \alpha$ and $\eta_k = \hat{\eta} \psi_k$,

$$\begin{aligned} &\mathbb{E}[f_\alpha(w^{k+1}) | \mathcal{F}_{k-1}] \\ &\leq f_\alpha(w^k) - \hat{\eta} \mathbb{E}[\psi_k \langle \nabla f_\alpha(w^k), \widehat{\nabla} \overline{F}^k(w^k) \rangle | \mathcal{F}_{k-1}] + \langle \nabla f_\alpha(w^k), \mathbb{E}[e^k | \mathcal{F}_{k-1}] \rangle \\ &+ \frac{\sqrt{d} L_0}{\alpha} (\hat{\eta}^2 \mathbb{E}[\psi_k^2 | \widehat{\nabla} \overline{F}^k(w^k)] | \mathcal{F}_{k-1} - 2\hat{\eta} \mathbb{E}[\psi_k \langle \widehat{\nabla} \overline{F}^k(w^k), e^k \rangle | \mathcal{F}_{k-1}] + \mathbb{E}[\|e^k\|_2^2 | \mathcal{F}_{k-1}]) \\ &\stackrel{\text{a.s.}}{\leq} f_\alpha(w^k) - \hat{\eta} \mathbb{E}[\psi_k \langle \nabla f_\alpha(w^k), \widehat{\nabla} \overline{F}^k(w^k) \rangle | \mathcal{F}_{k-1}] + \frac{\sqrt{d} L_0 \hat{\eta}^2}{\alpha} ((\overline{\Psi}^U)^2 c_2 Q + c_3) \\ &\stackrel{\text{a.s.}}{\leq} f_\alpha(w^k) + \hat{\eta} \left(\frac{\Psi_k^U}{2} - c_1 \underline{\Psi}^U - \frac{\Psi_k^L}{2} \right) \|\nabla f_\alpha(w^k)\|_2^2 + \hat{\eta} \left(\frac{\Psi_k^U}{2} - \frac{\Psi_k^L}{2} \right) c_2 Q + \frac{\sqrt{d} L_0 \hat{\eta}^2}{\alpha} ((\overline{\Psi}^U)^2 c_2 Q + c_3) \\ &= f_\alpha(w^k) - \hat{\eta} \left(c_1 \underline{\Psi}^U - \frac{\Delta_k}{2} \right) \|\nabla f_\alpha(w^k)\|_2^2 + \hat{\eta} \frac{\Delta_k}{2} c_2 Q + \frac{\sqrt{d} L_0 \hat{\eta}^2}{\alpha} ((\overline{\Psi}^U)^2 c_2 Q + c_3) \\ &\stackrel{\text{a.s.}}{\leq} f_\alpha(w^k) - \hat{\eta} \left(c_1 \underline{\Psi}^U - \frac{c_4 \hat{\eta}}{2\alpha} \right) \|\nabla f_\alpha(w^k)\|_2^2 + \hat{\eta} \frac{c_4 \hat{\eta}}{2\alpha} c_2 Q + \frac{\sqrt{d} L_0 \hat{\eta}^2}{\alpha} ((\overline{\Psi}^U)^2 c_2 Q + c_3) \\ &= f_\alpha(w^k) - \frac{c_5}{\sqrt{K}} \left(c_1 \underline{\Psi}^U - \frac{c_4 c_5}{2\alpha \sqrt{K}} \right) \|\nabla f_\alpha(w^k)\|_2^2 + \frac{c_4 c_5^2}{2\alpha K} c_2 Q + \frac{\sqrt{d} L_0 c_5^2}{\alpha K} ((\overline{\Psi}^U)^2 c_2 Q + c_3) \\ &\leq f_\alpha(w^k) - \frac{c_5 c_6}{\sqrt{K}} \|\nabla f_\alpha(w^k)\|_2^2 + \frac{c_4 c_5^2}{2\alpha K} c_2 Q + \frac{\sqrt{d} L_0 c_5^2}{\alpha K} ((\overline{\Psi}^U)^2 c_2 Q + c_3), \end{aligned}$$

where the second inequality holds using the same simplifications used to get inequality (25), and the third inequality was shown as inequality (26), both in the proof of Theorem 20. The fourth inequality uses Assumption 19, and the last inequality holds using the assumption

that $K \geq \left(\frac{c_4 c_5}{2\alpha(c_1 \bar{\Psi}^U - c_6)} \right)^2$. Dividing by $\frac{c_5 c_6}{\sqrt{K}}$ and rearranging,

$$\begin{aligned} \|\nabla f_\alpha(w^k)\|_2^2 &\stackrel{\text{a.s.}}{\leq} \frac{\sqrt{K}}{c_5 c_6} (f_\alpha(w^k) - \mathbb{E}[f_\alpha(w^{k+1}) | \mathcal{F}_{k-1}]) \\ &\quad + \frac{c_4 c_5 c_2 Q}{2\alpha c_6 \sqrt{K}} + \frac{\sqrt{d} L_0 c_5}{\alpha c_6 \sqrt{K}} ((\bar{\Psi}^U)^2 c_2 Q + c_3). \end{aligned}$$

Taking the expectation, summing the inequalities over $k \in [K]$, and dividing by K ,

$$\frac{1}{K} \sum_{k=1}^K \mathbb{E}[\|\nabla f_\alpha(w^k)\|_2^2] \leq \frac{1}{c_5 c_6 \sqrt{K}} (f_\alpha(w^1) - \mathbb{E}[f_\alpha(w^{K+1})]) + \frac{c_4 c_5 c_2 Q}{2\alpha c_6 \sqrt{K}} + \frac{\sqrt{d} L_0 c_5}{\alpha c_6 \sqrt{K}} ((\bar{\Psi}^U)^2 c_2 Q + c_3).$$

Noting that $\mathbb{E}[\|\nabla f_\alpha(\hat{w})\|_2^2] = \frac{1}{K} \sum_{k=1}^K \mathbb{E}[\|\nabla f_\alpha(w^k)\|_2^2]$, $\mathbb{E}[\text{dist}(0, \partial_{\frac{\alpha}{2}}^\infty f(\hat{w}))^2] \leq \mathbb{E}[\|\nabla f_\alpha(\hat{w})\|_2^2]$ from Proposition 4, and that $\mathbb{E}[f_\alpha(w^{K+1})] \geq 0$ by assumption,

$$\mathbb{E}[\text{dist}(0, \partial_{\frac{\alpha}{2}}^\infty f(\hat{w}))^2] \leq \frac{f_\alpha(w^1)}{c_5 c_6 \sqrt{K}} + \frac{c_4 c_5 c_2 Q}{2\alpha c_6 \sqrt{K}} + \frac{\sqrt{d} L_0 c_5}{\alpha c_6 \sqrt{K}} ((\bar{\Psi}^U)^2 c_2 Q + c_3).$$

Given that

$$\mathbb{E}[\text{dist}(0, \partial_{\frac{\alpha}{2}}^\infty f(\hat{w}))^2] \leq \mathbb{E}[\text{dist}(0, \partial_{\frac{\alpha}{2}}^\infty f(\hat{w}))^2]$$

by Jensen's inequality, the requirement that

$$\mathbb{E}[\text{dist}(0, \partial_{\frac{\alpha}{2}}^\infty f(\hat{w}))] \leq \nu$$

is satisfied when

$$\frac{f_\alpha(w^1)}{c_5 c_6 \sqrt{K}} + \frac{c_4 c_5 c_2 Q}{2\alpha c_6 \sqrt{K}} + \frac{\sqrt{d} L_0 c_5}{\alpha c_6 \sqrt{K}} ((\bar{\Psi}^U)^2 c_2 Q + c_3) \leq \nu^2.$$

After rearranging, we require

$$\frac{c_5^2}{c_6^2 \alpha^2 \nu^4} \left(\frac{\alpha f_\alpha(w^1)}{c_5^2} + \frac{c_4 c_2 Q}{2} + \sqrt{d} L_0 ((\bar{\Psi}^U)^2 c_2 Q + c_3) \right)^2 \leq K.$$

Choosing K as

$$K = \left\lceil \frac{c_5^2}{c_6^2 \alpha^2 \nu^4} \left(\frac{\alpha f_\alpha(w^1)}{c_5^2} + \frac{c_4 c_2 Q}{2} + \sqrt{d} L_0 ((\bar{\Psi}^U)^2 c_2 Q + c_3) \right)^2 \right\rceil = O\left(\frac{1}{\alpha^2 \nu^4}\right).$$

□

Lemma 31. *Let $R_t(\cdot)$ perform rounding to nearest into \mathbb{F}_t^d , and let $\frac{\alpha}{2} \in \mathbb{F}_t$ for an $\alpha > 0$. For any $y \in \bar{B}_{\frac{\alpha}{2}}^\infty \cap \mathbb{F}_t^d$, it holds that*

$$\bar{B}_{\frac{\alpha}{2}}^\infty \cap R_t^{-1}(y) \subseteq \prod_{i=1}^d \left[y_i - \frac{\beta e_i - t}{2}, y_i + \frac{\beta e_i - t}{2} \right] \quad (29)$$

and $m(\bar{B}_{\frac{\alpha}{2}}^\infty \cap R_t^{-1}(y)) \geq \prod_{i=1}^d \left(\frac{\beta e_i - t - 1}{2} \right)$, where e_i is the exponent of y_i when $\mathbb{F} = \mathbb{I}$ and $e_i = 0$ when $\mathbb{F} = \mathbb{I}$, for all $i \in [d]$.

Proof. The distance from a point $y \in \mathbb{L}_t$, for $y \notin \{\Lambda^-, \Lambda^+\}$, to the closest larger in magnitude element in \mathbb{L}_t equals β^{e-t} . The distance to the closest smaller in magnitude element for any $y \in \mathbb{L}_t$ equals β^{e-t-1} when $d_1 = 1$, $d_i = 0 \forall i > 1$, and $|y| \neq \lambda_N$, and β^{e-t} otherwise. When $\mathbb{F} = \mathbb{I}$, all points are β^{-t} apart. As $R_t(\cdot)$ rounds to nearest, it holds for $y \notin \{\Lambda^-, \Lambda^+\}$ that $\overline{B}_{\frac{\alpha}{2}}^\infty \cap R_t^{-1}(y) \subseteq R_t^{-1}(y) \subseteq [y - \frac{\beta^{e-t}}{2}, y + \frac{\beta^{e-t}}{2}]$. When $y \in \{\Lambda^-, \Lambda^+\}$ this bound also holds as $\overline{B}_{\frac{\alpha}{2}}^\infty \cap R_t^{-1}(y) \subseteq S$ for an $S \in \{[y, y + \frac{\beta^{e-t}}{2}], [y - \frac{\beta^{e-t}}{2}, y]\}$. Expanding this bound up to d dimensions results in (29).

From the previous paragraph, the lower bound in one dimension for $y \in [-\frac{\alpha}{2}, \frac{\alpha}{2}] \cap \mathbb{F}_t$, $m([-\frac{\alpha}{2}, \frac{\alpha}{2}] \cap R_t^{-1}(y)) \geq \frac{\beta^{e-t-1}}{2}$, is attained when considering $\mathbb{F} = \mathbb{L}$, $y = \frac{\alpha}{2}$, $d_1 = 1$, $d_i = 0 \forall i > 1$, and $|y| \neq \lambda_N$, as then $(y - \frac{\beta^{e-t-1}}{2}, y] \subseteq [-\frac{\alpha}{2}, \frac{\alpha}{2}] \cap R_t^{-1}(y)$. This lower bound is smaller than for when considering $\mathbb{F} = \mathbb{I}$, where a lower bound on the inverse image of any $y \in [-\frac{\alpha}{2}, \frac{\alpha}{2}] \cap \mathbb{L}_t$ can be determined by considering $y \in \{-\frac{\alpha}{2}, \frac{\alpha}{2}\}$, where for an $S \in \{[y, y + \frac{\beta^{-t}}{2}], (y - \frac{\beta^{-t}}{2}, y]\}$, it holds that $S \subseteq [-\frac{\alpha}{2}, \frac{\alpha}{2}] \cap R_t^{-1}(y)$. The lower-bound in d -dimensions follows directly. \square

Proof. (Theorem 27): This proof requires Lemma 31, which is given directly above this proof. For all $\hat{u}^k \in \hat{u}_\infty$, let $j_k := \min\{j \geq 1 : \hat{u}^k \in \mathbb{F}_{t_j}^d\}$ be the index of the minimum number of precision/fractional digits such that \hat{u}^k is representable in $\mathbb{F}_{t_j}^d$ for $j \geq j_k$. For any $\hat{u}^k \in \hat{u}_\infty$, $j \geq j_k$, and $i \in [d]$,

$$\begin{aligned} & \mathbb{E}[|\widehat{\nabla} F_i(w + \hat{u}^k, \xi, b) - \widehat{\nabla} F_i(w + u, \xi, b)| \mid u \in \overline{B}_{\frac{\alpha}{2}}^\infty \cap R_{t_j}^{-1}(\hat{u}^k)] \\ &= \frac{1}{\mathbb{P}(u \in \overline{B}_{\frac{\alpha}{2}}^\infty \cap R_{t_j}^{-1}(\hat{u}^k))} \mathbb{E}[|\widehat{\nabla} F_i(w + \hat{u}^k, \xi, b) - \widehat{\nabla} F_i(w + u, \xi, b)| \mathbb{1}_{u \in \overline{B}_{\frac{\alpha}{2}}^\infty \cap R_{t_j}^{-1}(\hat{u}^k)}] \\ &= \frac{m(\overline{B}_{\frac{\alpha}{2}}^\infty)}{m(\overline{B}_{\frac{\alpha}{2}}^\infty \cap R_{t_j}^{-1}(\hat{u}^k))} \mathbb{E}[|\widehat{\nabla} F_i(w + \hat{u}^k, \xi, b) - \widehat{\nabla} F_i(w + u, \xi, b)| \mathbb{1}_{u \in \overline{B}_{\frac{\alpha}{2}}^\infty \cap R_{t_j}^{-1}(\hat{u}^k)}] \\ &= \frac{1}{m(\overline{B}_{\frac{\alpha}{2}}^\infty \cap R_{t_j}^{-1}(\hat{u}^k))} \int_{\overline{B}_{\frac{\alpha}{2}}^\infty \cap R_{t_j}^{-1}(\hat{u}^k)} \mathbb{E}_{\xi, b}[|\widehat{\nabla} F_i(w + \hat{u}^k, \xi, b) - \widehat{\nabla} F_i(w + u, \xi, b)|] du \end{aligned}$$

for all $w \in \mathbb{R}^d$, given that $\mathbb{P}(u \in \overline{B}_{\frac{\alpha}{2}}^\infty \cap R_{t_j}^{-1}(\hat{u}^k)) = \frac{m(\overline{B}_{\frac{\alpha}{2}}^\infty \cap R_{t_j}^{-1}(\hat{u}^k))}{m(\overline{B}_{\frac{\alpha}{2}}^\infty)}$ for the second equality, and the final equality holds using Tonelli's theorem: The function $|\widehat{\nabla} F_i(w + \hat{u}^k, \xi, b) - \widehat{\nabla} F_i(w + u, \xi, b)| \mathbb{1}_{u \in \overline{B}_{\frac{\alpha}{2}}^\infty \cap R_{t_j}^{-1}(\hat{u}^k)} \in L^+(\overline{B}_{\frac{\alpha}{2}}^\infty \times \mathbb{R}^{d+s})$, the measures P_u and $P_\xi \times P_b$ are finite, where P_X denotes the probability measure induced by random variable X , and the associativity of the product of measures holds given that they are finite (Folland, 1999, Section 2.5, Exercise 45).

For any $w \in \mathbb{R}^d$, $i \in [d]$, and bounded measurable set $K \subset \mathbb{R}^d$,

$$\begin{aligned} & \int_{u \in K} |\mathbb{E}_{\xi, b}[\widehat{\nabla} F_i(w + u, \xi, b)]| du \\ & \leq \int_{u \in K} \|\mathbb{E}_{\xi, b}[\widehat{\nabla} F(w + u, \xi, b)]\|_2 du \\ & \leq \int_{u \in K} \sqrt{c_2 Q} du = m(K) \sqrt{c_2 Q} < \infty, \end{aligned}$$

where the second inequality holds given that $\|\mathbb{E}_{\xi, b}[\widehat{\nabla} F(w + u, \xi, b)]\|_2 \leq \sqrt{c_2 Q}$ for almost all $u \in K$ using Assumption 26 with Jensen's inequality, hence the functions $\mathbb{E}_{\xi, b}[\widehat{\nabla} F_i(w + u, \xi, b)]$ are locally integrable in $u \in \mathbb{R}^d$, and the Lebesgue differentiation theorem can be used to prove that for all $\hat{u}^k \in \hat{u}^\infty$, all $i \in [d]$, and almost all $w \in \mathbb{R}^d$,

$$\lim_{j \rightarrow \infty} \frac{1}{m(\overline{B}_{\frac{\alpha}{2}}^\infty \cap R_{t_j}^{-1}(\hat{u}^k))} \int_{\overline{B}_{\frac{\alpha}{2}}^\infty \cap R_{t_j}^{-1}(\hat{u}^k)} \mathbb{E}_{\xi, b}[\widehat{\nabla} F_i(w + \hat{u}^k, \xi, b) - \widehat{\nabla} F_i(w + u, \xi, b)] du = 0. \quad (30)$$

In particular, we verify that the requirements of (Folland, 1999, Theorem 3.21) hold: for any $k \in \mathbb{N}$, from Lemma 31,

$$\overline{B}_{\frac{\alpha}{2}}^\infty \cap R_{t_j}^{-1}(\hat{u}^k) \subseteq \prod_{i=1}^d \left[\hat{u}_i^k - \frac{\beta e_i^k - t_j}{2}, \hat{u}_i^k + \frac{\beta e_i^k - t_j}{2} \right] \subseteq \overline{B}_{\rho_j}^2(\hat{u}^k),$$

where e_i^k is the exponent of \hat{u}_i^k , $\rho_j := \sqrt{d} \frac{\beta e_{max}^k - t_j}{2}$, where $e_{max}^k := \max\{e_1^k, e_2^k, \dots, e_d^k\} \leq e_{max}$ when $\mathbb{F} = \mathbb{L}$ and $e_{max}^k := 0$ when $\mathbb{F} = \mathbb{I}$, with $m(\overline{B}_{\rho_j}^2(\hat{u}^k)) = \frac{(\sqrt{\pi} \rho_j)^d}{\Gamma(\frac{d}{2} + 1)}$. The measure $m(\overline{B}_{\frac{\alpha}{2}}^\infty \cap R_{t_j}^{-1}(\hat{u}^k)) \geq \prod_{i=1}^d \left(\frac{\beta e_i^k - t_j - 1}{2} \right) \geq \left(\frac{\beta e_{min}^k - t_j - 1}{2} \right)^d$, where $e_{min}^k := \min\{e_1^k, e_2^k, \dots, e_d^k\} \geq e_{min}$ when $\mathbb{F} = \mathbb{L}$ and $e_{min}^k := 0$ when $\mathbb{F} = \mathbb{I}$, hence

$$\begin{aligned} \frac{m(\overline{B}_{\frac{\alpha}{2}}^\infty \cap R_{t_j}^{-1}(\hat{u}^k))}{m(\overline{B}_{\rho_j}^2(\hat{u}^k))} & \geq \left(\frac{\beta e_{min}^k - t_j - 1}{2\sqrt{\pi} \rho_j} \right)^d \Gamma\left(\frac{d}{2} + 1\right) \\ & = \left(\frac{\beta e_{min}^k - t_j - 1}{2\sqrt{\pi} \sqrt{d} \frac{\beta e_{max}^k - t_j}{2}} \right)^d \Gamma\left(\frac{d}{2} + 1\right) \\ & = \frac{\Gamma\left(\frac{d}{2} + 1\right)}{(\beta^{1+e_{max}^k} - e_{min}^k \sqrt{\pi d})^d}. \end{aligned} \quad (31)$$

The sets $\overline{B}_{\frac{\alpha}{2}}^\infty \cap R_{t_j}^{-1}(\hat{u}^k)$ are said to *shrink nicely*, given that (31) is independent of t_j . A family of sets $\{E_\rho(\hat{u}^k)\}_{\rho > 0}$ can be considered, which all satisfy

$$E_\rho(\hat{u}^k) \subseteq \overline{B}_\rho^2(\hat{u}^k)$$

and

$$\frac{m(E_\rho(\hat{u}^k))}{m(\overline{B}_\rho^2(\hat{u}^k))} \geq \frac{\Gamma\left(\frac{d}{2} + 1\right)}{(\beta^{1+e_{max}^k} - e_{min}^k \sqrt{\pi d})^d}.$$

From (Folland, 1999, Theorem 3.21), for any $\hat{u}^k \in \hat{u}_\infty$ and $i \in [d]$,

$$\lim_{\rho \rightarrow 0} \frac{1}{m(E_\rho(\hat{u}^k))} \int_{E_\rho(\hat{u}^k)} \mathbb{E}_{\xi, b} [|\widehat{\nabla} F_i(w + \hat{u}^k, \xi, b) - \widehat{\nabla} F_i(w + u, \xi, b)|] du = 0 \quad (32)$$

for all $w \in \hat{S}^{k,i} \subset \mathbb{R}^d$, where $m((\hat{S}^{k,i})^c) = 0$. It follows that for all $\hat{u}^k \in \hat{u}_\infty$, $i \in [d]$, and $w \in \hat{S} := \bigcap_{k=1}^\infty \bigcap_{i=1}^d \hat{S}^{k,i}$, (32) holds with $m((\hat{S})^c) = 0$, as the union of a countable number of null sets. Considering the sequence $\{\rho_j\}$ and setting $E_{\rho_j}(\hat{u}^k) = \overline{B}_{\frac{\rho_j}{2}} \cap R_{t_j}^{-1}(\hat{u}^k)$, it follows from (32), taking the limit over the sequence $\{\rho_j\}$, that (30) holds for all $\hat{u}^k \in \hat{u}_\infty$, $i \in [d]$, and almost all $w \in \mathbb{R}^d$. \square

Appendix D Supplementary Material for Section 6

Choosing the Baseline SGD Model

Training R20C10, momentum = 0.9 and weight decay = 1e-4, following (He et al., 2016, Section 4.2), were tested without rounding these parameter values to avoid biasing these initial experiments. Using FL8N, plotted in Figure 1, it was found that plain SGD worked best: the minimum accuracy of SGD is greater than the maximum accuracy of the momentum variants, and the mean accuracy of SGD is similar to the maximum accuracy when using weight decay. Using FL16N, plotted in Figure 2, SGD+Weight Decay+Momentum has the best accuracy, though in this experiment all methods have similar accuracies. Being significantly better in the lower precision environment, plain SGD was chosen as the baseline SGD algorithm for further low-precision training experiments.

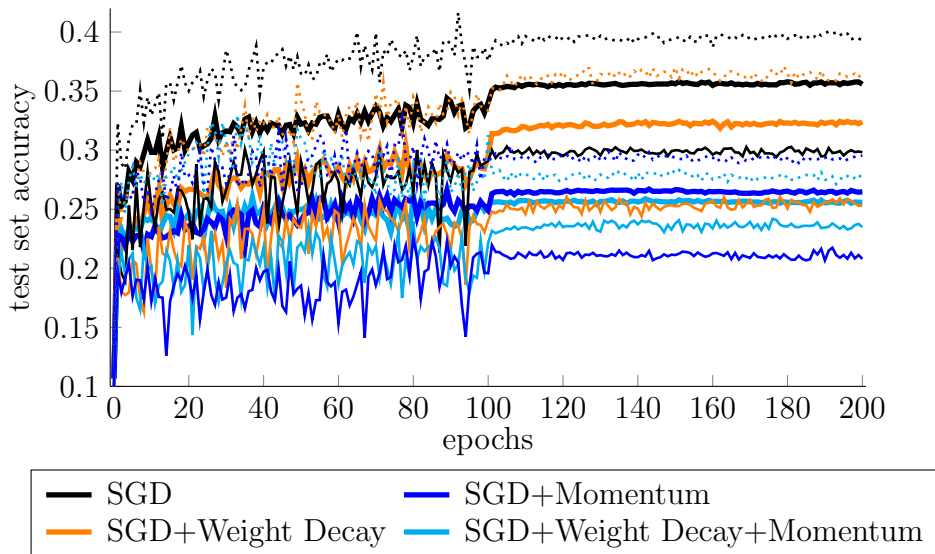


Figure 1: Comparison of popular variants of SGD. The mean (thick solid), minimum (thin solid), and maximum (dotted) test set accuracy over 10 runs of training R20C10 in FL8N is plotted.

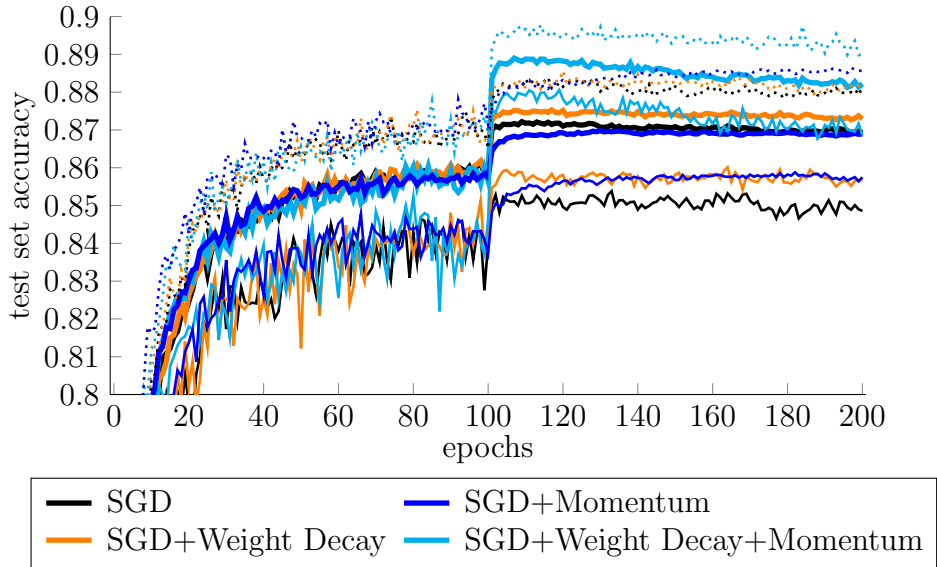


Figure 2: Comparison of popular variants of SGD. The mean (thick solid), minimum (thin solid), and maximum (dotted) test set accuracy over 10 runs of training R20C10 in FL16N is plotted.

Choosing the Variant of Gradient Normalization

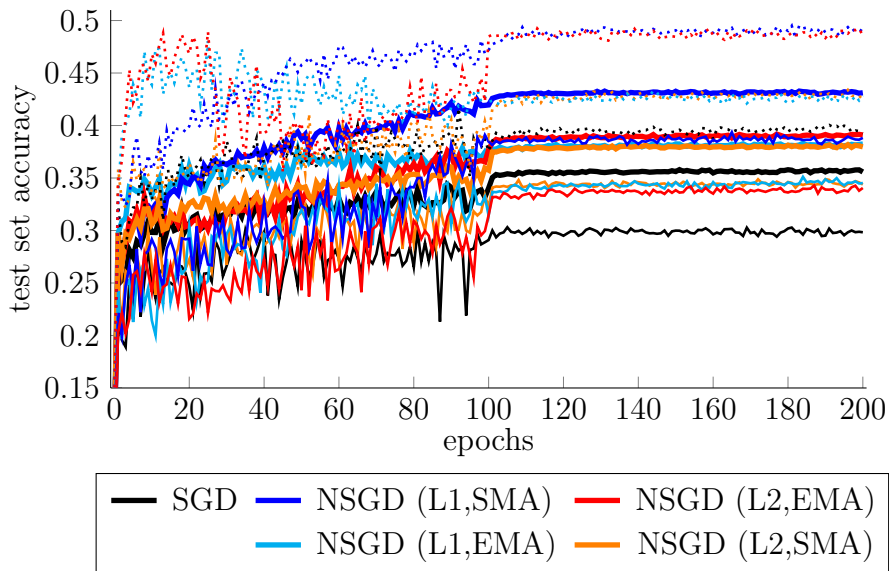


Figure 3: Comparison of different variants of NSGD with SGD. The mean (thick solid), minimum (thin solid), and maximum (dotted) test set accuracy over 10 runs training R20C10 in FL8N is plotted.

Results and Plots of Training in Low-Precision Environments

Table 2: Accuracies, relative accuracies, and scores of all algorithms in the fixed-point rounding to nearest (R=N) and stochastic rounding (R=S) experiments, with the resulting Sum of Accuracies (SoA), Sum of Relative Accuracies (SoR), and Sum of Scores (SoS) methods of ranking. The column Acc indicates whether each row contains the mean or minimum accuracies of each algorithm. Bold and underline indicate the highest and lowest value in each column.

R=N Experiments	Acc	SGD	NSGD	DNSGD	PSGD	PNSGD	PDNSGD
R20C10 FI24/19N	Mean	0.3326	0.3327	<u>0.3309</u>	0.3802	0.3804	0.3814
R20C10 FI24/19N	Min	0.0986	0.0990	0.0996	<u>0.0962</u>	0.0974	0.0981
R32C100 FI26/19N	Mean	<u>0.3690</u>	<u>0.3690</u>	<u>0.3690</u>	0.4274	0.4274	0.4273
R32C100 FI26/19N	Min	0.0100	0.0100	0.0100	0.0100	0.0100	0.0100
SoA		0.8103	0.8107	<u>0.8095</u>	0.9138	0.9152	0.9169
R20C10 FI24/19N	Mean	0.8721	0.8723	<u>0.8676</u>	0.9967	0.9972	1
R20C10 FI24/19N	Min	0.9908	0.9948	1	<u>0.9664</u>	0.9787	0.9858
R32C100 FI26/19N	Mean	<u>0.8634</u>	<u>0.8634</u>	<u>0.8634</u>	1	1	0.9998
R32C100 FI26/19N	Min	0.9993	<u>0.9977</u>	0.9987	1	1	1
SoR		<u>3.7256</u>	3.7281	3.7298	3.9631	3.9760	3.9856
R20C10 FI24/19N	Mean	<u>-3</u>	<u>-3</u>	<u>-3</u>	3	3	3
R20C10 FI24/19N	Min	0	0	0	0	0	0
R32C100 FI26/19N	Mean	<u>-3</u>	<u>-3</u>	<u>-3</u>	3	3	3
R32C100 FI26/19N	Min	0	0	0	0	0	0
SoS		<u>-6</u>	<u>-6</u>	<u>-6</u>	6	6	6

R=S Experiments	Acc	SGD	NSGD	DNSGD	PSGD	PNSGD	PDNSGD
R20C10 FI20/15S	Mean	0.8640	0.8601	0.8588	0.8608	0.8641	<u>0.8564</u>
R20C10 FI20/15S	Min	0.8456	0.8507	0.8475	0.8484	0.8566	<u>0.8326</u>
R32C100 FI24/17S	Mean	<u>0.5902</u>	0.5982	0.5973	0.5953	0.6015	0.6013
R32C100 FI24/17S	Min	<u>0.5749</u>	0.5754	0.5850	0.5794	0.5872	0.5873
SoA		<u>2.8745</u>	2.8845	2.8886	2.8840	2.9094	2.8777
R20C10 FI20/15S	Mean	0.9998	0.9954	0.9938	0.9962	1	<u>0.9911</u>
R20C10 FI20/15S	Min	0.9871	0.9931	0.9893	0.9905	1	<u>0.9720</u>
R32C100 FI24/17S	Mean	<u>0.9812</u>	0.9945	0.9931	0.9898	1	0.9997
R32C100 FI24/17S	Min	<u>0.9788</u>	0.9797	0.9961	0.9866	0.9998	1
SoR		<u>3.9469</u>	3.9628	3.9722	3.9629	3.9998	3.9629
R20C10 FI20/15S	Mean	4	<u>-2</u>	<u>-2</u>	<u>-2</u>	4	-2
R20C10 FI20/15S	Min	-1	3	-1	-1	5	<u>-5</u>
R32C100 FI24/17S	Mean	<u>-5</u>	-1	-1	-1	4	4
R32C100 FI24/17S	Min	<u>-3</u>	<u>-3</u>	3	<u>-3</u>	3	3
SoS		-5	-3	-1	<u>-7</u>	16	0

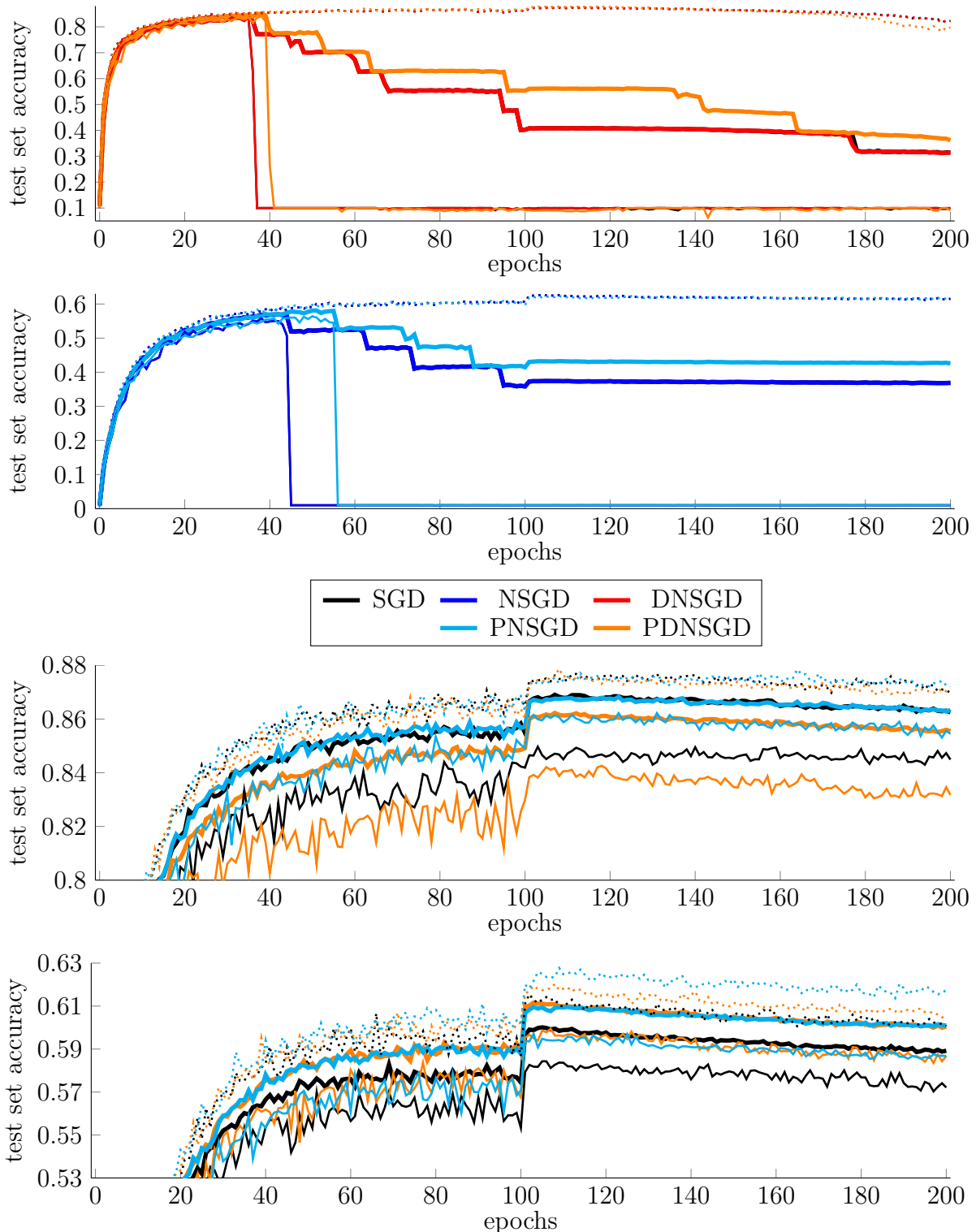


Figure 4: Plots of SGD and the best (and worst) performing algorithms. The mean (thick solid), minimum (thin solid), and maximum (dotted) test set accuracy from training, from top to bottom, R20C10 in FI24/19N, R32C100 in FI26/19N, R20C10 in FI20/15S, and R32C100 in FI24/17S over 10 runs is plotted.

Table 3: Accuracies, relative accuracies, and scores of all algorithms in the floating-point rounding to nearest experiments, with the resulting Sum of Accuracies (SoA), Sum of Relative Accuracies (SoR), and Sum of Scores (SoS) methods of ranking. The column Acc indicates whether each row contains the mean or minimum accuracies of each algorithm. Bold and underline indicate the highest and lowest value in each column.

R=N Experiments	Acc	SGD	NSGD	DNSGD	PSGD	PNSGD	PDNSGD
R20C10 FL8N	Mean	0.3565	0.4315	0.3683	<u>0.3226</u>	0.3890	0.3673
R20C10 FL8N	Min	0.2984	0.3868	0.3180	<u>0.2798</u>	0.2950	0.3038
R20C10 FL9N	Mean	0.7804	0.7730	0.7744	<u>0.7730</u>	0.7706	<u>0.7655</u>
R20C10 FL9N	Min	0.7359	0.7620	0.7592	0.7344	0.7587	<u>0.7018</u>
R32C100 FL9N	Mean	0.1974	0.2052	0.2043	0.1840	<u>0.1837</u>	0.1854
R32C100 FL9N	Min	0.1590	0.1750	0.1755	0.1572	<u>0.1515</u>	0.1674
R32C100 FL10N	Mean	0.4369	0.4405	<u>0.4344</u>	0.4347	0.4372	0.4356
R32C100 FL10N	Min	0.4250	0.4214	<u>0.4213</u>	0.4229	0.4258	0.4263
SoA		3.3896	3.5955	3.4552	<u>3.3086</u>	3.4115	3.3531
R20C10 FL8N	Mean	0.8263	1	0.8537	<u>0.7477</u>	0.9015	0.8514
R20C10 FL8N	Min	0.7714	1	0.8220	<u>0.7233</u>	0.7626	0.7854
R20C10 FL9N	Mean	1	0.9905	0.9923	<u>0.9905</u>	0.9875	<u>0.9809</u>
R20C10 FL9N	Min	0.9657	1	0.9962	0.9637	0.9956	<u>0.9209</u>
R32C100 FL9N	Mean	0.9618	1	0.9955	0.8969	<u>0.8954</u>	0.9034
R32C100 FL9N	Min	0.9063	0.9975	1	0.8959	<u>0.8636</u>	0.9539
R32C100 FL10N	Mean	0.9919	1	<u>0.9861</u>	0.9868	0.9926	0.9889
R32C100 FL10N	Min	0.9970	0.9886	<u>0.9882</u>	0.9922	0.9988	1
SoR		7.4205	7.9766	7.6340	<u>7.1970</u>	7.3975	7.3849
R20C10 FL8N	Mean	-3	5	0	<u>-5</u>	3	0
R20C10 FL8N	Min	-2	5	3	<u>-5</u>	-2	1
R20C10 FL9N	Mean	5	0	0	0	0	<u>-5</u>
R20C10 FL9N	Min	-2	3	3	-2	3	<u>-5</u>
R32C100 FL9N	Mean	1	4	4	<u>-3</u>	<u>-3</u>	<u>-3</u>
R32C100 FL9N	Min	-2	4	4	-2	<u>-5</u>	1
R32C100 FL10N	Mean	<u>-1</u>	5	<u>-1</u>	<u>-1</u>	<u>-1</u>	<u>-1</u>
R32C100 FL10N	Min	3	<u>-3</u>	<u>-3</u>	<u>-3</u>	3	3
SoS		-1	23	10	<u>-21</u>	-2	-9

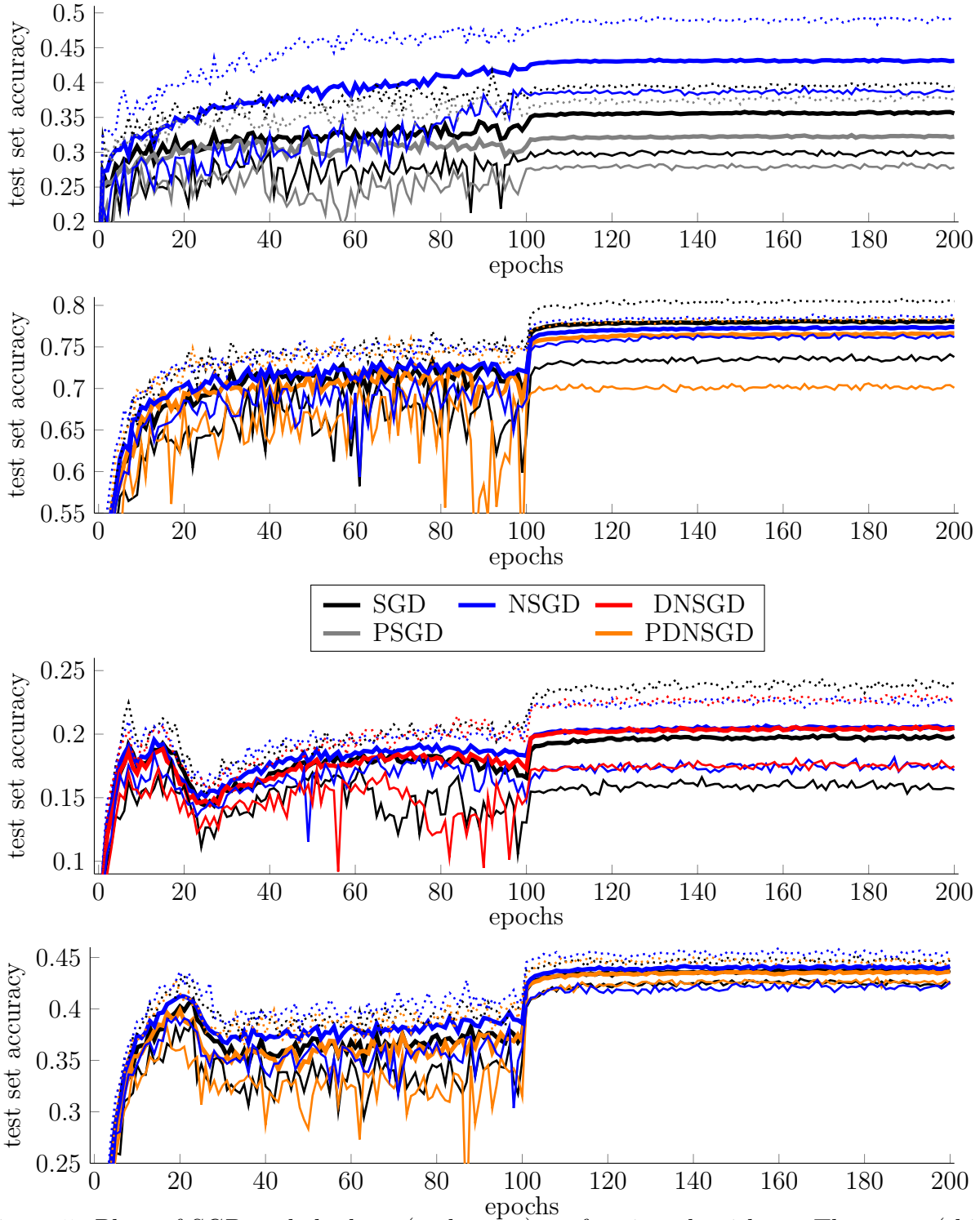


Figure 5: Plots of SGD and the best (and worst) performing algorithms. The mean (thick solid), minimum (thin solid), and maximum (dotted) test set accuracy from training, from top to bottom, R20C10 in FL8N, R20C10 in FL9N, R32C100 in FL9N, and R32C100 in FL10N over 10 runs is plotted.

Table 4: Accuracies, relative accuracies, and scores of all algorithms in the floating-point stochastic rounding experiments, with the resulting Sum of Accuracies (SoA), Sum of Relative Accuracies (SoR), and Sum of Scores (SoS) methods of ranking. The column Acc indicates whether each row contains the mean or minimum accuracies of each algorithm. Bold and underline indicate the highest and lowest value in each column.

R=S Experiments	Acc	SGD	NSGD	DNSGD	PSGD	PNSGD	PDNSGD
R20C10 FL8S	Mean	0.4559	0.4644	0.4873	0.4709	0.4844	<u>0.4404</u>
R20C10 FL8S	Min	0.3912	0.4271	0.4316	0.4285	0.4069	<u>0.3907</u>
R20C10 FL8S WD	Mean	0.5130	<u>0.5094</u>	0.5159	0.5144	0.5211	0.5292
R20C10 FL8S WD	Min	0.4764	<u>0.4242</u>	0.4735	0.4590	0.4828	0.4814
R32C100 FL9S	Mean	0.3776	0.3746	0.3695	0.3716	0.3826	<u>0.3679</u>
R32C100 FL9S	Min	0.3504	<u>0.3489</u>	0.3512	0.3558	0.3682	0.3518
R32C100 FL9S WD	Mean	0.4072	<u>0.3994</u>	0.4023	0.4121	0.4100	0.4084
R32C100 FL9S WD	Min	0.3864	0.3794	<u>0.3789</u>	0.3900	0.3940	0.3906
SoA		<u>2.8745</u>	2.8845	2.8886	2.8840	2.9094	2.8777
R20C10 FL8S	Mean	0.9356	0.9531	1	0.9663	0.9940	<u>0.9038</u>
R20C10 FL8S	Min	0.9065	0.9895	1	0.9928	0.9427	<u>0.9051</u>
R20C10 FL8S WD	Mean	0.9694	<u>0.9627</u>	0.9750	0.9722	0.9848	1
R20C10 FL8S WD	Min	0.9867	<u>0.8787</u>	0.9807	0.9507	1	0.9972
R32C100 FL9S	Mean	0.9870	0.9791	0.9657	0.9712	1	<u>0.9616</u>
R32C100 FL9S	Min	0.9518	<u>0.9477</u>	0.9537	0.9663	1	0.9555
R32C100 FL9S WD	Mean	0.9880	<u>0.9692</u>	0.9762	1	0.9949	0.9910
R32C100 FL9S WD	Min	0.9807	0.9629	<u>0.9617</u>	0.98980	1	0.99120
SoR		7.7057	<u>7.6428</u>	7.8131	7.8092	7.9163	7.7054
R20C10 FL8S	Mean	-3	-1	4	1	4	<u>-5</u>
R20C10 FL8S	Min	<u>-4</u>	3	3	3	-1	<u>-4</u>
R20C10 FL8S WD	Mean	-1	<u>-5</u>	-1	-1	3	5
R20C10 FL8S WD	Min	0	<u>-5</u>	0	-3	4	4
R32C100 FL9S	Mean	2	2	<u>-3</u>	<u>-3</u>	5	<u>-3</u>
R32C100 FL9S	Min	<u>-2</u>	<u>-2</u>	<u>-2</u>	3	5	<u>-2</u>
R32C100 FL9S WD	Mean	2	<u>-4</u>	<u>-4</u>	2	2	2
R32C100 FL9S WD	Min	-1	<u>-4</u>	<u>-4</u>	3	3	3
SoS		-7	<u>-16</u>	-7	5	25	0

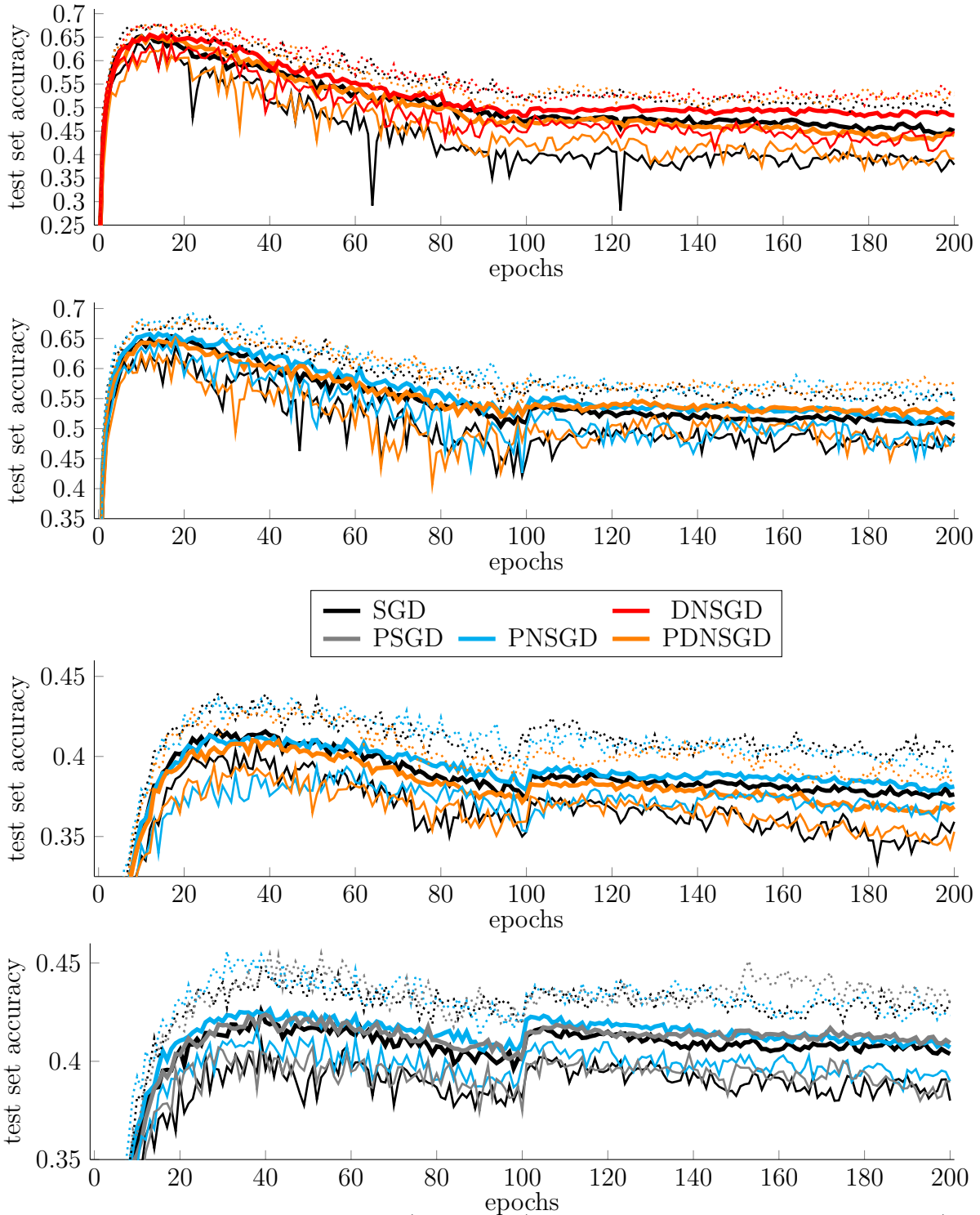


Figure 6: Plots of SGD and the best (and worst) performing algorithms. The mean (thick solid), minimum (thin solid), and maximum (dotted) test set accuracy from training, from top to bottom, R20C10 in FL8S, R20C10 in FL8S with weight decay (WD), R32C100 in FL9S, and R32C100 in FL9S with WD over 10 runs is plotted.